# Posttranslational modifications of human M3 muscarinic acetylcholine receptor

## zooming in its functional implications

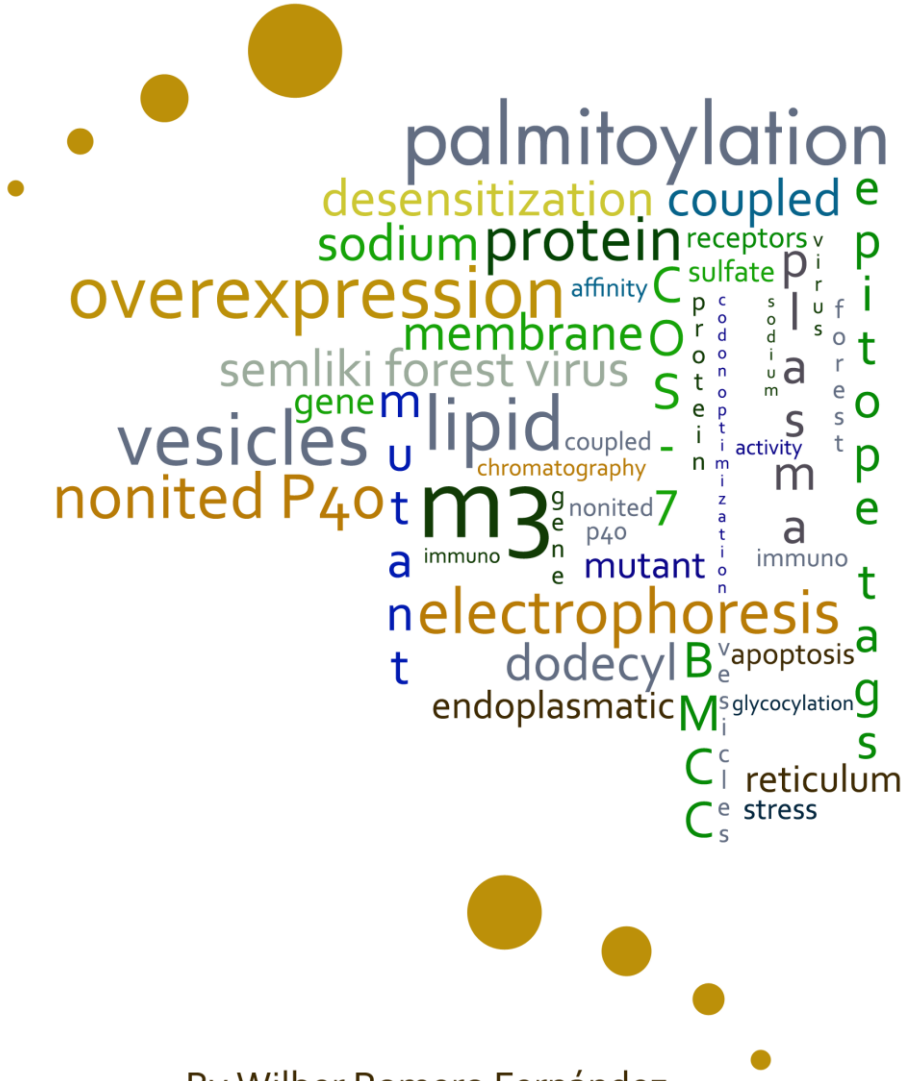


By Wilber Romero Fernández

Cover made by Martín Herrera Ardila

Technical University of Catalonia

# Posttranslational modifications of human $M_3$ muscarinic acetylcholine receptor: zooming in its functional implications

A dissertation submitted in partial fulfillment
of the requirements for the degree of
DOCTOR
by
Technical University of Catalonia

**Wilber Romero Fernández**
B.S. Havana University

Barcelona, 2011

The present Ph.D. thesis has been carried out at the Terrassa campus
Industrial and Molecular Biotechnology Group
Department of Chemical Engineering
Technical University of Catalonia
supervised
by

Dr. Pere Garriga Solé

This work has been financially supported by the
Professor University training Program (FPU-AP2004-6658)
from Spanish Ministry of Education
and grants
SAF 2008-04943-C02-02 and SAF 2005-08148-C04-02
from Spanish Ministry of Science
Government of Spain

*A mi madre y abuelas*

## Ph.D. thesis abstract

The human $M_3$ muscarinic acetylcholine receptor ($M_3R$) regulates many important physiological roles in the central and peripheral nervous systems, and it is involved in the pathophysiology of several neurodegenerative and autoimmune diseases, representing attractive potential pharmacological target for intervention. However, the lack of structural information on this receptor hampered the development of new potent antagonist with increased selectivity and lower side effects. Such structural information can be only achieved by means of experimental biophysical techniques, which require large quantities of pure receptor. Considering that under physiological conditions the expression of G-protein coupled receptors (GPCRs) is relatively low, optimization of the receptor overexpression is a pre-requisite for structural studies efforts to be performed. In addition, although is has well established that GPCR undergo post-translational and increase evidences support that these are tight links to receptor roles, little progress has been made in the post-translational modifications field in some GPCRs, such as the case of $M_3R$.

In this study, we provide some strategies to improve muscarinic receptor heterologous expression in mammalian cells guaranteeing proper post-translational modifications. In addition, we have been able to extract high levels of functional receptor from COS-7 cells using a detergent combination tested, and to purify the receptor to near homogeneity -keeping the full wild type receptor properties- by means of different affinity purification methods. Regarding the post-translational modifications studied, our findings provide the first evidence of the critical role that N-glycan chains play in determining muscarinic receptor distribution and localization, as well as in cell integrity. Furthermore, our data reveal a role for palmitoylation in determining $M_3R$ residence within lipid raft, as well as in receptor internalization and down-regulation

In summary, the strategies used could help increasing $M_3R$ expression not only in order to start purification efforts, but also for subsequent structural analysis, functional assays, and potential three-dimensional structural determination. In addition, we suggest a possible map site for N-glycosylation and palmitoylation of $M_3R$ in COS-7 cells and provide further experimental evidence that post-translational modifications of $M_3R$ determine receptor expression and functionality.

## Table of Content

# CHAPTER 1

## GENERAL INTRODUCTION

# General Introduction

## 1.1 G-Proteins-Coupled Receptors

**G-Protein-Coupled Receptors:** G-protein-coupled receptors (GPCRs) are a broad class of integral membrane proteins that comprise a larg superfamily of proteins that plays an important role in signal transduction [1]. GPCR acronym derives from their function in G-protein binding and activation [2]. GPCRs are characterized by a highly specific structural architecture formed by helices, which cross the membrane seven times. The seven transmembrane-spanning α-helixes are connected by intracellular and extracellular loop domains. When properly folded, the extracellular and intracellular domains form very specific active sites for binding ligands and GTP-binding proteins respectively. The orientation of the N- and C-terminus is also conserved across all GPCRs. The N-terminal tail is exposed to the extracellular environment and the C-terminal tail is located in the cytosol of the cell and thought to maintain an interaction with cytosolic G-proteins (Fig. 1) [3,4]. GPCRs are also referred to as heptahelical, serpentine or 7-transmembrane receptors. It is important to note that not all proteins that bind G-proteins are GPCRs, and that GPCRs are able to signal through G-protein independent pathways mediated by molecules like chaperones and scaffolding proteins [5].

GPCRs are activated by specific ligands and this promotes the activation of specific intracellular heterotrimeric G-proteins. Activated G-proteins bind to various downstream effectors inducing a cellular response by initiating complex intracellular cascades [6]. There is a wide chemical diversity among the endogenous ligands that bind and activate these GPCRs, ranging from pheromones, hormones, lipids and peptides to biogenic amines, nucleotides and ions [7]. Further, the sensation of exogenous stimuli, including light, odor and taste, is mediated through GPCRs [8]. Over 1000 seven-transmembrane helix encoded GPCR-like sequences have been identified in the human genome [9]. It is not surprising that they are involved in many disorders, making them medical relevant targets for drug development [10]. The presence of GPCRs at the cell surface

makes these receptors very accessible to therapeutic drugs. It is estimated that more than half of drugs under current investigation are targets at GPCRs [10,11].

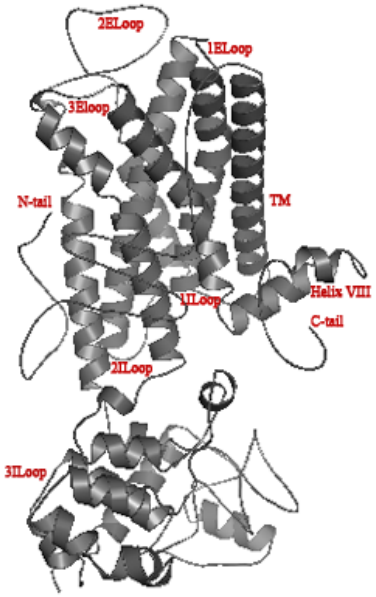


**Figure 1.** Computer model of the human muscarinic acetylcholine receptor as GPCR archetype based on the crystal structure of rhodopsin and β-adrenergic receptor using I-TASSER algorithms and prepared using PyMOL. The structure is viewed from parallel to the cell membrane and has six key features. 1: seven transmembrane α-helices; 2: three external loops (1Eloop-3Eloop); 3: three cytosolic loops (1ILoop-3ILoop); 4: N-terminal tail (N-tail) and a C-terminal tail (C-tail); and 5: a possible cytosolic helix VIII (Helix VIII).

## GPCR classification

GPCRs do not share any overall sequence homology among the different subfamilies; the only structural feature common to all GPCRs is the presence of seven transmembrane-spanning α-helical segments connected by alternating intracellular and extracellular loops. Two cysteine residues (one in ECL 1 and one in ECL 2) which are conserved in most GPCRs, form a disulfide link which is probably important for the packing and for the stabilization of a restricted number of conformations of these seven transmembrane domains. Aside from sequence variations, GPCRs differ in the length and function of their N-terminal extracellular

domain, their C-terminal intracellular domain and their intracellular loops. Each of these domains provides specific properties to these various receptor proteins. However, significant sequence homology is found, within several subfamilies. GPCRs can be subdivided into smaller families on the basis of sequence homology and/or pharmacological characteristics. In general, GPCRs are divided into three major subfamilies: rhodopsin/β2-adrenergic-receptor-like family (family A or class A), glucagon-receptor-like family (family B or class B) and metabotropic glutamate neurotransmitter receptors family (family C or class C). Yeast pheromone receptors (family D, STE2 receptors), the cAMP receptors (family E, STE3 receptors) and the frizzled/smoothened family make up three minor subfamilies (family F). A schematic representation, of subfamilies A to C, is shown in Fig. 2.

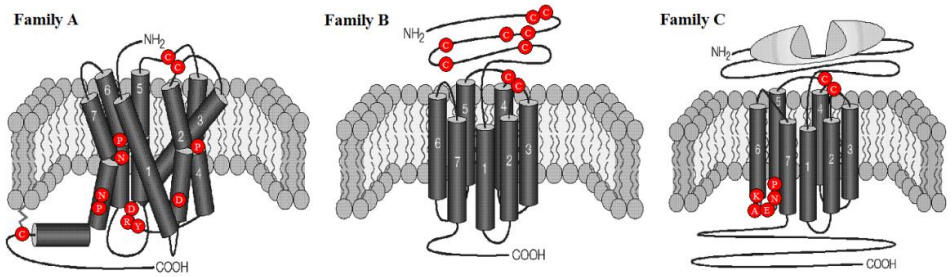


**Figure 2**. GPCRs can be divided into different families based on their structural and genetic characteristics. The figure shows schematic representations of receptor monomers, and illustrates in red circles some key structural aspects of the three main GPCR families (A, B, C). Figure adapted from 16

Family A that comprises the rhodopsin/β2 adrenergic receptor-like receptors, contains 90% of all GPCRs and is by far the largest and the most studied. Family A includes, among others, aminergic receptors (muscarinergic, dopaminergic, histaminergic, serotonergic and adrenergic receptors), peptides, and rhodopsin, as well as the large subfamily of olfactory receptors. The overall homology among all type A receptors is low and restricted to a number of highly conserved key residues. The high degree of conservation among these key residues suggests that they play an essential role in the structural or functional integrity of the receptors. The only residue consistently present among all family A receptors is arginine,

found in the Asp-Arg-Tyr (DRY) motif located on the cytoplasmic side of TM-3, which is believed to be involved in G-protein activation [12] . However, other fingerprint elements such as the conserved NsxxNPxxY motif are also clearly associated with the rhodopsin family. In addition, six different groups of receptors have been further classified within this subfamily with regard to their phylogeny .

Family B receptors include approximately 25 different receptors for a variety of peptide hormones and neuropeptides, such as vasoactive intestinal peptide, calcitonin, PTH, and glucagon. Except for the disulfide bridge connecting the first (ECL 1) and second extracellular loops (ECL 2), family B receptors do not contain any of the structural features characterizing family A receptors. Notably, the important DRY motif is absent in family B receptors. The most prominent characteristic of family B receptors is a large extracellular amino terminus containing several cysteines, presumably forming a network of disulfide bridges.

An exceptionally long amino terminus characterizes Family C receptors. This family includes the metabotropic glutamate, the γ-aminobutyric acid (GABA), the calcium, the vomeronasal, the mammalian pheromone receptors, and the recently identified putative taste receptors. Family C include a short and highly conserved intracellular loop 3 (3ILoop), a relatively long C-terminal tail, and an exceptionally long N-terminal tail, which is shaped like a Venus-fly trap to facilitate ligand binding. This region shares a low but significant sequence similarity to bacterial periplasmic binding proteins (PBPs) and is considered the glutamate binding site equivalent to the known amino acid binding site of PBPs [13]. As with subfamilies A and B, subfamily C receptors contain two putative disulfide-forming cysteines in extracellular loops 1 and 2 (ECL 1 and 2). Otherwise, they do not share any conserved residues with subfamily A or B receptors.

The A-F sub-classification of the GPCR superfamily is widely accepted. However, Fredriksson et al. performed the first phylogenetic study of the entire superfamily of GPCRs (comprising about 2% of the genes in the human genome) and proposed a different, more accurate classification [14]. Their analysis showed that there are five main subfamilies of human GPCRs, and that they share a common

evolutionary origin within each subfamily: glutamate, rhodopsin, adhesion, frizzled/taste2, and secretin otherwise known as the GRAFS classification, based on the initials of each of the subfamily names. Three of these subfamilies, the rhodopsin (A), secretin (B), and glutamate (C) families, correspond to the A-F clan system, whereas the two other families, adhesion and frizzled, were not included in the clan system [15]. The rhodopsin receptors make up the largest family, divided into four main groups with 13 distinct branches.

## GPCR signalling

GPCRs share a seven-transmembrane $\alpha$-helical domain topology and coupling to heterotrimeric G-proteins ($G_{\alpha\beta\gamma}$). GPCRs mediate the effect of numerous ligands. Binding of those extracellular ligands initiates the signal transduction cascade. This is supposed to trigger conformational changes in the receptor that promotes subsequent nucleotide exchange by the $G_{\alpha}$ subunit. Following GDP replacement by GTP, the tightly associated $G_{\alpha}$ and $G_{\beta\gamma}$ subunits dissociate from each other and from the receptor. Both components are then free to interact with downstream elements of the signalling cascades such as adenylate cyclase or ion channels and to modulate their activity. Signal transduction is tightly regulated by receptor phosphorylation and subsequent interaction with arrestins as well as by interplay of G-protein subunits with "regulators of G-protein signalling" (RGS). Tremendous progress has been accomplished within the last few years in dissecting GPCR mediated signal transduction pathways, but the molecular mechanisms underlying ligand recognition and signal transduction through the membrane are restrained by the lack of receptor structures at high resolution.

## Regulation of GPCR signalling and desensitization

Desensitization means a weakening of the signal transmission under conditions of a long-lasting stimulation by ligands. Despite the persistent effect of extracellular stimuli, the signal is no longer passed into the cell interior, or only in a weakened form, during desensitizing conditions. Receptor desensitization is achieved by three mechanisms that are different in their time courses; (1) uncoupling between the

receptor and the G protein (~ 2-3 min), (2) reversible decrease in the number of cell surface receptors by internalization (~10-30 min), and (3) down-regulation of the GPCR transcription (~2-3 h) [16]. For mAChRs and most other GPCRs, agonist-induced phosphorylation of the receptor facilitates receptor internalization. Receptor phosphorylation is mediated by kinases, including G protein receptor kinases (GRKs), casein kinase 1α (CK1α), and diacylglycerol-regulated protein kinase C (PKC) [17]. PKC, phosphorylated in an agonist-independent and Gβγ-independent manner both *in vitro* and *in vivo* alike, has been shown for $M_1$R and $M_3$R. Once they are phosphorylated by GRKs, mAChRs bind β-arrestin, and can then interact with clathrin, the major structural component of the clathrin based endocytic machinery [18]. Phosphorylated and β-arrestin bound receptors are then internalized within clathrin-coated vesicles. The budding of clathrin-coated vesicles from the plasma membrane is regulated by dynamin GTPases, which are also activated by β-arrestin *via* the action of c-Src. In the GTP-bound form, dynamin is thought to form a collar at the neck of the clathrin coated pit and to catalyze the fission of the vesicles [19]. In many cells, exposure to muscarinic agonists induces rapid desensitization and internalization of the cell surface mAChRs that is followed by a loss of total number of cellular receptors in the following hours. This process, also termed down-regulation, can only be overcome by *de novo* receptor synthesis. This process requires an intact cytoskeleton, as demonstrated by the inhibitory effect of colchicines, on agonist-induced mAChR down-regulation [20]. Until now, only a few domains in $M_1$R and $M_3$R have been involved in modulating mAChR down-regulation.

## Constitutive activity of GPCRs

The ability of G protein coupled receptors (GPCR) to activate their cognate G-proteins in the absence of an agonist is termed ‘constitutive’ receptor activity [21] and it depends on the concentration and expression level of the free activated receptor. The discovery of constitutive active GPCRs was accompanied by the finding that certain ligands formerly known as antagonists were actually able to inhibit the constitutive receptor activity. In contrast to agonist, these ligands posses a negative intrinsic activity and are now known as inverse agonists [22]. One of the

most powerful tools used by researchers in this area has been the discovery of specific mutations which enhance the agonist independent activity, namely, constitutive active mutant receptors (CAM) [23]. The concept of constitutive activity has now been firmly established and has been shown to occur for over 60 GPCRs. Constitutive active GPCRS may be the cause of several diseases, such as male precocious puberty, dwarfism, Kaposi's sarcoma and congenital night blindness. The detection of constitutive activity also had implications for the ternary model describing receptor activation.

The two state model portrayed only the binding of an agonist (A) to the receptor (R), causing the activation of the formed complex (AR). The ternary model also took the G-protein (G) coupling into account, which would coupled to the activated AR complex ($AR^*$), forming the ternary $AR^*G$ complex. Constitutive activity demanded an extension of this ternary model. Allowing for receptors to be activated and bind G proteins in the absence of agonist. An even more complex, but thermodynamically more complete is the cubic ternary model [24] (Fig. 5). This model also allows for the formation of a non-signalling complex between the inactive receptor and the G-protein. Monczor and co-workers found evidences to support the cubic ternary complex, using the $H_2$ inverse agonist tiotidine [25]. The discovery that GPCRs can for oligomeric structures, which exhibit different affinities for certain G-proteins, will undoubtedly result in models with even higher levels of complexity. An example of such a model has been described by Durrox [26].

In the case of the mAChRs, a number of studies have identified constitutively activating mutations, particularly in the predominantly Gq/11- coupled $M_1R$, $M_3R$, and $M_5R$ subtypes [27]. Spalding et al., 1997 first identified that mutation of adjacent serine (Ser465) and threonine (Thr466) residues at the junction between TM VI and the third extracellular loop results in a CAM-$M_5R$ [28]. The serine residue conserved in $M_1R$ and $M_5R$ and the equivalent asparagine residue corresponding to $M_3R$, $M_2R$ and $M_4R$ are thus implicated in constraining the receptor to inactive state. The mutant receptors displayed many of the characteristic properties of CAM-GPCRs, including enhanced agonist affinity and potency, in

addition to an elevated basal functional activity (proportional to the receptor expression level), which was sensitive to the inverse agonist atropine [29].

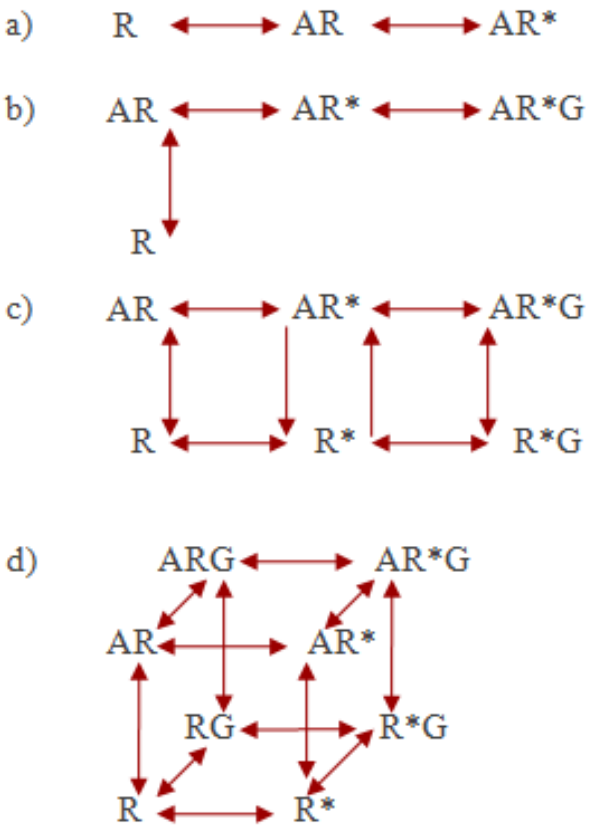


**Figure 5.** Models describing GPCR system. The traditional model merely describes the binding of agonist (A) to the receptor (R) and subsequent activation of this complex (AR). The ternary complex introduces the G-protein (G) as a third partner, which can interact with the activated agonist-receptor complex (AR*). The ternary complex was extended after the discovery of ligand-independent activation of the receptor, allowing for the formation of R*G. The cubic ternary complex makes up a thermodynamically more complete model. Figure adapted from 27.

## Heterologous expression of G-protein-coupled receptors

Structural characterization of a protein may be achieved using different biophysical and biochemical approaches which require protein amounts ranging from a few micrograms up to several milligrams per assay. Rhodopsin excepted, the low abundance of GPCRs often precludes such methods of investigation. In the past decade, heterologous organisms were used increasingly for protein production. The priority was often set upon achievement of high expression levels and production systems were chosen according to easiness of scaling up. Nevertheless functional as well as structural studies require that recombinant proteins exhibit characteristics indistinguishable from the native ones. Moreover the functional behaviour of a GPCR is strongly dependent upon cell type and receptor density: for instance the presence and relative concentrations of signal transduction elements may drastically affect ligand and G-protein binding properties. All these parameters ought to be taken into account when addressing pharmacological properties such as ligand affinity or when depicting the relations taking place between signal transduction key elements.

Over the last years several methods have been described to overexpress GPCRs [30,31]. Heterologous expression has been evaluated in several different expression systems including bacterial, yeast, insect and mammalian, but with varying degree of success because of differences in the host cell environment [32]. Among bacteria *E. coli* is a popular organism for heterologous expression. It is often described as an easy way to produce large amounts of eukaryotic proteins, mainly because of its facility of use and its cost-effectiveness. Interestingly, the baculovirus-infected system can be used for production of multimeric proteins, up to 4 genes can be introduced in a single viral recombinant. Protocols are well established, most tools are commercially available and companies are still improving the system's simplicity and flexibility. Great attention is also given to speed up the generation of recombinant viruses and the constitution of large viral stocks to infect insect cells. Baculovirus-infected insect cells have proven very efficient for membrane protein production and successful overexpression of several GPCRs. Insect cells perform the same post-translational modifications as

mammalian cells with the exception of N-glycosylations, which remain often more simple and are of the high-mannose type.

Expression of GPCRs in non-mammalian cells suffers from the lack of post-translational modifications, such as N-glycosylation, fatty acid acylation, phosphorylation some of which are known to be of critical relevance for optimal protein function [33]. The lipidic composition of bacterial membranes is different from the eukaryotic cell membrane, for instance no cholesterol is present in the bacterial inner membrane possibly altering GPCR properties. Overexpression of heterologous proteins may also lead to the formation of cytoplasmic inclusion bodies, high-density bodies of almost pure but misfolded protein, resistant to proteolysis and easy to isolate. Yet these seductive aspects are usually outbalanced by one major inconvenience: the necessity of refolding the protein, an arduous process with uncertain outcome. Other *E. coli* properties may hinder heterologous protein expression too such as the low percentage of GC in the genome when compared to mammalian genes or the existence of rare codons. The availability of different tRNAs may be another limiting factor especially if clusters of rare codons are located close to the protein N-terminus possibly generating frameshifts. Such side-products could hamper structural studies for which homogeneity of the protein is critical.

Among heterologous expression systems, mammalian cells offer to GPCRs the closest alternative to their native environment. Therefore they are widely used for functional studies especially when post-translational modifications such as N-glycosylation or proteolytic processing are a prerequisite to function. However, differences in post-translational processing may be observed depending on the cell line. Moreover, the type of cell may affect functional studies by presenting a different G-protein content to the heterologous protein pointing out the crucial importance of the host cell when investigating signalling properties. Heterologous protein production may be achieved through transient or stable expression. In both cases, intrinsic characteristics of the protein as well as mRNA stability seem to influence expression levels.

## Post-translational modifications of GPCRs

Post-translational modifications (PTMs) add an additional level of complexity to topographical organization of GPCRs. The N-glycosylation of GPCRs, usually on one or more asparagine residues, was elucidated very early in the characterization of these receptors (for reviews, see [34,35]. However, O-glycosylation has been recently documented for some GPCRs. In addition to glycosylation, GPCRs are also extensively phosphorylated by several kinases. The sites of phosphorylation have been mapped mainly to the carboxyl tail and the third intracellular loop, and have been linked to regulatory processes, such as desensitization and internalization (for review, see [16]. In addition to these well-characterized modifications, GPCRs are subject to covalent modification with the fatty acid palmitate [36].

N-linked glycosylation is the most common PTMs of GPCRs with approximately 70-90% of occurrence in the consensus sequences. N-glycosylation has been shown to enhance protein thermal stability and to facilitate folding kinetics may play important roles in receptor expression, structure and/or function. Increasing amounts of evidence support that core N-glycan contributes not only to receptor folding, but also to the cell surface transport [37-40]. Analysis by SDS-PAGE, disruption of N-glycosylation by site-direct mutagenesis, prevention of N-glycan add by tunicamycin, removal of the glycan by glycosidases (N-glycosidase F, endoglycosidase H, neuraminidase, O-glycosidase) constitutes tools for establishing that a consensus sequence for N-glycosylation site is actually modified (see, review [35].

Protein palmitoylation is an important post-translational lipid modification in which a 16-carbon palmitate group is attached to a cysteine residue of specific proteins via a thioester bond. Similar to other lipid modifications, such as myristoylation and isoprenylation, palmitoylation increases the hydrophobicity of a protein and promotes association of these proteins with specific membranes [36]. Palmitoylation facilitates the localization of proteins to the plasma membrane, and more particularly to microdomains called lipid rafts or caveolae within the plasma

membrane [41]. Compared with other stable lipid modifications, palmitoylation is a reversible lipid modification under the control of two types of enzyme[36]: (i) palmitoyl-acyl transferases (PATs) that catalyse the attachment of palmitate to proteins and (ii) thioesterases that cleave the palmitate from proteins (Figure 6). Although palmitate cleavage has been well characterized through the identification, purification and cloning of several thioesterases, the mechanism and enzymic properties of the palmitoylation reaction remain relatively unstudied, due to the lack of success in purifying and cloning PATs.

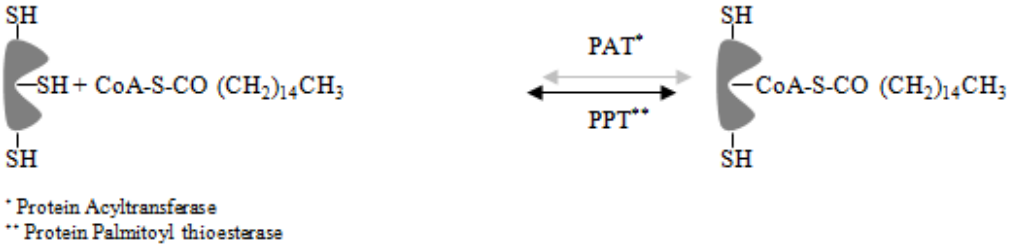


**Figure 6.** Protein palmitoylation is dynamic. Specific enzymes (PATs), which have recently been discovered to be a family of proteins known as DHHC proteins, catalyze the addition of palmitate to cysteine residues via a thioester bond. A different set of enzymes (PPTs) remove palmitate from proteins. Figure adaptated from [42].

By far the most commonly used assay for protein palmitoylation has been metabolic labeling of cultured cells with radiolabeled palmitate ($^{3}$H-palmitate, $^{125}$I-palmitate). The labeled palmitate is added to the culture medium, taken up by the cells and metabolically incorporated into protein palmitoylation sites. The labeled proteins are usually purified and analyzed on sodium dodecyl sulfate polyacrylamide **(**SDS-PAGE). $^{3}$H-palmitate is the most widely used form of radiolabeled palmitate [42]. Enzyme-mediated *in vitro* palmitoylation has recently been performed using purified and partially purified DHHC PATs discovered first in yeast and later in mammals [43]. *In vitro* palmitoylation using DHHC palmitoyl-transferases is likely to become a method of choice to assay protein palmitoylation.

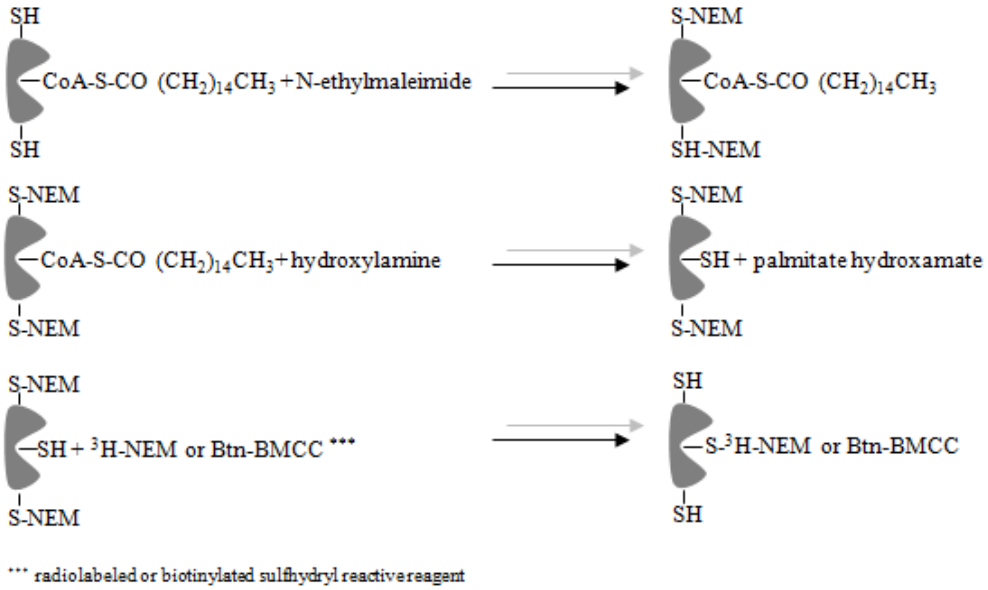


**Figure 7.** Fatty acyl exchange assays of protein palmitoylation. These methods are based on the ability to specifically remove palmitate from proteins with hydroxylamine treatment resulting in free sulfhydryl groups at the palmitoylation sites. Prior to hydroxylamine treatment, any preexisting free sulfhydryl group is blocked with NEM. Unlike thioester bonds, the covalent attachment of NEM to a cysteine side groups is not sensitive to hydroxylamine. The free sulfhydryls generated by hydroxylamine treatment are then reacted with an appropriate alkylating reagent such as $^{3}$H-NEM or btn-BMCC to label the sites. Figure Adapted from [42].

However, fatty acyl exchange chemistry is an important new alternative to study the palmitoylation on the GPCRs. The general methodology is diagrammed in Figure 7. In the first step, all pre-existing, free sulfhydryl groups are blocked by incubation with *N*-ethylmaleimide (NEM). In the second step, the fatty acyl group is removed using hydroxylamine to specifically cleave the thioester bond that covalently attaches the fatty acyl group to the cysteine residue at the palmitoylation site. The hydroxylamine cleavage leaves the cysteine residue with a free sulfhydryl group. The third step, is to label the newly created free sulfhydryl group with thiol-specific reagents. A highly sensitive and quantitative assay for protein palmitoylation can be performed by using $^{3}$H-NEM to label cysteines in the last step of the fatty acyl exchange method. Alternatively, non-radioactive sulfhydryl-

specific compounds containing biotin (btn), such as btn-BMCC (Fig. 7), btn-PEO-maleimide or btn-PEO-iodoacetamide can be used to specifically label the free sulfhydryls on cysteine residues at the palmitoylation sites.

### 1.2 Muscarinic Receptor Family

Acetylcholine (ACh) is a major neurotransmitter in the central and peripheral nervous systems. The many important physiological actions of ACh are initiated by its binding to two distinct classes of plasma membrane receptors: the nicotinic (nAChRs) and muscarinic ACh receptors (mAChRs). Whereas nAChRs function as ACh-gated cation channels, mAChRs are prototypical members of the superfamily of GPCRs. Within these two classes of receptors, a large amount of heterogeneity has been discovered that further complicates the assignment of specific physiological functions. Five genes ($M_1R$-$M_5R$) encode mAChRs proteins. The muscarinic receptor family has been classified as a member of biogenic amine receptor group inside the rhodopsin/adrenergic-like receptors family or class A in the GPCRs superfamily classification system [44].

Based on their ability to activate different classes of heterotrimeric G proteins, the five mAChR subtypes can be subdivided into two major functional classes. The $M_2$ and $M_4$ receptors show selectivity for G proteins of the $G_i$ family, whereas the $M_1$, $M_3$, and $M_5$ receptors selectively couple to G proteins of the $G_q$ class [45] (Figure 8). $M_2R$ and $M_4R$ are coupled primarily to to the Gi/o class of G proteins, and inhibit adenylyl cyclase activity. The activation of αGi inhibits adenylyl cyclase (AC) which primarily decreases the cellular cAMP level. The βγ subunits activate fast inward rectifier potassium channels and inhibit voltage sensitive calcium channels. Pertussis toxin treatment, which blocks Gi/Go function, increases the likelihood of Gs and muscarinic receptor interaction suggesting that G-protein stoichiometry within the cell plays a key role in directing the signalling potential of each receptor. $M_2R$ and $M_4R$ stimulate phospholipase C in some cell lines that is thought to be mediated, in part, by βγ-subunits released following heterotrimeric G-protein activation. A novel signalling pathway involving the activation of phospholipase $A_2$ by Gi-coupled receptors, including $M_2R$ and $M_4R$ is stimulated

when phospholipase $A_2$ is preactivated either directly or with calcium-mobilizing agonists. In this study, $M_2R$ and $M_4R$ augmented purinergic receptor-stimulated phospholipase $A_2$ activation [49]. This may be physiologically relevant since the purinergic receptor agonist, ATP, is co-released with many neurotransmitters, including Ach, and may serve to prime arachidonic acid mobilizing other signal transduction pathways.

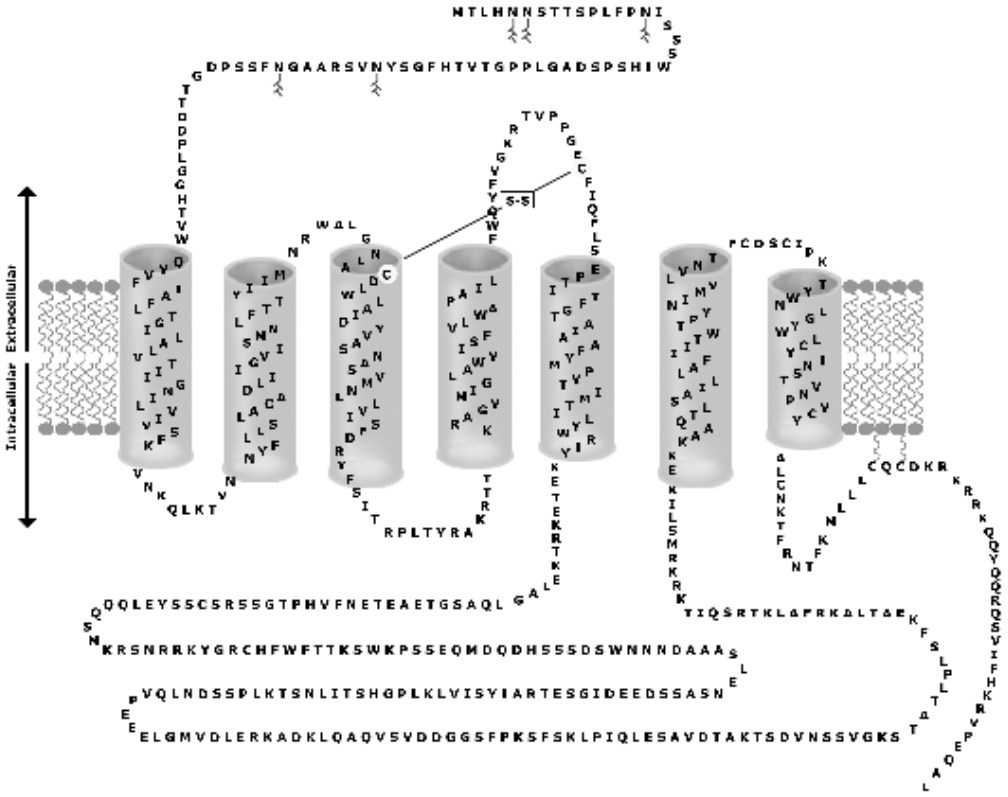


**Figure 8** Amino acid sequence and secondary structure model of human $M_3R$. The residues crucial for the binding to ACh, shown , are found within the TM regions. Cysteine residues, in the 1Eloop and 2Eloop, form a disulphide bridge that is shown as a solid line. The most conserved motifs (DRY and NPxxY) are represented. Predicted N-glycosylation sites are shown in the N-terminal tail. Palmitoylation of two conserved cysteines in the C-terminal tail is also highlight. Adapted from [46].

$M_1R$, $M_3R$ and $M_5R$ mAChR subtypes activate primarily the Gq/G11 class of G-proteins stimulating phospholipase Cβ isoforms to break down inositol 4,5 bisphosphate (PIP2). Upon agonist binding to the receptor, the latter undergoes a conformational change exposing a high affinity binding site for the G-protein heterotrimer which has GDP bound in an inactive state. Once the G protein binds to the receptor, the GDP is released leaving an empty space for the nucleotide GTP, which exists at a higher intracellular concentration than GDP, to bind. This exchange of GDP for GTP induces a conformational change causing dissociation of Gα from the Gβγ dimer. The Gβ and Gγ subunits remain tightly associated and anchored to the lipid bilayer. Gα, with GTP bound, activates phospholipase C (PLC) which promotes the hydrolysis of phosphatidylinositol 4,5-biphosphate (PIP2) into the intracellular messengers 1,2- diacylglycerol (DAG) and inositol 1,4,5-triphosphate (IP3). DAG remains bound to the membrane and activates protein kinase C (PKC) leading to effects including modulating slow potassium and calcium conductances. PKC also phosphorylates several mitogen-activated protein kinases (MAPKs), like ERK-1 and ERK-2, and activating various gene transcription factors involved in promoting smooth muscle growth. This activation appears to be dependent on PKC, although a PKC-independent pathway has been proposed involving phosphorylation on sites in the third intracellular loop of the $M_3R$ by casein kinase 1α (CK1α) [47]. The other product of PIP2 hydrolysis, IP3, translocates and binds to IP3 receptors locatedin the sarcoplasmic calcium stores. When IP3 receptors are activated they release $Ca^{2+}$ into the cytosol by opening $Ca^{2+}$ channels. Intracellular calcium stores are the major source of $Ca^{2+}$ for muscle contraction although influx from calcium channel receptors in the membrane can also contribute.

In addition to their ability to stimulate phospholipase C through Gq, $M_1R$, $M_3R$ and $M_5R$ have also been shown to stimulate phospholipase A2 and phospholipase D in various cell lines and primary cultured cells. Phospholipase $A_2$ or D activation has a common requirement for extracellular calcium. A cation channel mediating muscarinic receptor-dependent calcium influx has been initially characterized and may provide the regulatory step essential for phospholipase activation. These studies showed that the muscarinic receptor-operated calcium channel is voltage-

independent, has a low conductance, and in the cell lines studied may be under the regulation of a small-molecular-weight G protein. Expression studies with a mammalian homologue of the Drosophila Trp/Trpl cation channels indicated that the Trp6 channel was under the regulation of the $M_5$ receptor. Receptor-operated calcium channels may be a key signalling pathway for other calcium-mobilizing receptors. Additional signal transduction activation has been associated with $M_1R$, $M_3R$ and $M_5R$ including the inefficient stimulation of adenylate cyclase through both Gs and G protein-independent pathways.

## Physiological roles and functions of muscarinic receptor subtypes

During the past two decades, numerous studies have explored the roles of specific mAChR subtypes ($M_1-M_5$) in mediating the diverse physiological actions of ACh. Such knowledge is considered essential for the development of novel therapeutic approaches aimed at inhibiting or enhancing signalling through specific mAChR subtypes. However, the task of assigning specific physiological functions to distinct mAChR subtypes has proven very challenging, primarily owing to the lack of muscarinic agonists and antagonists that show a high degree of subtype selectivity for the individual mAChR subtypes. Another complicating factor is that most organs, tissues, or cell types express multiple mAChRs. These factors have led to conflicting reports regarding the potential physiological and pathophysiological roles of specific mAChR subtypes, particularly as far as the central muscarinic actions of ACh are concerned. Several studies indicate that disruption of one specific mAChR gene does not seem to have major effects on the expression levels of the remaining four mAChRs, at least not in the limited number of tissues that have been studied so far. This observation suggests that it is unlikely that compensatory changes in mAChR expression levels have a major impact on the outcome of mouse phenotyping studies.

**$M_1R$.** The $M_1R$ receptor gene was the first gene encoding for a mAChR that was ablated in mice, founding predominantly in all the major regions of the forebrain, particularly the cerebral cortex, hippocampus and the corpus striatum and are the most abundantly expressed subtype in those regions. At these locations, $M_1R$ is

involved in higher cognitive processes such as learning and memory. $M_1R$ mediates most of the ACh-stimulated PIP2 breakdown and MAP kinase activation in the hippocampus and cerebral cortex and activate ion channels underlying prolonged oscillations in the hippocampus [48, 49].

**$M_2R$.** This receptor subtype is expressed throughout the central nervous system and in the periphery, especially in smooth muscle and tissues of the heart. In the heart, $M_2R$ is involved in the regulation of the force and rate of heart beating. Stimulation of the parasympathetic nervous system releases ACh from vagal nerve endings, which binds to $M_2R$ in the sinoatrial node, reducing heart beat frequency. $M_2R$ appears to be solely responsible for these regulatory effects despite the presence of the other mAChR subtypes in heart cardiac muscle. In $M_2R$-deficient mice, oxotremorine-mediated antinociceptive response was greatly attenuated in both tail-flick and hot plate tests, suggesting that $M_2R$ plays a crucial role in muscarinic agonist-induced analgesia. On the other hand, electrophysiological examination demonstrated that the mAChR-dependent inhibition of the neuronal calcium channel was abolished in sympathetic ganglion neurons from $M_2R$-deficient mice. Carbachol, induced bradycardia in spontaneously beating sinoatrial node cells and atria; an effect that was completely abolished in $M_2R$ deficient mice, indicating that $M_2R$ is responsible for cholinergic deceleration of the beating heart. In $M_2R$ knockout mice, the carbachol-mediated contraction of a smooth muscle preparation slightly attenuated [48, 49].

**$M_3R$.** Receptors are broadly expressed in the brain, although the expression level is not high when compared to other receptor subtypes. A striking feature of $M_3R$ observed was significant loss of body mass accompanied by reductions in serum leptin and insulin levels as a result of reduced food intake. Expressed at relatively high levels in the hypothalamus, $M_3R$ may be responsible, in part, for the regulation of appetite. At present little is known about the central physiological roles of $M_3R$. In the periphery, it is located in organs and tissues that are innervated by the parasympathetic nervous system. They play a key role in actions associated with glandular function and regulation of smooth muscle contraction. They have been found in salivary glands mediating primarily the stimulation of salivation and

in the airway smooth muscle producing its contraction. $M_3R$ is also involved in the parasympathetic control of pupillary sphincter muscle contractility. *In vitro* pharmacological studies using different isolated smooth muscle preparations (urinary bladder, ileum, stomach fundus, trachea and gall bladder) have shown the predominant role of $M_3R$ in ACh-mediated regulation of the contraction of these smooth muscle tissues. This $M_3R$ smooth muscle mediation is especially important in the bladder, where enhanced urinary retention is present in $M_3R$-deficient mice, suggesting this subtype is critical to urinary bladder voiding [48, 49].

**$M_4R$.** This receptor is known to be abundantly expressed in the striatum and is believed to regulate striatal dopamine release through action on the cell bodies of striatal GABAergic projection neurons. $M_4R$-deficient mice showed significant increases in basal locomotor activity. This may also be caused by an increase in dopamine release from the striatum, as administration of a dopamine $D_1$ receptor agonist enhanced the locomotor activity. This highlights the fact that functional interactions between the cholinergic and dopaminergic pathways are important for striatal function and its control is relevant to the treatment of Parkinson's disease [48, 49].

**$M_5R$.** This receptor was the last mAChR cloned, it is found in both neuronal and non-neuronal cells and it is expressed at low levels. Localization studies have revealed that $M_5R$ is abundantly expressed in dopamine-containing neurons of the *substantia nigra par compacta*, an area of the midbrain providing dopaminergic innervation to the striatum. Until recently, little was known about their physiological functions. The discovery of $M_5R$ receptors in peripheral and cerebral blood vessel endothelium, has led to the proposal of $M_5R$ as being able to mediate Ach-induced dilation of arteries and arterioles. $M_5R$ knockout mice have been shown to change drug seeking behaviours where effects of morphine and opioids were significantly reduced. The expression of $M_5R$ in the *substantia nigra* and the *nucleus accumbens* is consistent with their role as modulators of dopamine release in the mid-brain and their involvement in the rewarding effects of drug abuse. However, the complex neuronal pathways that are regulated by these modulatory effects remain to be discovered [48, 49].

## 1.3 Aims of the study

The human $M_3$ muscarinic acetylcholine receptor ($M_3R$) regulates many important functions of the central and peripheral nervous system, representing an attractive potential pharmacological target for intervention. Considering that under physiological conditions the expression of $M_3R$ is relatively low, optimization of the receptor overexpression is a pre-requisite for structural studies efforts can be performed. In addition, although is has well established that G protein-coupled receptors (GPCRs) undergo post-translational, increased evidence supports that these modifications have tight links to receptor physiological roles. In spite of this, little progress has been made in the detailed study of post-translational modifications in some specific GPCRs, like in the case of $M_3R$.

**The overall aim of this thesis was to gain new insights into molecular aspects of overexpression/purification and post-translational modifications of the $M_3$ muscarinic receptor and its relationship to the receptor structure and function.**

Specifically, the present work is focused on:

1. Improving $M_3R$ heterologous overproduction in mammalian cells by keeping proper post-translational modifications.
2. Obtaining a purified $M_3R$, by means of affinity purifications methods, while keeping its full wild-type biological functionality.
3. Describing N-glycoylation sites of $M_3R$, expressed in COS-7 cells, as well as determining the role of these N-glycan chains on $M_3R$ structure and function.
4. Unveiling the occurrence and role(s) of palmitoylation at the C-terminal domain of $M_3R$ expressed in COS-7 cells.

## References


[1] Perez, D.M. (2003). The evolutionarily triumphant G-protein-coupled receptor. Mol Pharmacol 63, 1202-5.

[2] Kristiansen, K. (2004). Molecular mechanisms of ligand binding, signaling, and regulation within the superfamily of G-protein-coupled receptors: molecular modeling and mutagenesis approaches to receptor structure and function. Pharmacol Ther 103, 21-80.

[3] Palczewski, K. et al. (2000). Crystal structure of rhodopsin: A G protein-coupled receptor. Science 289, 739-45.

[4] Rosenbaum, D.M. et al. (2007). GPCR engineering yields high-resolution structural insights into beta2-adrenergic receptor function. Science 318, 1266-73.

[5] Hill, S.J. (2006). G-protein-coupled receptors: past, present and future. Br J Pharmacol 147 Suppl 1, S27-37.

[6] Ma, P. and Zemmel, R. (2002). Value of novelty? Nat Rev Drug Discov 1, 571-2.

[7] Klabunde, T. and Hessler, G. (2002). Drug design strategies for targeting G-protein-coupled receptors. Chembiochem 3, 928-44.

[8] Gether, U. (2000). Uncovering molecular mechanisms involved in activation of G protein-coupled receptors. Endocr Rev 21, 90-113.

[9] Strosberg, A.D. and Nahmias, C. (2007). G-protein-coupled receptor signalling through protein networks. Biochem Soc Trans 35, 23-7.

[10] Mailman, R.B. (2007). GPCR functional selectivity has therapeutic impact. Trends Pharmacol Sci 28, 390-6.

[11] Flower, D.R. (1999). Modelling G-protein-coupled receptors for drug design. Biochim Biophys Acta 1422, 207-34.

[12] Probst, W.C., Snyder, L.A., Schuster, D.I., Brosius, J. and Sealfon, S.C. (1992). Sequence alignment of the G-protein coupled receptor superfamily. DNA Cell Biol 11, 1-20.

[13] Conn, P.J. and Pin, J.P. (1997). Pharmacology and functions of metabotropic glutamate receptors. Annu Rev Pharmacol Toxicol 37, 205-37.

[14] Fredriksson, R., Lagerstrom, M.C., Lundin, L.G. and Schioth, H.B. (2003). The G-protein-coupled receptors in the human genome form five main families. Phylogenetic analysis, paralogon groups, and fingerprints. Mol Pharmacol 63, 1256-72.

[15] Attwood, T.K. and Findlay, J.B. (1994). Fingerprinting G-protein-coupled receptors. Protein Eng 7, 195-203.

[16] van Koppen, C.J. and Kaiser, B. (2003). Regulation of muscarinic acetylcholine receptor signaling. Pharmacol Ther 98, 197-220.

[17] Budd, D.C., McDonald, J.E. and Tobin, A.B. (2000). Phosphorylation and regulation of a Gq/11-coupled receptor by casein kinase 1alpha. J Biol Chem 275, 19667-75.

[18] Krupnick, J.G., Santini, F., Gagnon, A.W., Keen, J.H. and Benovic, J.L. (1997). Modulation of the arrestin-clathrin interaction in cells. Characterization of beta-arrestin dominant-negative mutants. J Biol Chem 272, 32507-12.

[19] Takei, K. and Haucke, V. (2001). Clathrin-mediated endocytosis: membrane factors pull the trigger. Trends Cell Biol 11, 385-91.

[20] Maloteaux, J.M. and Hermans, E. (1994). Agonist-induced muscarinic cholinergic receptor internalization, recycling and degradation in cultured neuronal cells. Cellular mechanisms and role in desensitization. Biochem Pharmacol 47, 77-88.

[21] Costa, T. and Herz, A. (1989). Antagonists with negative intrinsic activity at delta opioid receptors coupled to GTP-binding proteins. Proc Natl Acad Sci U S A 86, 7321-5.

[22] Bond, R.A. and Ijzerman, A.P. (2006). Recent developments in constitutive receptor activity and inverse agonism, and their potential for GPCR drug discovery. Trends Pharmacol Sci 27, 92-6.

[23] Seifert, R. and Wenzel-Seifert, K. (2002). Constitutive activity of G-protein-coupled receptors: cause of disease and common property of wild-type receptors. Naunyn Schmiedebergs Arch Pharmacol 366, 381-416.

[24] Kenakin, T. (2002). Drug efficacy at G protein-coupled receptors. Annu Rev Pharmacol Toxicol 42, 349-79.

[25] Monczor, F., Fernandez, N., Legnazzi, B.L., Riveiro, M.E., Baldi, A., Shayo, C. and Davio, C. (2003). Tiotidine, a histamine H2 receptor inverse agonist that binds with high affinity to an inactive G-protein-coupled form of the receptor. Experimental support for the cubic ternary complex model. Mol Pharmacol 64, 512-20.

[26] Durroux, T. (2005). Principles: a model for the allosteric interactions between ligand binding sites within a dimeric GPCR. Trends Pharmacol Sci 26, 376-84.

[27] Dowling, M.R., Willets, J.M., Budd, D.C., Charlton, S.J., Nahorski, S.R. and Challiss, R.A. (2006). A single point mutation (N514Y) in the human M3 muscarinic acetylcholine receptor reveals differences in the properties of antagonists: evidence for differential inverse agonism. J Pharmacol Exp Ther 317, 1134-42.

[28] Spalding, T.A., Burstein, E.S., Wells, J.W. and Brann, M.R. (1997). Constitutive activation of the m5 muscarinic receptor by a series of mutations at the extracellular end of transmembrane 6. Biochemistry 36, 10109-16.

[29] Ford, D.J., Essex, A., Spalding, T.A., Burstein, E.S. and Ellis, J. (2002). Homologous mutations near the junction of the sixth transmembrane domain and the third extracellular loop lead to constitutive activity and enhanced agonist affinity at all muscarinic receptor subtypes. J Pharmacol Exp Ther 300, 810-7.

[30] Hassaine, G. et al. (2006). Semliki Forest virus vectors for overexpression of 101 G protein-coupled receptors in mammalian host cells. Protein Expr Purif 45, 343-51.

[31] Sarramegna, V., Talmont, F., Demange, P. and Milon, A. (2003). Heterologous expression of G-protein-coupled receptors: comparison of expression systems fron the standpoint of large-scale production and purification. Cell Mol Life Sci 60, 1529-46.

[32] Tate, C.G. and Grisshammer, R. (1996). Heterologous expression of G-protein-coupled receptors. Trends Biotechnol 14, 426-30.

[33] Massotte, D. (2003). G protein-coupled receptor overexpression with the baculovirus-insect cell system: a tool for structural and functional studies. Biochim Biophys Acta 1610, 77-89.

[34] Shental-Bechor, D. and Levy, Y. (2009). Folding of glycoproteins: toward understanding the biophysics of the glycosylation code. Curr Opin Struct Biol 19, 524-33.
[35] Wheatley, M. and Hawtin, S.R. (1999). Glycosylation of G-protein-coupled receptors for hormones central to normal reproductive functioning: its occurrence and role. Hum Reprod Update 5, 356-64.
[36] Qanbar, R. and Bouvier, M. (2003). Role of palmitoylation/depalmitoylation reactions in G-protein-coupled receptor function. Pharmacol Ther 97, 1-33.
[37] Duvernay, M.T., Filipeanu, C.M. and Wu, G. (2005). The regulatory mechanisms of export trafficking of G protein-coupled receptors. Cell Signal 17, 1457-65.
[38] Markkanen, P.M. and Petaja-Repo, U.E. (2008). N-glycan-mediated quality control in the endoplasmic reticulum is required for the expression of correctly folded delta-opioid receptors at the cell surface. J Biol Chem 283, 29086-98.
[39] Roy, S., Perron, B. and Gallo-Payet, N. Role of asparagine-linked glycosylation in cell surface expression and function of the human adrenocorticotropin receptor (melanocortin 2 receptor) in 293/FRT cells. Endocrinology 151, 660-70.
[40] Lanctot, P.M., Leclerc, P.C., Escher, E., Guillemette, G. and Leduc, R. (2006). Role of N-glycan-dependent quality control in the cell-surface expression of the AT1 receptor. Biochem Biophys Res Commun 340, 395-402.
[41] Renner, U. et al. (2007). Localization of the mouse 5-hydroxytryptamine(1A) receptor in lipid microdomains depends on its palmitoylation and is involved in receptor-mediated signaling. Mol Pharmacol 72, 502-13.
[42] Drisdel, R.C., Alexander, J.K., Sayeed, A. and Green, W.N. (2006). Assays of protein palmitoylation. Methods 40, 127-34.
[43] Fukata, Y., Bredt, D.S. and Fukata, M. (2006). Protein Palmitoylation by DHHC Protein Family.
[44] Ishii, M. and Kurachi, Y. (2006). Muscarinic acetylcholine receptors. Curr Pharm Des 12, 3573-81.
[45] Caulfield, M.P. and Birdsall, N.J. (1998). International Union of Pharmacology. XVII. Classification of muscarinic acetylcholine receptors. Pharmacol Rev 50, 279-90.
[46] Borroto-Escuela, D.O., Correia, P.A., Romero-Fernandez, W., Narvaez, M., Fuxe, K., Ciruela, F. and Garriga, P. Muscarinic receptor family interacting proteins: Role in receptor function. J Neurosci Methods
[47] Nahorski, S.R., Tobin, A.B. and Willars, G.B. (1997). Muscarinic M3 receptor coupling and regulation. Life Sci 60, 1039-45.
[48] Allosteric interactions at the M3 muscarinic acetylcholine receptor. Ph.D. Thesis, Laura Iarriccio Silva, Barcelona 2008.
[49] Human M3 muscarinic acetylcholine receptor protein-protein interactions: roles in receptor signaling and regulation. Ph.D. Thesis, Dasiel Oscar. Borroto Escuela, Barcelona 2008.

# CHAPTER 2

## OVERPRODUCTION OF $M_3$ MUSCARINIC RECEPTOR: A REQUIRED IMPORTANT STEP IN RECEPTOR PURIFICATION

(contents of this chapter is a manuscript accepted for publications in Biotechnology Progress Journal)

## Overeproduction of $M_3$ muscarinic receptor: a required important step in receptor purification

### Abstract

The human $M_3$ muscarinic acetylcholine receptor ($M_3R$), present in both the central and peripheral nervous system is involved in several neurodegenerative and autoimmune diseases [1,2]. Recently, $M_3R$ overexpression has been suggested to play a role in certain forms of cancer [3,4], showing promise as a new potential pharmacological target. However, the lack of structural information on this receptor subtype hampered the development of new potent antagonist with increased selectivity and lower side effect. A large amount of pure receptor is required to get this purpose. This chapter describes our attempts to overexpress functional $M_3R$ on the perspective of future biophysical studies. In order to achieve this goal, four tagged receptor genes were engineered and codon optimized $M_3R$ gene suitable for high-level expression in mammalian systems. In addition, different heterologous expression systems, including mammalian cells and viral transfection, were employed to overexpress $M_3R$. While codon optimization resulted in an only 2-fold to 3-fold increase of $M_3R$ expression, we found that epitope tagging of the synthetic $M_3R$, especially with Haemagglutinin and Flag epitope tags could improve $M_3R$ expression levels. Confocal microscopy signalled localization of the tagged synthetic receptor to the cell membrane, with a receptor density ($B_{max}$) of 9.27 ± 0.13 pmol/mg protein, as measured by saturation assays using [$^3$H]-N-methylscopolamine. On the other hand, viral transfection led to a yield of 27 pmol/mg protein, which is the highest level reported so far for this receptor subtype in mammalian cells. Takening together, the strategies used could help increasing $M_3R$ expression not only in order to start purification efforts, but also for later secondary structural analysis, functional assays, and potential three-dimensional structural determination. Results may be useful in future efforts for overproduction of other muscarinic acetylcholine receptor subtypes.

## Introduction

The muscarinic acetylcholine receptors (mAChRs) are prototypic and a well-characterized member of the G protein-coupled receptor (GPCR) family represented by five distinct subtypes ($M_1R$-$M_5R$). Experimental studies using genetically modified knock-out mice have clarified the function of each subtype, suggesting a key role in essential processes like memory, locomotion, temperature regulation, urinary bladder and trachea, control of salivary secretion, pupillary constriction, immunity and food intake [5-7]. As mAChRs are involved in different roles and disorders at various locations, mAChR agonists or antagonists represent attractive pharmacological targets for intervention. To facilitate the discovery of high affinity and selective ligands targeting each subtype the availability of detailed structural information is extremely helpful. However, no detailed structure exists for any mAChRs. Such structural information can be only achieved by means of experimental biophysical techniques that require large quantities of pure receptor.

Traditionally, the drug discovery has relied on screening chemical libraries in search of compounds interacting favourably with the GPCR of interest. Despite its drawbacks, this procedure has been a widely used tool. However, there is still a great need for development on drugs with raised affinity and selectivity. The drug design based in the information of the high-resolution three-dimensional (3D) structures of their target protein has become a powerful tool for drug development. However, only a few high-resolution structures are available. Up to now the molecular structures of six unique GPCRs have been determined [8]. This lack of structural data mainly originates in the membranous nature of these proteins and in their low natural plenty. Thus, their heterologous overexpression is an unavoidable step, and it is essential to develop efficient expression strategic.

Over the last years several methods have been described to overexpress GPCRs [9,10]. Heterologous expression has been evaluated in several different expression systems including bacterial, yeast, insect and mammalian, but with varying degree of success because of differences in the host cell environment [11]. *Pichia*

*pastoris*-based GPCR expression resulted in 40 pmol/mg protein yields [12,13]. Furthermore, high-level expressions of neurokinin-1, rhodopsin, purinergic receptor 12, β-adrenergic and histamine H1 receptors have been reported in baculovirus/Spodoptera frugiperda (*Sf9*) insect cells system [10,14].

Expression of GPCRs in non-mammalian cells suffers from the lack of post-translational modifications, such as N-glycosylation which are known to be important for optimal receptor functionality [15]. However, the expression of GPCRs in mammalian cells involves a time-consuming and labour-intensive with a costly process with of the low yields of protein that are able achieve. To guarantee specific post-translational modifications and receptor functionality, several GPCR like the neurokinin-1, histamine H2, $CB_2$ cannabinoid and $\alpha_2$-adrenergic receptors have been efficiently expressed using the Semliki Forest virus-based (SFV) expression system in mammalian cell suspension with specific binding activities in the 50–200 pmol/mg protein range, and yields rising up to 10 mg/l [9]. In addition, rhodopsin expression from a tetracycline-inducible stable HEK293S cell line resulted in yields of 10 mg/l opsin [16], while $\beta_2$-adrenergic receptor expression achieved 220 pmol/mg protein in the same expression system [17]. Also, codon optimization is considered to ease the transcription/translation machinery by removing rare codon from the gene of interest [17], becoming as a useful tool that provides the ability to the increase gene expression expression yields [18-20]. However, reports on the use of this approach in the GPCR field are limited [21,22].

Heterologous expression of muscarinic receptor family in different systems has been previously reported: for $M_2R$ in *E. Coli* (6 pmol/mg protein); $M_1R$ in *S. Cerevisiae* (0.02 pmol/mg protein); $M_1R$, $M_2R$, $M_3R$ and $M_5R$ in insect cells (0.8 to 36 pmol/mg protein) and $M_1R$-$M_4R$ in HEK cells (1-3 $x10^{-5}$ sites/cells) [10,23]. In this study, we evaluate different methods aimed at overexpressing $M_3R$, as an example of muscarinic acetylcholine family, in different eukaryotic expression systems. In our hands, higher level of $M_3R$ resulted using Semliki Forest virus (SFV) transfection. We used as well different epitope tagging, incubation strategies and codon optimization tools to improve receptor expression levels. The codon optimized of $M_3R$ showed 2-3 time enhanced expression level over the wild-type

receptor ($M_3R^{WT}$). Flag-tagged receptor resulted in a 5-fold increase expression level over the $M_3R^{WT}$ level. The feasibility of each system was ascertained by evaluating the expression levels using immune detection and pharmacological analysis. Taken together, the strategies used could help increasing $M_3R$ expression not only in order to start purification efforts, but also for secondary structural analysis, functional assays and potential three-dimensional structural determination. Results may be useful in future efforts for overproduction of other mAChRs.

## Materials and Methods

### Plasmid constructs

The sequence encoding the human $M_3R$ gene was optimized for mammalian cell codon usage following the instruction of the supplier (Encorbio, FL, USA). The codon optimized human M3 gene ($coM_3R$) consisted of 1672 bp, of which 1600 bp encoded the $M_3R$ gene. The salient features of the codon-optimized $coM_3R$ gene included a Kozak consensus (GCCACCATGG) 5′ sequence adjacent to the ATG start codon, an increase in the GC content of the gene from 52% to 61.5%, and restriction sites for EcoRI at the 5′ end, and BamHI at the 3′ end in order to facilitate cloning. The use of repetitive codons for any particular amino acid was also avoided wherever possible, to ensure that the total tRNA pool of the cell was not adversely affected. PCR primers were designed using the Vector NTI® software (USA). The cDNAs for the $coM_3R$ were subcloned into the mammalian expression vector pcDNA3.1, pcDNA3.1/3xHA or pcDNA3.1/myc (both gifts from P. Calvo, SFU, CA, USA) or InterPlay® mammalian TAP system, pNTAP-B vector (Stratagene, La Jolla, CA, USA) or pcDNA3.1/Flag-His10 vector (kind gift of M. Bini), thus resulting in the pcDNA3.1-coM3R, pcDNA3.1-3xHA-$coM_3R$, pcDNA3.1-myc-$coM_3R$, pTAP-$coM_3R$ and pcDNA3.1-Flag-$coM_3R$-His10 vectors.

### Cell culture and transfection

African green monkey kidney (COS-7), Chinese hamster ovary (CHO), Baby hamster kidney (BHK) and human embryonic kidney (HEK 293T) cells were grown in Dulbecco's modified Eagle's medium and neuroblastoma cells (SK-N-

MC) in RPMI medium both, supplemented with 2 mM L-glutamine, 100 units/ml penicillin/streptomycin, and 10% (v/v) fetal bovine serum (FBS) at 37°C and in an atmosphere of 5% $CO_2$. For transfection, cells were grown in 6-well dishes at a concentration of $1\times10^6$ cells/well or in 75cm$^2$ flasks and cultured overnight before transfection. Cells were transiently transfected using linear PolyEthylenImine reagent (PEI) (Polysciences Inc., Warrington PA, USA). Cells were harvested 48 hours after transfection and centrifuged at 30000 x g for 30 min. Membrane fractions were frozen as aliquots in 5 mM phosphate buffer saline (PBS), pH 7.4, and stored at -80°C until required. For $M_3R$ overexpression using incubation strategies, cells were incubated in the absence or presence of increasing concentration of atropine (0.5 or 1 µM) or sodium butyrate (5 mM up to 50 mM) at 24 h and 48 h respectively.

## Generation of stable cell lines

COS-7 cells (6-well plates, $1x10^6$ adherent cells) were transfected with pcDNA3.1-co$M_3R$ using lipid based transfection protocol in serum and antibiotic-free. Briefly, cells were transfected with 4 µg of cDNA using Lipofectamine™ 2000 (Invitrogen, Carlsbad, CA, USA). The cells were incubated at 37°C in a $CO_2$ incubator for 4 h and then the media was replaced with complete DMEM containing 10% Fetal Bovine Serum (FBS) for 24 h allowing express the protein for Geneticin (G418) resistance under non-selective conditions (for sensitive cells, G418 selection may begin after 48 h). For the selection cells were cultured in DMEM containing 500 µg/ml of G418. The cells were kept at 37°C in a $CO_2$ incubator, replacing with fresh DMEM media containing 10% FBS and 500 µg/ml G418 every two days until colonies were obtained. These colonies were collected and passaged 5 times to get cells stably transfected with co$M_3R$ gene. Single colonies of cells were picked and co$M_3R$ expression was verified through radioligand binding and immunoblots to select clones highly expressing the co$M_3R$. For selection, non-transfected cells were used as negative control. For transfection efficiency and positive control, measured by fluorescence microscopy, a GFP-expression vector (pmaxFP®-Green-N Vector, Lonza, Ibérica, S.A) was used.

## Generation of recombinant Semliki Forest virus particles and infection of mammalian cell lines

A N-terminally tagged Flag-co$M_3$R-His10 gene in a suitable vector for creation of Semliki Forest virus (SFV) was obtained by polymerase chain reaction (PCR) in two steps. The Flag-co$M_3$R-His10 gene was amplified from the pcDNA3.1-Flag-co$M_3$R-His10 by PCR without start and stop codon with a 5´BamHI and 3´SpeI sites using the following sense 5´-CGGGATCCAAGCTTGGTACCACCATGTAC-3´ and antisense 5´-GGACTAGTTCTACTGTCGAATCTACCGG -3´ primers. The gene was directly cloned into the pSFV2genB vector (PSFV2genB-Flag-co$M_3$R-His10).Correct orientation was verified by restriction analysis and sequence analysis.

PSFV2genB-Flag-co$M_3$R-His10 and pSFV-helper2 plasmids were linearised with *SapI* and *SpeI*, respectively, and were purified by phenol/chloroform extraction prior to in vitro transcription. Expression of the recombinant receptor is driven by the bacterial SP6 promoter. 2.5 µg of linearised plasmid were transcribed with 7 U SP6 RNA polymerase (Amersham Biosciences, Germany) in a buffer containing 40 mM HEPES (pH 7.4), 6 mM magnesium acetate, 2 mM spermidine, 1 mM of ATP, CTP and UTP, 0.5 mM GTP, 1 mM m7G (5´) ppp (5´) G (CAP; Amersham Biosciences), 1.5 U RNAsin (Roche, Spain) and 5 mM dithiothreitol in a final volume of 50 µl for 1 h at 37°C. A BHK cells from a semi-confluent 150 $cm^2$ flask were detached with Versene/Trypsine solution. Cells were collected by centrifugation for 5 min at 500 x g and washed twice with 10 ml PBS. Cells were resuspended in 2.5 ml PBS prior to electroporation with the in vitro synthesized RNA. 400 µl of BKH cell suspension was transferred and electroporated on a Bio-rad Genepulser cuvette (Bio-rad, 165-2086) together with 50 µl of transcribed PSFV2genB-Flag-co$M_3$R-His10 RNA and 25 µl of transcribed pSFV-helper2 RNA *(settings: 20 µF, 1300V, ∞Ω)*. Following electroporation cells were immediately resuspended in a growth medium and seeded in 25 $cm^2$ flasks, and 24 h after electroporation, cell media was collected, passed thought a 0.22 µm filter and viral particles were stored at -80°C.

The recombinant virus was activated by chymotrypsin treatment prior infection. 500 µg chymotrypsin (Roche, Spain) was added per 10 ml of virus suspension and incubated for 15 min at room temperature. Subsequently, chymotrypsin was inactivated by the addition of 250 µl aprotinin (10 mg/ml, Sigma-Aldrich, St. Louis, MO, USA). Infection of mammalian cells with the activated viral particles was similar in all used cell lines. Cells were grown to 80% confluence, the medium was aspirated and cells were washed once with PBS. Diluted viral suspensions were added in a small volume, just enough to cover the cells. Cells were incubated with the virus suspension at 37°C for 1 h which the appropriate culture medium and cultured after 24-48 h.

### Membrane preparation and [$^3$H]-N-methylscopolamine binding assay

About 48 h after transfection, cells were washed twice with cold phosphate buffered saline (PBS), harvested and homogenized in binding buffer (20 mM HEPES, pH 7.4, 5 mM $MgCl_2$, 1 mM EDTA), using a Polytron tissue homogeniser. Cell membranes were collected by centrifugation at 20000 x g for 15 min and homogenized as above. After centrifugation at 40000 x g for 20 min at 4ºC, the final pellet was resuspended in binding buffer, and membranes were either used immediately or frozen in liquid nitrogen until needed. Protein concentration was determined by using the Bradford protein assay kit (Bio-Rad, Hercules, CA, USA). To determine the affinity of NMS for each sample, membranes were incubated with different concentrations of [$^3$H]-NMS (ranging from 12.5 pM to 1.5 nM) in 5 mM sodium phosphate (pH 7.4) containing 5 mM $MgCl_2$ at 30°C for 2h. The incubations were stopped by filtration through Whatman (Maidstone, Kent, UK) GF/B filters and washed extensively with ice-cold PBS before scintillation counting. Nonspecific binding was determined in the presence of 10 µM atropine.

### Western blot

Proteins separated on 12% SDS-PAGE electrophoresis were immunoblotted to Immobilon P polyvinylidene difluoride membranes (PVDF, Millipore, Bedford, MA) using a semidry transfer system (Bio-Rad, USA). Membranes were blocked for 1 h in 5% dried milk, Tris-buffered saline, pH 7.5 with 0,1 % Tween-20

(TBST) prior to overnight incubation with primary antibody. Protein immunodetection on membranes was assessed using a rabbit anti-$M_3R$ antibody (1:1000; Santa Cruz Biotechnology, CA, USA) as the primary antibody; and then horseradish-peroxidase (HRP)-conjugated goat anti-rabbit IgG (1:2000; Santa Cruz Biotechnology) as secondary antibody, and developed using SuperSignal West Pico Chemiluminescent Substrate detection kit (Pierce Biotechnology), and HyBlot CL autoradiography film (Denville Scientific, Metuchen, NJ).

**Immunocytochemistry Staining**

Cells were cultured on 35-mm glass coverslips coated with 0.1 mg/ml poly-D-lysine in DMEM supplemented with 2 mM L-glutamine, 100 units/ml penicillin, 100 µg/ml streptomycin, and 10% (v/v) fetal bovine serum (FBS) at 37 °C and in an atmosphere of 5% $CO_2$ in six-well plates. Subconfluent cultures in Log phase were transfected with Fugene® HD transfection (Roche Applied Science, USA) with 2 µg of cDNA according to the manufacturer's instructions. The nuclei were stained with Hoechst 33342 (dilution 1:4000, Invitrogen, Molecular Probes, USA) 3 min at room temperature and washed with PBS 1X. The cells were fixed in 4% paraformaldehyde, incubated 20 min at room temperature and washed with PBS 1X/Glycine 20 mM to quench the remaining free aldehyde groups. The cells were permeabilized with PBS 1X/Glycine 20mM/Triton X-100 0.05%, 5 min at room temperature and washed with PBS 1X/Glycine 20 mM. The cells were blocked with PBS 1X/Glycine 20 mM/BSA 1%, 1 h 37 $^{o}$C and washed in PBS 1X/Glycine 20 mM. The cells were immunostained with rabbit anti-$M_3R$ polyclonal antibody (1:50, Santa Cruz Biotechnology) for 1 h 37 $^{o}$C, and washed three times 5 min each with PBS 1X/Glycine 20 mM. Followed, the cells were stained with FITC-conjugated goat anti-rabbit IgG (1:1000, Santa Cruz Biotechnology) in the same manner. After three PBS washes, the cells were rinsed with water and the coverslips were mounted onto glass slides using Fluorescent Mounting Medium (Dako Diagnostic). Microscope observations were performed with a Leica TCS-SL confocal microscope (Leica, Bannockburn, IL, USA).

### Guanosine 5'-[γ-$^{35}$S]-thiotriphosphate binding assays

The Guanosine 5'-[γ-$^{35}$S]-thiotriphosphate ([$^{35}$S]-GTPγS, 1250 Ci/mmol Perkin-Elmer Life Sciences) binding assays were conducted as described previously [24]. Briefly, membrane homogenate fractions (5 µg total protein) were incubated with 0.2 nM [$^{35}$S]-GTPγS and 1 µM guanosinne-5'-diphosphate (GDP, Sigma Aldrich), in the absence (basal) or presence of 100 µM carbamoylcholine chloride (Cch, Sigma-Aldrich) in 200 µl of 10 mM Hepes, pH 7.4, 10 mM $MgCl_2$, 1 mM EGTA, 100 mM NaCl, 0,2% BSA and 10 µg/ml saponin. Reactions were incubated at 30°C for 1 h. Nonspecific binding was determined by incubation of samples in the presence of 5 µM unlabeled GTPγS, and was subtracted from total basal and total agonist-stimulated binding. Reactions were terminated by addition of 1 ml of ice-cold assays buffer, centrifuged and solubilized with 0.2% SDS. The supernatants were vortex and roll overnight at 4°C with heterotrimeric $G_{\alpha q/11}$ protein antibody (1:50, Santa Cruz Biotechnology), followed of incubation with protein-A sepharose suspension 1 h to room temperature. The washed protein-A beads (10 mM sodium phosphate buffer, pH. 7.4) were resuspended in 1 ml cocktail, vortex mixed and radioactivity was detected by liquid scintillation counting.

### Statistical analysis

All binding data were analyzed using the commercial program GraphPad PRISM 5.0 (GraphPad Prism, San Diego, CA, USA). The number of samples *(n)* for each experimental condition is indicated in the figure legends. For statistical evaluation of the biochemical data, unless otherwise specified, one-way analysis of variance (ANOVA) was used. Group differences after significant ANOVAs were measured by post hoc Bonferroni´s Multiple Comparison test.

## Results

### 2.1 Overexpression of $M_3R$ through codon optimization

To find out whether codon optimization of the $M_3R$ ($coM_3R$) would help increasing its expression level, we developed a $coM_3R$ for expression in mammalian cell. The

gene for the co$M_3R$ was constructed to mainly use only the most frequently codon for each amino acid. The use of repetitive codons for any particular amino acid was also avoided wherever possible, to ensure that the total tRNA pool of the cell was not adversely affected (Table. 1). The following codon was used: alanine (GCC), arginine (AGA), asparagine (AAC), aspartate (GAC), cysteine (TGC), glutamate (GAG), glutamine (CAG), glycine (GGC), histidine (CAC), isoleucine (ATC), methionine (ATG), leucine (CTG), lysine (AAG), phenylalanine (TTC), proline (CCC), serine (AGC or TCC), threonine (ACC), tryptophan (TGG), tyrosine (TAC), valine (GTG) (Table. 1).

**Table 1.** Codon optimized human $M_3$ muscarinic acetylcholine receptor $M_3R$ sequence. The sequence encoding the human $M_3R$ gene (ACM3_HUMAN) was optimized for mammalian cell codon usage. The codon optimize human $M_3$ gene (co$M_3R$) consisted of 1672 bp, of which 1600 bp encodes $M_3R$. The salient features of the codon-optimized co$M_3R$ gene include a Kozak consensus (GCCACCATGG) 5′ to the ATG start codon, an increase in the GC content of the gene from 52% to 61.5%, and restriction sites for EcoRI at the 5′ end and BamHI at the 3′ end to facilitate cloning. In red below the nucleotide sequence of co$M_3R$, where the ***** represent the position of amino acids conserved and the ***letter*** the amino acids replaced. Transversion change (purines <-> pyrimidines), transition change (purines <-> purines/pyrimidines <-> pyrimidines)

ACM3_HUMAN

ACM3_HUMAN Optimized

| | | | | | | | | | | | |
|---|---|---|---|---|---|---|---|---|---|---|---|
| ATG | ACC | TTG | CAC | AAT | AAC | AGT | ACA | ACC | TCG | CCT | TTG |
| *** | *** | C** | *** | **C | *** | **C | **C | *** | AGC | **C | C** |
| TTT | CCA | AAC | ATC | AGC | TCC | TCC | TGG | ATA | CAC | AGC | CCC |
| **C | **C | *** | *** | *** | AG* | AG* | *** | **C | *** | *** | *** |
| TCC | GAT | GCA | GGG | CTG | CCC | CCG | GGA | ACC | GTC | ACT | CAT |
| AG* | **C | **C | **C | *** | *** | **C | **C | *** | *** | **C | **C |
| TTC | GGC | AGC | TAC | AAT | GTT | TCT | CGA | GCA | GCT | GGC | AAT |
| *** | *** | *** | *** | **C | **G | AGC | A*C | **C | **C | *** | **C |
| TTC | TCC | TCT | CCA | GAC | GGT | ACC | ACC | GAT | GAC | CCT | CTG |
| *** | AG* | AGC | **C | *** | **C | *** | *** | **C | *** | **C | *** |
| GGA | GGT | CAT | ACC | GTC | TTG | CAA | GTG | GTC | TTC | ATC | GCT |
| **C | **C | **C | *** | *** | *** | **G | *** | **G | *** | *** | **C |
| TTC | TTA | ACG | GGC | ATC | CTG | GCC | TTG | GTG | ACC | ATC | ATC |

| | | | | | | | | | | | |
|---|---|---|---|---|---|---|---|---|---|---|---|
| *** | C*G | **C | *** | *** | *** | *** | C** | *** | *** | *** | *** |
| GGC | AAC | ATC | CTG | GTA | ATT | GTG | TCA | TTT | AAG | GTC | ACC |
| *** | *** | *** | *** | **G | **C | *** | AGC | **C | *** | **G | *** |
| AAG | CAG | CTG | AAG | ACG | GTC | AAC | AAC | TAC | TTC | CTC | TTA |
| *** | *** | *** | *** | **C | **G | *** | *** | *** | *** | **G | C*G |
| AGC | CTG | GCC | TGT | GCC | GAT | CTG | ATT | ATC | GGG | GTC | ATT |
| *** | *** | *** | **C | *** | **C | *** | **C | *** | **C | **G | **C |
| TCA | ATG | AAT | CTG | TTT | ACG | TAC | ATC | ATC | ATG | AAT | CGA |
| AGC | *** | **C | *** | **C | **C | *** | *** | *** | *** | **C | A** |
| TGG | GCC | TTA | GGG | AAC | TTG | GCC | TGT | GAC | CTC | TGG | CTT |
| *** | *** | C*G | **C | *** | C** | *** | **C | *** | **G | *** | **G |
| GCC | ATT | GAC | TAC | GTA | GCC | AGC | AAT | GCC | TCT | GTT | ATG |
| *** | **C | *** | *** | **G | *** | *** | **C | *** | AGC | **G | *** |
| AAT | CTT | CTG | GTC | ATC | AGC | TTT | GAC | AGA | TAC | TTT | TCC |
| **C | **G | *** | *** | *** | *** | **C | *** | *** | *** | **C | AG* |
| ATC | ACG | AGG | CCG | CTC | ACG | TAC | CGA | GCC | AAA | CGA | ACA |
| *** | **C | **A | **C | **G | **C | *** | A*A | *** | **G | A** | **C |
| ACA | AAG | AGA | GCC | GGT | GTG | ATG | ATC | GGT | CTG | GCT | TGG |
| **C | *** | *** | *** | **C | *** | *** | *** | **C | *** | **C | *** |
| GTC | ATC | TCC | TTT | GTC | CTT | TTG | GCT | CCT | GCC | ATC | TTG |
| **G | *** | AG* | TTC | **G | **G | *** | **C | **C | *** | *** | C** |
| TTC | TGG | CAA | TAC | TTT | GTT | GGA | AAG | AGA | ACT | GTG | CCT |
| *** | *** | **G | *** | **C | **G | **C | *** | *** | **C | *** | **C |
| CCG | GGA | GAG | TGC | TTC | ATT | CAG | TTC | CTC | AGT | GAG | CCC |
| **C | **C | *** | *** | *** | **C | *** | *** | **G | **C | *** | *** |
| ACC | ATT | ACT | TTT | GGC | ACA | GCC | ATC | GCT | GCT | TTT | TAT |
| *** | **C | **C | **C | *** | **C | *** | *** | **C | **C | **C | **C |
| ATG | CCT | GTC | ACC | ATT | ATG | ACT | ATT | TTA | TAC | TGG | AGG |
| *** | **C | **G | *** | **C | *** | **C | **C | C*G | *** | *** | **A |
| ATC | TAT | AAG | GAA | ACT | GAA | AAG | CGT | ACC | AAA | GAG | CTT |
| *** | **C | *** | **G | **C | **G | *** | A*A | *** | **G | *** | **G |
| GCT | GCT | GGC | CTG | CAA | GCC | TCT | GGG | ACA | GAG | GCA | GAG |
| **C | **C | *** | *** | **G | *** | AGC | **C | **C | *** | **C | *** |
| ACA | GAA | AAC | TTT | GTC | CAC | CCC | ACG | GGC | AGT | TCT | CGA |
| **C | **G | *** | **C | **G | *** | *** | **C | *** | **C | AGC | A*A |
| AGC | TGC | AGC | AGT | TAC | GAA | CTT | CAA | CAG | CAA | CAA | AGC |
| *** | *** | *** | **C | *** | **G | **G | **G | *** | **G | **G | *** |
| ATG | AAA | CGC | TCC | AAC | AGG | AGG | AAG | TAT | GGC | CGC | TGC |
| *** | **G | A*A | AG* | *** | **A | **A | *** | **C | *** | A*A | *** |
| CAC | TTC | TGG | TTC | ACA | ACC | AAG | AGC | TGG | AAA | CCC | AGC |
| *** | *** | *** | *** | **C | *** | *** | *** | *** | **G | *** | *** |
| TCC | GAG | CAG | ATG | GAC | ATG | GAC | CAA | GAC | CAC | AGC | AGC |
| AG* | *** | *** | *** | *** | *** | *** | **G | *** | *** | *** | *** |
| AGT | GAC | AGT | TGG | AAC | AAC | AAT | GAT | GCT | GCT | GCC | TCC |
| **C | *** | **C | *** | *** | *** | **C | **C | **C | **C | *** | AG* |

| | | | | | | | | | | | |
|---|---|---|---|---|---|---|---|---|---|---|---|
| CTG | GAG | AAC | TCC | GCC | TCC | TCC | GAC | GAG | GAG | GAC | ATT |
| *** | *** | *** | AG* | *** | AG* | AG* | *** | *** | *** | *** | **C |
| GGC | TCC | GAG | ACG | AGA | GCC | ATC | TAC | TCC | ATC | GTG | CTC |
| *** | AG* | *** | **C | *** | *** | *** | *** | AG* | *** | *** | **G |
| AAG | CTT | CCG | GGT | CAC | AGC | ACC | ATC | CTC | AAC | TCC | ACC |
| *** | **G | **C | **C | *** | *** | *** | *** | **G | *** | AG* | *** |
| AAG | TTA | CCC | TCA | TCG | GAC | AAC | CTG | CAG | GTG | CCT | GAG |
| *** | C*G | *** | AGC | AGC | *** | *** | *** | *** | *** | **C | *** |
| GAG | GAG | CTG | GGG | ATG | GTG | GAC | TTG | GAG | AGG | AAA | GCC |
| *** | *** | *** | **C | *** | *** | *** | C** | *** | **A | **G | *** |
| GAC | AAG | CTG | CAG | GCC | CAG | AAG | AGC | GTG | GAC | GAT | GGA |
| *** | *** | *** | *** | *** | *** | *** | *** | *** | *** | **C | **C |
| GGC | AGT | TTT | CCA | AAA | AGC | TTC | TCC | AAG | CTT | CCC | ATC |
| *** | **C | **C | **C | **G | *** | *** | AG* | *** | **G | *** | *** |
| CAG | CTA | GAG | TCA | GCC | GTG | GAC | ACA | GCT | AAG | ACT | TCT |
| *** | **G | *** | AGC | *** | *** | *** | **C | **C | *** | **C | AGC |
| GAC | GTC | AAC | TCC | TCA | GTG | GGT | AAG | AGC | ACG | GCC | ACT |
| *** | **G | *** | AG* | AGC | *** | **C | *** | *** | **C | *** | **C |
| CTA | CCT | CTG | TCC | TTC | AAG | GAA | GCC | ACT | CTG | GCC | AAG |
| **G | **C | *** | AG* | *** | *** | **G | *** | **C | *** | *** | *** |
| AGG | TTT | GCT | CTG | AAG | ACC | AGA | AGT | CAG | ATC | ACT | AAG |
| **A | **C | **C | *** | *** | *** | *** | **C | *** | *** | **C | *** |
| CGG | AAA | AGG | ATG | TCC | CTG | GTC | AAG | GAG | AAG | AAA | GCG |
| A*A | **G | **A | *** | AG* | *** | **G | *** | *** | *** | **G | **C |
| GCC | CAG | ACC | CTC | AGT | GCG | ATC | TTG | CTT | GCC | TTC | ATC |
| *** | *** | *** | **G | **C | **C | *** | C** | **G | *** | *** | *** |
| ATC | ACT | TGG | ACC | CCA | TAC | AAC | ATG | GTT | CTG | GTG | AAC |
| *** | **C | *** | *** | **C | *** | *** | *** | **G | *** | *** | *** |
| TTT | TGT | GAC | AGC | TGC | ATA | CCC | AAA | ACC | TTT | TGG | AAT |
| **C | **C | *** | *** | *** | **C | *** | **G | *** | **C | *** | **C |
| CTG | GGC | TAC | TGG | CTG | TGC | TAC | ATC | AAC | AGC | ACC | GTG |
| *** | *** | *** | *** | *** | *** | *** | *** | *** | *** | *** | *** |
| AAC | CCC | GTG | TGC | TAT | GCT | CTG | TGC | AAC | AAA | ACA | TTC |
| *** | *** | *** | *** | **C | **C | *** | *** | *** | **G | **C | *** |
| AGA | ACC | ACT | TTC | AAG | ATG | CTG | CTG | CTG | TGC | CAG | TGT |
| *** | *** | **C | *** | *** | *** | *** | *** | *** | *** | *** | **C |
| GAC | AAA | AAA | AAG | AGG | CGC | AAG | CAG | CAG | TAC | CAG | CAG |
| *** | **G | **G | *** | **A | A*A | *** | *** | *** | *** | *** | *** |
| AGA | CAG | TCG | GTC | ATT | TTT | CAC | AGG | CGC | GAC | CCC | GAG |
| *** | *** | AGC | **G | **C | **C | *** | *** | A*A | **C | *** | *** |
| CAG | GCC | TTG | TAG | | | | | | | | |
| *** | *** | C** | *GA | | | | | | | | |

Western blot analysis shows a correct expression of $coM_3R$ in COS-7 cells by a clear definite band migrating around 75 kDa. Another band can also be detected around 132 kDa which is consistent with the presence of a dimeric species (Fig. 1). In addition, we tested the ability of $coM_3R$ binding [$^3$H]-NMS (Fig. 2). Saturation data showed that the affinity dissociation constants ($K_D$) values of $coM_3R$ for [$^3$H]-N-methylscopolamine ([$^3$H]-NMS) was comparable to the values find out for the $M_3R^{WT}$ in all expression system used (data not shown), Also agonist-induced activation of G protein by $coM_3R$ (Fig. 3).

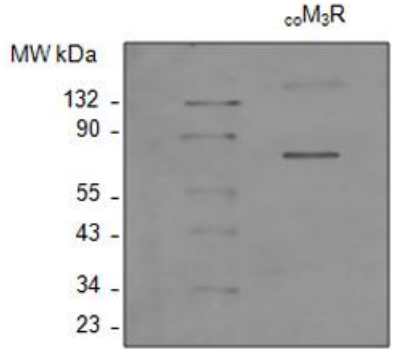


**Figure 1.** Expression of $coM_3R$ on COS-7 cells. Cells transfected with optimized ACM3_Human-pcDNA were lysed in CelLytic™ M buffer and resolved on 10% SDS-PAGE. Receptors were subject to immunoblotting using the anti-$M_3$ polyclonal antibody and HRP-conjugated goat anti-rabbit IgG as a secondary antibody. *Lane 1*, 5 µl Cruz Marker™ molecular weight standard. *Lane 2*, loading 10 µl of sample (1 mg/ml).

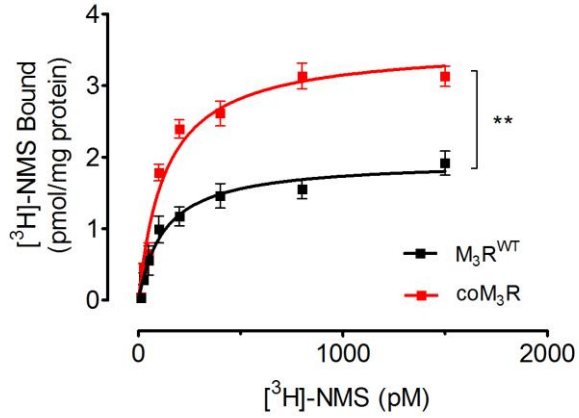


**Figure 2.** [$^3$H]-NMS saturation binding of $M_3R^{WT}$ or $coM_3R$ membrane homogenates (5 µg total protein). [$^3$H]-NMS binding in the presence of 10 µM atropine was defined as nonspecific binding. Binding reactions were stopped by rapid filtration through Whatman GF/B filters and filters washed extensively with ice-cold PBS before counting. Data points were fitted to non-linear regression equations using GraphPad PRISM 5.0. Data are presented as means ± S.E.M *(n=3)*, performed in duplicate by (two-way ANOVA, (**$P$<0.01).

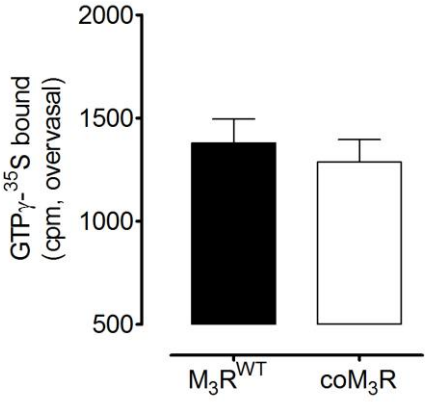


**Figure 3.** [$^{35}$S]-GTPγS binding assay of $M_3R^{WT}$ or co$M_3R$ membrane homogenates (5 µg), carbachol 10 µM, [$^{35}$S]-GTPγS 0.2 nM in binding buffer for 2 h at 30°C. After reaction stop, $G_{\alpha q}$ proteins was immnunoprecipitate using anti-$G_{\alpha q}$ antibody. Followed incubation with protein-A sepharose the radioactivity of washed beads was detected by scintillation counting. Binding in the presence of 5 µM of unlabeled GTPγS was defined as nonspecific binding. Data are expressed as specific binding respect to a sample in the absence of ligand, as mean ± S.E.M *(n=2)*.

Expression of the co$M_3R$ in different mammalian cells lines resulted in a maximal increase of 2.5-fold to 3-fold in the expression level in comparison to that of the $M_3R^{WT}$. Significantly, the higher total number of co$M_3R$ was obtained in the case COS-7 cells ($B_{max}$, 3.25 ± 0.13 vs. 1.26 ± 0.18 pmol/mg protein on $M_3R^{WT}$ (Fig. 4). In addition, we confirm by immunochemistry experiments the location of both, the synthetic and the $M_3R^{WT}$. Figure 5 shows that in all heterologous systems assayed a similar distribution of the receptor on plasma membrane was observed. However, an in depths study of the subcellular localization showed a slightly higher reticular distribution for the $M_3R^{WT}$ compared to the synthetic receptor (Fig. 5).

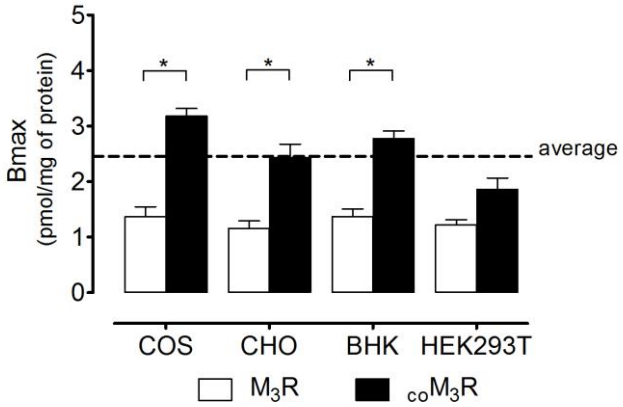


**Figure 4**. Quantitative determination of co$M_3R$ expression level transiently expressed on different mammalian cell lines. Membranes prepared from PolyEthylenImine transfected mammalian cells (10 µg/ml) expressing $M_3R$ or co$M_3R$ were incubated with [$^3$H]-NMS (6.25-1500 pM) in Hepes buffer at 30ºC for 2 h. The non-specific binding was measured

using 10 µM atropine. To analyze the saturation binding data, the nonlinear curve-fitting program Prism 5.0 was used. Data are presented as means ± S.E.M *(n=3)*, performed in duplicate. *: Significant different compared to cells expressing $M_3R^{WT}$, ($P$<0.05) by Student's *t* test.

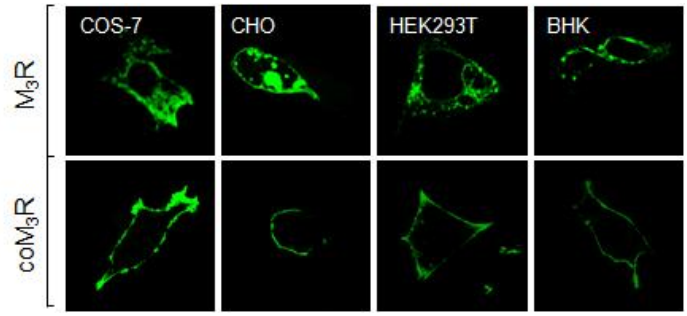


**Figure 5.** $M_3$ muscarinic receptor subcellular localization. Cells were cultured as adherent monolayers on glass slides and transfected with $M_3R$ or $coM_3R$ using FuGENE®HD and then visualized 48 h after transfection. Preparations were fixed, and stained with rabbit antibodies against $M_3$ followed the bound primary antibodies were detected using FITC-conjugated goat anti-rabbit. Cells were visualized by confocal microscopy. These pictures are representative of four different experiments with similar qualitative results.

### 2.2 Effect sodium butyrate and inverse agonist incubation in $M_3R$ expression

Another method used to increase the receptor expression level was adding sodium butyrate (NaBut) in the growth medium [25]. NaBut is a histone deacetylase inhibitor found to inhibit growth and to induce differentiation in various cell types by modulating transcription factors activity [26]. For several GPCRs, the cells incubation with NaBut was shown enhance membrane protein expression [21].

We obtained s COS-7 cell line stably expressing the $coM_3R$ in order to efficiently test whether NaBut had a positive effect on $coM_3R$ expression levels. Results showed that 48 h incubation of stably COS-7-$coM_3R$ cells from 5 mM up to 50 mM. NaBut has a slight positive effect on the expression of $coM_3R$ (Fig. 6), and the chemical change on medium conditions did not alter the pharmacological properties of $coM_3R$ (data not shown). Similar results were obtained using western blot methods (Fig. 7).

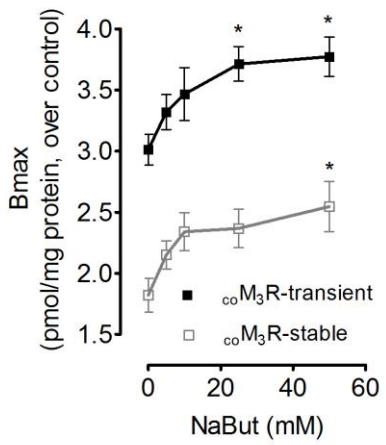


**Figure 6.** Effect of the NaBut incubation on $coM_3R$ expression level in COS-7 cells. Both, stable and transient COS-7 cells expressing $coM_3R$ were cultured in absence (control) or presence of increasing concentration of NaBut (5mM up to 50mM) for 48 h. Expression level was then determined by [$^3$H]-NMS binding. Data represent the means ± S.E.M. of three independent experiments performed in triplicate. *: Significantly different compared to control (two-way ANOVA, $P$<0.05).

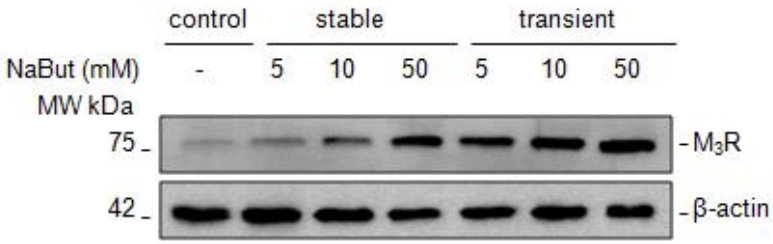


**Figura 7.** Western blots analysis of receptor expression level under different incubation condition. Sodium butyrate-treated stable and transient COS-7 cells expressing $coM_3R$ were lysed in CelLytic$^{TM}$ M buffer. Aliquots of 10 µl (1 mg/ml) were separated on 12% SDS-PAGE followed by electro-blotting using the anti-$M_3$ antibody and HRP-conjugated goat anti-rabbit IgG as a secondary antibody. Blots are representative of two independent experiments.

It was previously shown that incubation of the $M_3R$ inverse agonist atropine acting as a pharmacological chaperone has a positive effect on its [27]. These receptor ligands may act to stabilize the newly synthesized receptor in the native or intermediate state of its folding pathway, possibly by inducing stabilizing conformational constraints within the hydrophobic core of the protein. In our hands, incubation of stable and transient COS-7-$coM_3R$ cells during 24 h with antagonist atropine concentration ranging from 0.5 or 1 µM results in a boost $coM_3R$ expression (Fig. 8). Similar results were obtained using western blot methods (Fig. 9).

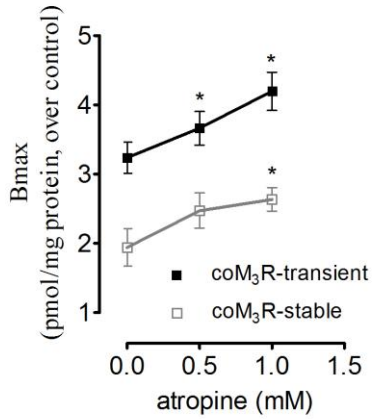


**Figure 8.** Effect of atropine incubation on $coM_3R$ expression level in COS-7 cells. Both, stable and transient COS-7 cells expressing $coM_3R$ were cultured in absence (control) or presence of atropine (0.5 µM or 1 µM) for 24 h. Expression level was then determined by [$^3$H]-NMS binding. The data represent the means ± S.E.M. (*n=3*), performed in triplicate. *: Significantly different compared to control (two-way ANOVA, $P<0.05$).

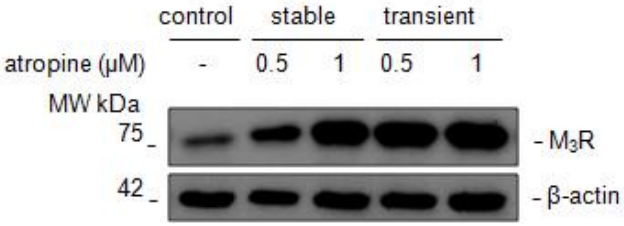


**Figura 9.** Western blots analysis of receptor level under different incubation condition. Atropine-treated stable and transient COS-7 cells expressing $coM_3R$ were lysed in CelLytic$^{TM}$ M buffer. Aliquots of 20 µl (1 mg/ml) were separated on 12% SDS-PAGE followed by electro-blotting using the anti-$M_3$ antibody and HRP-conjugated goat anti-rabbit IgG as a secondary antibody. Blots are representative of two independent experiments.

## 2.3 Overexpression of $M_3R$ through epitope tagging expressed in different mammalian expression systems

Introducing a short epitope tag in N or C-terminal of the receptor gene allows detection and subsequent GPCRs purification. Often adding such tag in GPCR gene sequence has not influence on the receptor expression level [28]. However, occasionally introducing epitope tagging can have a significant effect on the protein expression levels [10]. To find out the effect of N-terminal epitope tags on the expression level of the synthetic $coM_3R$, we generated several $coM_3R$ constructs; a haemagglutinin tagged $M_3R$ (3xHA-$coM_3R$), a CBP-SBP tagged

(CBP-SBP-co$M_3$R), a c-myc tagged (c-myc-co$M_3$R) and a Flag tagged (Flag-coM3R) plus C-terminally histidines tagged (Flag-co$M_3$R-His10).When transiently expressed in COS-7 cells, a 3 and a 5-fold increase in expression level was achieved for the HA- and Flag-His10 tagged synthetic receptor respectively. BHK cell system turned out into similar results to those gained in COS-7 cells. The introduction of a c-myc-epitope tag did not show a significant effect on co$M_3$R expression level whereas a small 1.5-fold enhancement was observed by introducing the CBP-SBP tagged (Fig. 10). The improvement in the Flag-co$M_3$R-His10 expression level on COS-7 cell was also confirmed by Western blot analysis (Fig. 11).

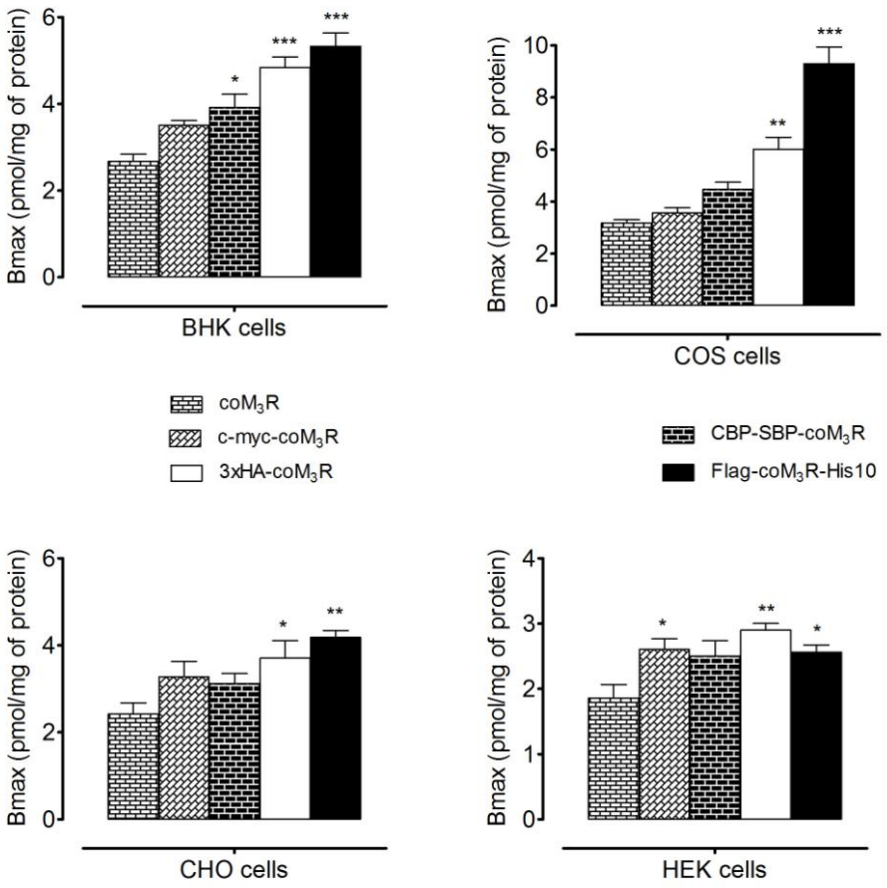

**Figure 10.** Recombinant expression of $coM_3R$ and differentially tagged $coM_3R$ in mammalian cell lines. Cells were transiently transfected with $coM_3R$, c-myc-$coM_3R$, CBP-SBP-$coM_3R$, 3xHA-$coM_3R$ and Flag-$coM_3R$-His10 expression levels were determined by [$^3$H]-NMS binding as described previously. The non-specific binding was measured using 10 µM atropine. To analyze the saturation binding data, the nonlinear curve-fitting program Prism 5.0 was used. Bars represent the mean ± S.E.M of expression level calculated from two separate experiments, each one performed in triplicate. ***: Significantly different compared to $coM_3R$ (one-way ANOVA, ***$P$<0.001, ** $P$<0.01).

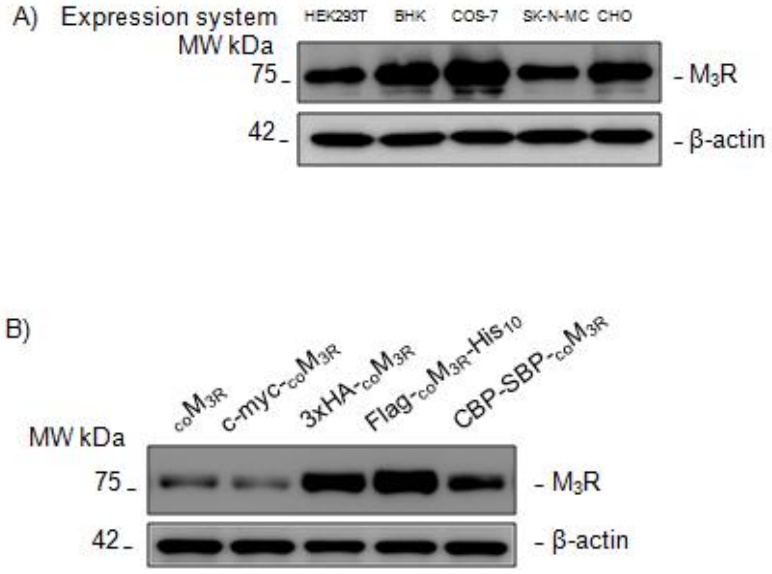


**Figure 11.** (A) Expression level of Flag-$coM_3R$-His10 in different expression systems and (B) Expression level of $coM_3R$ and tagged $coM_3R$ was measured by Western blot. Proteins were resolved on 12% SDS-PAGE, and Western blot was performed with antibody against $M_3R$ and HRP-conjugated goat anti-rabbit IgG as a secondary antibody. SK-N-MC expressing endogenously $M_3R$ was use as control. Blots are representative of two independent experiments.

### 2.4 Overexpression of the $M_3R$ using Semliki Forest virus

Semliki Forest virus (SFV) vectors have been useful for high-level expression of many proteins [29] .The short virus generation time, the fact that they infect a wide host range including mammalian cells lines and primary cell cultures [30], their

extensive replication of RNA in the cytoplasm of the host cell resulting in high-level expression of genes interest, are some advantages that make the use of SFV vectors is attractive for GPCRs overexpression [31]. To research the ability of the SFV expression system to promote high expression of the M3R, we constructed an N-terminally Flag tagged co$M_3$R-His10 in the pSFVgenB vector as described in *Materials and Methods*.

Some critical factors to be controlled during of Semliki Forest virus mediated GPCR expression methods are the time of post-infection and some variations in expression levels occurring among different host cell lines [32]. CHO cells infected with SFV vectors carrying a neurokinin-1 receptor showed maximal binding agonist activity at 12 h post infection, whereas BHK cells infected with SFV-α1b-adrenergic receptor and COS-7 cells with SFV-rat histamine H2 receptor needed 40 h after infection for maximal specific agonist-binding activity [32]. By harvesting cells at different times points, we determined the optimal time of infections, in when the maximal receptor expression was achieved for different cell lines. In general, all infected cells reached maximal expression around 15 h reaching an extended sustained plateau at least until 24 h (Fig. 12).

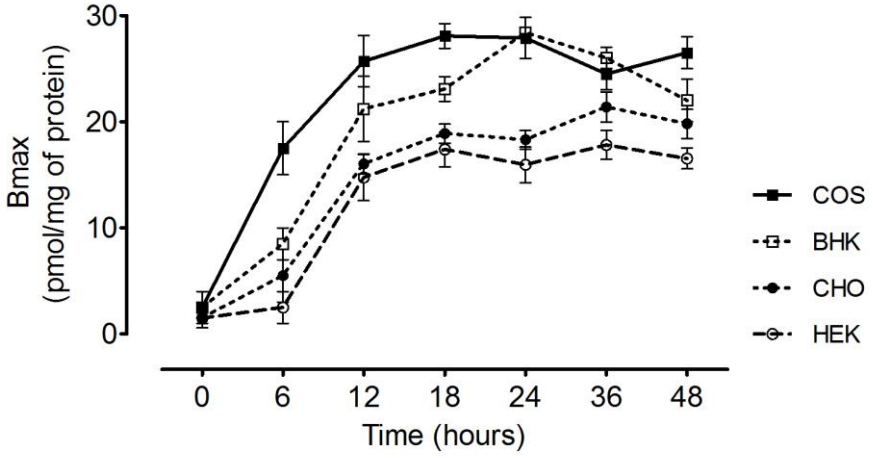

**Figure 12.** Time course of $coM_3R$ expression levels in COS-7 cells. The time course was evaluated by [$^3$H]-NMS saturation binding assay as described previously. Points are the means mean ± S.E.M of three independent experiments.

Therefore, in our case, cells were harvested 20 h after infection as an optimal time to find out expression levels in each expression system. As shown SFV-Flag-$coM_3R$-His10 infection in COS-7 cells resulted in >2.3-fold increase of receptor expression compared to infected HEK cells (approximately 27 pmol/mg protein, which is the highest level reported so far for this receptor subtype in mammalian cells) (Fig 13). In a similar way, the expression level achieved for BHK cells was slightly higher than the expression in CHO and HEK cells (1-fold vs. CHO cells and 2-fold vs. HEK293T cells) (Fig 13).

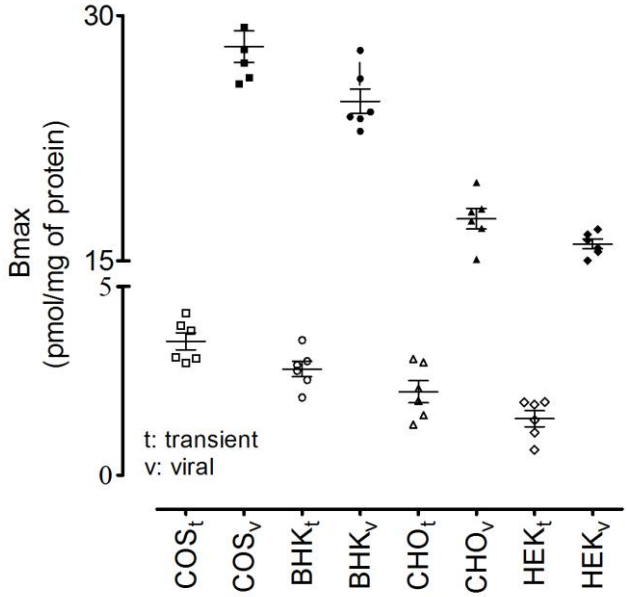


**Figure 13.** Expresssion of Flag-$coM_3R$-His10 in mammalian cell lines with recombinant Semliki Forest virus. COS-7, BHK, CHO and HEK293T cells were infected with recombinant PSFV2genB-Flag-$coM_3R$-His10. PolyEthylenImine transfected cell lines with $coM_3R$ were used as a control. $M_3R$ level was determined using [$^3$H]-NMS binding. Data represent the means ± S.E.M. of two independent experiments performed in triplicate.

## Discussion

G-protein-coupled receptors (GPCRs) represent one of the largest superfamily of protein in the human body with about 1% of the human genome being encoded by over 1000 genes. Many GPCRs are involved in the pathophysiology of diseases, making them interesting targets for therapeutic intervention. It is estimated that more than half of drugs under current investigation are targets for GPCRs. However, only a small percentage of the drugs under investigation are successfully brought to the market [33]. Part of this growing problem lies in the difficulty to produce an enough quantity of pure receptor for structural analysis. In fact, so far only a few high-resolution structures are available [8]. Considering that under physiological conditions the expression of GPCRs is relatively low, optimization of the receptor overexpression is a pre-requisite for obtaining large amounts of pure receptor. In the perspective of future biophysical studies, we have overexpressed M3R using different expression systems, as a first step in the process of large-scale purification. To achieve this goal, a codon optimized $M_3R$ gene suitable for high-level expression in mammalian systems has been used. In addition, four tagged codon optimized gene were engineered and different heterologous expression systems, including viral transfection, were assayed.

Previous studies have shown that by removing rare codons from the gene of interest facilitate the proper work of transcription/translation machinery [17], making this approach an emerging useful to optimize protein expression levels [20]. Currently, reports on the use of this codon-optimization tool in the GPCR field are sparse [22]. However, studies on the improved expression of CCR5 chemokine receptor (2-5 folds) [21], CXCR4 receptor (~400-folds) [22] and β2-adrenergic receptor (130 to 220 pmol/mg protein) [17] have shown that codon optimization can enhance receptor expression levels. We development a codon optimized $M_3R$ for expression in mammalian cells in order to find out whether codon optimization of $M_3R$ would help increase its expression level. The results showed that codon optimization of the $M_3R$ gene did not result in a marked increase of receptor expression. Maximally a 2.5-3 fold increase in protein production was observed in transiently transfected COS-7 cells. This indicates that

the substitution of common codons for rare ones in M3R receptor is not the bottleneck step in the expression of the receptor in a mammalian system.

In addition to codon optimization, other techniques have been used to increase the receptor expression with a variable degree of success; for example, amino acid substitution [34], vector optimization [35], and co-expression with chaperones and other GPCRs [36,37]. Therefore, a possible alternative for improving $M_3R$ expression was the use of sodium butyrate and atropine preincubation. The addition of sodium butyrate (NaBut) in the growth medium induces differentiation in various cell types by modulating gene expression [25,26]. For several GPCRs, incubation of the cells with NaBut has been shown to enhance receptor expression [21]. So far, our results have shown a slight positive effect on expressing $M_3R$ after 48 hours preincubation for both stably and transiently transfected COS-7 cells. Furthermore, a boost on the receptor expression level in cells treated with atropine was confirmed by saturation binding assays and Western blot analysis.

On the other hand, introducing a short epitope tag in N or C-terminal of the receptor gene allows detection and subsequent GPCRs purification. Usually adding such kind of tag onto the GPCR gene sequence has not influenced on the receptor expression level, as in the case of serotonin 5-HT1B receptor [28]. However, occasionally introducing epitope tagging can have a significant effect on the protein expression levels [10]. Double tagging recombinant A1- and A2A – adenosine receptors resulted in an increase of the receptor expression levels compared to the wild-type receptor [38]. We set out to design and use four engineered tagged receptors which were constructed and their effect on the expression level in COS-7 mammalian cells was examined. The addition of CBP-SBP and c-myc tags to the N-terminal site of $coM_3R$ had no significant effect on [$^3$H]-NMS ligand binding when compared to the wild-type receptor, but resulted in 5-fold increasing on receptor expression when tagged the Flag-His10 epitope was used [39-41].

GPCR expression in mammalian cells based on Semliki Forest virus (SFV) vectors has proved to be a useful method which guarantees specific functionally-required

post-transductional modifications of the receptor [10]. SFV has been employed for large-scale recombinant protein production in mammalian culture to produce enough receptor quantities for structural biology of more than 50 different GPCRs [9,29]. For example, neurokinin-1 receptor, histamine H2 receptor, CB2 cannabinoid receptor and α2-adrenergic receptor, have been efficiently expressed in the SFV-based expression system with a specific binding of 50–200 pmol/mg of protein and the yields in large-scale production in mammalian cell suspension cultures have been up to 10 mg/l [9]. So far, only a few reports have been described the use for large-scale production of mAChRs using SFV [9]. Herein, we have shown that infection of recombinant SFV-Flag-co$M_3$R-His10 in a set of different mammalian cell lines significantly improves receptor expression levels. SFV-Flag-co$M_3$R-His10 infection in BHK and COS-7 cells resulted in >10-fold increase in comparison to transiently transfected wild-type co$M_3$R. Expression levels achieved in BHK and COS-7 cells were higher than the expression in the other cell lines used. We achieved a receptor density of 27 pmol/mg protein as the highest level reported so far for this human mAChR subtype, although it is slightly lower than the values reported for other GPCRs using the same expression system [42].

In summary, we have examined several different methods for overexpressing human $M_3R$ in different mammalian expression systems. We found that codon optimization of the $M_3R$ resulted in a slight increase on $M_3R$ overexpression, but this may not be significant for large scale-up purification. However, introduction of a HA-tag or Flag-tag can result in 5-fold receptor expression increase [38]. In addition, viral transfection system allowed obtaining a significant increase (up to 10-fold, 27 pmol/mg protein) in a time-dependent fashion, which is the highest level reported so far for this receptor subtype in a mammalian system. The successful strategies used can be helpful tools to increase $M_3R$ expression not only to facilitate purification efforts, but also for subsequent secondary structural trials, functional analyses and three-dimensional structure determination. Furthermore, the results may be useful in future efforts for overproduction of other mAChRs.

## References


[1] Gautam, D. et al. (2008). Metabolic roles of the M3 muscarinic acetylcholine receptor studied with M3 receptor mutant mice: a review. J Recept Signal Transduct Res 28, 93-108.

[2] Levey, A.I. (1993). Immunological localization of m1-m5 muscarinic acetylcholine receptors in peripheral tissues and brain. Life Sci 52, 441-8.

[3] Cheng, K. et al. (2008). Acetylcholine release by human colon cancer cells mediates autocrine stimulation of cell proliferation. Am J Physiol Gastrointest Liver Physiol 295, G591-7.

[4] Bowers, J.W., Schlauder, S.M., Calder, K.B. and Morgan, M.B. (2008). Acetylcholine receptor expression in Merkel cell carcinoma. Am J Dermatopathol 30, 340-3.

[5] Eglen, R.M. (2006). Muscarinic receptor subtypes in neuronal and non-neuronal cholinergic function. Auton Autacoid Pharmacol 26, 219-33.

[6] Ishii, M. and Kurachi, Y. (2006). Muscarinic acetylcholine receptors. Curr Pharm Des 12, 3573-81.

[7] Khattar, S.K. et al. (2006). High level stable expression of pharmacologically active human M1-M5 muscarinic receptor subtypes in mammalian cells. Biotechnol Lett 28, 121-9.

[8] Kobilka, B. and Schertler, G.F. (2008). New G-protein-coupled receptor crystal structures: insights and limitations. Trends Pharmacol Sci 29, 79-83.

[9] Hassaine, G. et al. (2006). Semliki Forest virus vectors for overexpression of 101 G protein-coupled receptors in mammalian host cells. Protein Expr Purif 45, 343-51.

[10] Sarramegna, V., Talmont, F., Demange, P. and Milon, A. (2003). Heterologous expression of G-protein-coupled receptors: comparison of expression systems fron the standpoint of large-scale production and purification. Cell Mol Life Sci 60, 1529-46.

[11] Tate, C.G. and Grisshammer, R. (1996). Heterologous expression of G-protein-coupled receptors. Trends Biotechnol 14, 426-30.

[12] Minic, J., Sautel, M., Salesse, R. and Pajot-Augy, E. (2005). Yeast system as a screening tool for pharmacological assessment of g protein coupled receptors. Curr Med Chem 12, 961-9.

[13] Schiller, H., Haase, W., Molsberger, E., Janssen, P., Michel, H. and Reilander, H. (2000). The human ET(B) endothelin receptor heterologously produced in the methylotrophic yeast Pichia pastoris shows high-affinity binding and induction of stacked membranes. Receptors Channels 7, 93-107.

[14] Aloia, A.L., Glatz, R.V., McMurchie, E.J. and Leifert, W.R. (2009). GPCR expression using baculovirus-infected Sf9 cells. Methods Mol Biol 552, 115-29.

[15] Massotte, D. (2003). G protein-coupled receptor overexpression with the baculovirus-insect cell system: a tool for structural and functional studies. Biochim Biophys Acta 1610, 77-89.

[16] Reeves, P.J., Callewaert, N., Contreras, R. and Khorana, H.G. (2002). Structure and function in rhodopsin: high-level expression of rhodopsin with restricted and homogeneous N-glycosylation by a tetracycline-inducible N-

acetylglucosaminyltransferase I-negative HEK293S stable mammalian cell line. Proc Natl Acad Sci U S A 99, 13419-24.

[17] Chelikani, P., Reeves, P.J., Rajbhandary, U.L. and Khorana, H.G. (2006). The synthesis and high-level expression of a beta2-adrenergic receptor gene in a tetracycline-inducible stable mammalian cell line. Protein Sci 15, 1433-40.

[18] Grisshammer, R., Duckworth, R. and Henderson, R. (1993). Expression of a rat neurotensin receptor in Escherichia coli. Biochem J 295 ( Pt 2), 571-6.

[19] Bane, S.E., Velasquez, J.E. and Robinson, A.S. (2007). Expression and purification of milligram levels of inactive G-protein coupled receptors in E. coli. Protein Expr Purif 52, 348-55.

[20] Bradel-Tretheway, B.G., Zhen, Z. and Dewhurst, S. (2003). Effects of codon-optimization on protein expression by the human herpesvirus 6 and 7 U51 open reading frame. J Virol Methods 111, 145-56.

[21] Mirzabekov, T., Bannert, N., Farzan, M., Hofmann, W., Kolchinsky, P., Wu, L., Wyatt, R. and Sodroski, J. (1999). Enhanced expression, native purification, and characterization of CCR5, a principal HIV-1 coreceptor. J Biol Chem 274, 28745-50.

[22] Babcock, G.J., Mirzabekov, T., Wojtowicz, W. and Sodroski, J. (2001). Ligand binding characteristics of CXCR4 incorporated into paramagnetic proteoliposomes. J Biol Chem 276, 38433-40.

[23] Kukkonen, J.P., Nasman, J., Ojala, P., Oker-Blom, C. and Akerman, K.E. (1996). Functional properties of muscarinic receptor subtypes Hm1, Hm3 and Hm5 expressed in Sf9 cells using the baculovirus expression system. J Pharmacol Exp Ther 279, 593-601.

[24] Borroto-Escuela, D.O., Correia, P.A., Perez Alea, M., Narvaez, M., Garriga, P., Fuxe, K. and Ciruela, F. Impaired M(3) muscarinic acetylcholine receptor signal transduction through blockade of binding of multiple proteins to its third intracellular loop. Cell Physiol Biochem 25, 397-408.

[25] Van Craenenbroeck, K., Gellynck, E., Lintermans, B., Leysen, J.E., Van Tol, H.H., Haegeman, G. and Vanhoenacker, P. (2006). Influence of the antipsychotic drug pipamperone on the expression of the dopamine D4 receptor. Life Sci 80, 74-81.

[26] Archer, S., Meng, S., Wu, J., Johnson, J., Tang, R. and Hodin, R. (1998). Butyrate inhibits colon carcinoma cell growth through two distinct pathways. Surgery 124, 248-53.

[27] Han, S.J., Hamdan, F.F., Kim, S.K., Jacobson, K.A., Brichta, L., Bloodworth, L.M., Li, J.H. and Wess, J. (2005). Pronounced conformational changes following agonist activation of the M(3) muscarinic acetylcholine receptor. J Biol Chem 280, 24870-9.

[28] Ng, G.Y., George, S.R., Zastawny, R.L., Caron, M., Bouvier, M., Dennis, M. and O'Dowd, B.F. (1993). Human serotonin1B receptor expression in Sf9 cells: phosphorylation, palmitoylation, and adenylyl cyclase inhibition. Biochemistry 32, 11727-33.

[29] Lundstrom, K. (2003). Semliki Forest virus vectors for rapid and high-level expression of integral membrane proteins. Biochim Biophys Acta 1610, 90-6.

[30] Ehrengruber, M.U., Lundstrom, K., Schweitzer, C., Heuss, C., Schlesinger, S. and Gahwiler, B.H. (1999). Recombinant Semliki Forest virus and Sindbis virus efficiently infect neurons in hippocampal slice cultures. Proc Natl Acad Sci U S A 96, 7041-6.

[31] Lundstrom, K. (1997). Alphaviruses as expression vectors. Curr Opin Biotechnol 8, 578-82.

[32] Lundstrom, K., Schweitzer, C., Rotmann, D., Hermann, D., Schneider, E.M. and Ehrengruber, M.U. (2001). Semliki Forest virus vectors: efficient vehicles for in vitro and in vivo gene delivery. FEBS Lett 504, 99-103.

[33] Mailman, R.B. (2007). GPCR functional selectivity has therapeutic impact. Trends Pharmacol Sci 28, 390-6.

[34] Parker, E.M., Kameyama, K., Higashijima, T. and Ross, E.M. (1991). Reconstitutively active G protein-coupled receptors purified from baculovirus-infected insect cells. J Biol Chem 266, 519-27.

[35] Pickering, B.M. and Willis, A.E. (2005). The implications of structured 5' untranslated regions on translation and disease. Semin Cell Dev Biol 16, 39-47.

[36] Huang, D., Gore, P.R. and Shusta, E.V. (2008). Increasing yeast secretion of heterologous proteins by regulating expression rates and post-secretory loss. Biotechnol Bioeng 101, 1264-75.

[37] Leskela, T.T., Markkanen, P.M., Pietila, E.M., Tuusa, J.T. and Petaja-Repo, U.E. (2007). Opioid receptor pharmacological chaperones act by binding and stabilizing newly synthesized receptors in the endoplasmic reticulum. J Biol Chem 282, 23171-83.

[38] Robeva, A.S., Woodard, R., Luthin, D.R., Taylor, H.E. and Linden, J. (1996). Double tagging recombinant A1- and A2A-adenosine receptors with hexahistidine and the FLAG epitope. Development of an efficient generic protein purification procedure. Biochem Pharmacol 51, 545-55.

[39] Park, P.S. and Wells, J.W. (2003). Monomers and oligomers of the M2 muscarinic cholinergic receptor purified from Sf9 cells. Biochemistry 42, 12960-71.

[40] Hayashi, M.K. and Haga, T. (1996). Purification and functional reconstitution with GTP-binding regulatory proteins of hexahistidine-tagged muscarinic acetylcholine receptors (m2 subtype). J Biochem 120, 1232-8.

[41] Zeng, F.Y. and Wess, J. (1999). Identification and molecular characterization of m3 muscarinic receptor dimers. J Biol Chem 274, 19487-97.

[42] Hoffmann, M., Verzijl, D., Lundstrom, K., Simmen, U., Alewijnse, A.E., Timmerman, H. and Leurs, R. (2001). Recombinant Semliki Forest virus for over-expression and pharmacological characterisation of the histamine H(2) receptor in mammalian cells. Eur J Pharmacol 427, 105-14.

# CHAPTER 3

## POST-TRANSLATIONAL MODIFICATIONS OF A FUNCTIONALLY SOLUBILIZED AND PURIFIED $M_3$ MUSCARINIC RECEPTOR FROM COS-7 CELLS

(contents of this chapter is a manuscript submitted for publications in Protein Journal)

## Post-translational modifications processing of a functional purified $M_3$ Muscarinic receptor from COS-7 cells


### Abstract

The human muscarinic acetylcholine receptor ($M_3R$), as potential therapeutic target, is under intensive investigations. This chapter discusses improving in solubilization and purifications of $M_3R$ so that structural studies efforts can be performed. Here, we examined two-engineered $M_3R$ for their purification followed by biochemical characterization. A mixture of n-dodecyl-β-D-maltoside/Nonited P40/cholesterol hemisuccinate allowed high level of functional receptors to be extracted from COS-7 cells. MALDI-TOF mass spectrometry analysis confirmed the presence of a specific band corresponding to the receptor obtained after affinity purification. Purified receptor yield varied slightly between preparations but was always in the range 8-14 nmol/l, and immobilized-nickel affinity chromatography proved to be the best purification method. Purified receptor reconstructed in phospholipid vesicles showed wild-type fully functional behavior. In addition, we found that the receptor suffers higher post-translational modifications and suggest a possible map site for N-glycosylation and S-palmitoylation occurrence in $M_3R$ expressed in COS-7 cells. Collectively, our data provide strategies should guide efforts to solubilization and subsequent purification of muscarinic receptors, not only in order to start structural analysis, but also for functional assays.

## Introduction

The human $M_3$ muscarinic acetylcholine receptor ($M_3R$) is a member of the G-protein-coupled receptor (GPCR) superfamily and is present in the central and peripheral nervous system [1]. This receptor mediates important cellular functions, and it has been linked to several neurodegenerative and autoimmune diseases including diabetes type-2, Sjögren's syndrome, chronic obstructive pulmonary disease, overactive bladder, obesity, irritable bowel syndrome, gastrointestinal spasms and cancer [2].

As the $M_3R$ are involved in different roles and disorders at various locations, this represent attractive pharmacological target for intervention in the search for selective agonists or antagonists. However, the lack of structural information on this receptor subtype hampered the development of new potent drugs with increased selectivity and lower side effects. Such structure-function studies can be achieved by means of biophysical and biochemical techniques, which require large quantities of pure receptor. In addition, although increase evidence suggests the important role of post-translational modification in the GPCRs field, only few studies have been reported to date for muscarinic acetylcholine receptors (mAChRs). Thus, the precise role of these $M_3R$ post-translational modifications, in the structure and function of the receptor, remains to be established.

Solubilization of GPCRs is a required important step for receptor purification. Methods for effective solubilization of GPCRs have been previously discussed [3]. Due to low natural abundance of GPCR, another early main step is receptor heterologous expression. Heterologous expression of $M_3R$ has been evaluated in several different expression systems including bacterial, yeast, insect and mammalian cells, but with varying degree of success due to differences in host cell metabolism [4]. The expression of GPCRs in non-mammalian cells suffers from the lack of post-translational modifications such as N-glycosylation, which are known to be important for optimal receptor functionality [5]. Recently, we reported the $M_3R$ overexpression in COS-7 cells guaranteeing specific post-translational modification and receptor functionality *(Romero-Fernandez et al., in press)*.

mAChRs were initially purified from calf forebrain by affinity chromatography with dexetimide coupled to Affi-Gel 10 as the immobilized ligand [6]. Also, mAChRs monomers or oligomers were purified from porcine atria [7,8], porcine cerebrum [9], rat brain [10], CHO cells [11], *sf9* cells [12,13] by mean of affinity chromatography with ABT as the ligand. Furthermore, addition of HA-, Flag- and c-myc tags to N-terminal or Rho-1D4 and $His_6$ tags to the C-terminal of $M_3R$ had no significant effect on [$^3$H]-NMS ligand binding and G-protein coupling properties of tagged-$M_3R$ when compared with wild-type receptor [12-15], and have been used as mAChRs purification strategies.

In this study, we tested different affinity chromatography system using two-engineered synthetic $M_3R$, an N-terminal Haemagglutinin tagged-$M_3R$ (3x HA-$M_3R$) and a Flag-$M_3R$ plus C-terminally histidines tagged (Flag-$M_3R$-His10) described previously *(Romero-Fernandez et al., in press)*, with the perspective to subsequently undertake structural and functional studies. The methods described will enable progress in structural studies of the muscarinic receptors and they provide an efficient and general technique that can be also adapted to promote the production and purification other GPCR.

## Material and Methods

### Generation of $M_3R$ mutants

To generate cDNA construct encoding simple mutation point, we replaced the asparagine residue in each N-glycosylation consensus sequence of the $M_3R^{WT}$ ($M_3R$ wild-type receptor) with glutamine residue using the Quick-Change site-directed mutagenesis kit (Stratagene, La Jolla, CA, USA). In addition, we substituted two cysteines residues at consensus sequences for S-palmitoylation at carboxyl tail of $M_3R$ by alanine. Simple mutations were confirmed by DNA sequencing. The primers (from Sigma Aldrich, St. Louis, MO, USA) used for mutagenesis (5'→3') were as follows: For $M_3R$ N-glycosylation deficient mutants: $M_3R^{N5Q}$: 5'-gAgAgTCACAATgACCTTgCACCAgAACAgTACAACCTCgCCTTTg-3'.
$M_3R^{N6Q}$: 5'-

gAgAgTCACAATgACCTTgCACAATCAgAgTACAACCTCgCCTTTg-3'. $M_3R^{N15Q}$: 5'-CCTCgCCTTTgTTTCCACAgATCAgCTCCTCCTgg-3'. $M_3R^{N41Q}$: 5'-CATTTCggCAgCTACCAggTTTCTCgAgCAgCTggC-3'.$M_3R^{N48Q}$: 5'-CTCgAgCAgCTggCCAgTTCTCCTCTCCAgACgg-3'. For $M_3R$ S-palmitoylation-deficient mutants: $M_3R^{C561A}$: 5'-CAAgATgCTgCTgCTggCCCAgTgTgACAAAAAAAAgAggCgC-3'. $M_3RC^{563A}$: 5'-CAAgATgCTgCTgCTgTgCCAggCTgACAAAAAAAAgAggCgC-3'.

## Cell culture and transfection

COS-7 cells (American Type Culture Collection) were grown in Dulbecco's modified Eagle's medium (DMEM), supplemented with 2 mM of L-glutamine, 100 units/ml penicillin, 100 µg/ml streptomycin, and 10% (v/v) fetal bovine serum (Invitrogen, Carlsbad, CA, USA) at 37°C and in an atmosphere of 5% $CO_2$. For transfection, cells were plated in 175 $cm^2$ flasks at concentration of $1\times10^6$ cells/well and cultured overnight before transfection. Cells were transiently transfected using linear Polyethylenimine transfection reagent (PEI, Polysciences Inc., Warrington PA, USA) according to the manufacturer's protocol. As chemical blockage of post-translational modifications used as control, cells were incubated, at 4 h post-transfection, in the absence or presence of 5 µg/ml tunicamycin (TM) or 100 µM of 2-bromopalmitate (2-BP) (Sigma Aldrich) and cells were harvested after 48 h.

## Membranes Preparation

To prepare cell membranes, cells were harvested 48 h after transfection. Initially, cells were washed twice with 10 ml (175 $cm^2$ flask) of ice-cold phosphate-buffered saline (1x PBS), pH 7.4. Subsequently, 10 ml of ice-cold buffer A (50 mM Tris-HCl, pH 7.5, 5 mM $MgCl_2$) was added to each flask, followed by 10 min incubation at 4°C. Cells were then scraped off the plates, centrifuged at 500 × g for 5 min and homogenized using a Polytron tissue homogenizer (for 30 s five times each 30 seconds on ice). After a 15 min centrifugation at 40,000 x g, 4°C, membrane pellets were washed three times in buffer B (10 mM Tris-HCl, pH 7.5, 5

mM $MgCl_2$) and then incubated on ice for 20 min with 0.2% digitonin in buffer B containing an protease inhibitor cocktail (Roche Diagnostics, USA), in order to remove soluble as well as peripheral membrane proteins. Following centrifugation at 40,000 x g for 15 min, supernatants were discarded, and crude membrane preparation was used immediately or frozen in liquid nitrogen and stored at -80°C until required.

**Membrane solubilization**

Membrane pellets preparation were incubated in a solubilization buffer containing 50 mM Tris–HCl, pH 7.5, 150 mM NaCl, 1 mM $CaCl_2$, 1 mM $MgCl_2$, 1% of glycerol, a cocktail of protease inhibitors, and mixed with selected detergent (1%) during 1 h at 4°C with mild agitation. Solubilized membrane proteins were recovered by collection of the supernatant, after ultra centrifugation at 100,000 x g for 30 min at 4°C. Protein concentrations were determined using the Micro BCA protein assay reagent kit, using bovine serum albumin (BSA) as a standard (Bio-Rad, USA). Solubilized receptors were either used immediately or frozen in liquid nitrogen, and stored at -80 °C until required.

**ABT-agarose affinity chromatography purification**

Here we described the procedures for affinity chromatography purification of $M_3R$ using 3-(2'-aminobenzhydryloxy)-tropane (ABT) as the ligand. ABT-agarose gel is not available commercially. Therefore, the preparations of ABT and ABT-agarose have been previously described [16]. Solubilized receptor prepared from 100 g of rat brain was subjected to affinity chromatography using ABT-agarose gel (kindly provided by Dr. T. Haga, University of Tokyo, Japan, essentially as described by Haga and Haga [9].

One hundred grams of rat brain were homogenized in 0.5 l of 0.32 M sucrose, 10 mM Hepes buffer, pH 7.5 and protease inhibitors cocktail with polytron tissue homogenizer for 30 s three times each 30 seconds on ice. The homogenate was dilute with 1 l the same buffer and centrifuged at 10,000 x g for 60 minutes at 4°C. The pellet was suspended in 0.5 l of 10 mM Tris-HCl buffer, pH 7.5 and

homogenized and centrifuged was repeated one once more to the same conditions. The final pellet was suspended in 0.5 l of 0.32 M sucrose, 20 mM Tris-HCl, pH 7.5 and stored at -80°C. The 50 ml of the membrane preparation were suspended in 450 mL of 20 mM Tris–HCl and pH 7.5, 150 mM NaCl, 1 mM $CaCl_2$, 1 mM $MgCl_2$, protease inhibitors cocktail and supplemented with a mixture digitonin/sodium cholate (1% + 0.1% v/v, respectively). The suspension was stirred during 1 hour at 4°C and centrifuged 100,000 x g 30 minutes at 4°C. The supernatant was used immediately.

All procedures are performed a 4°C, unless otherwise specified. In brief, prevail wash of the ABT-gel (50 ml) with 100 ml of 0.1% digitonin/20mM potassium phosphate *buffer*, pH 7.0 (KPB) at a flow rate of 0.8 ml/min using a peristaltic pump. The supernatants containing digitonin/cholate solubilized rat mAChRs were loading to the ABT-agarose gel column at the same flow rate. Non-specifically bound proteins were washed out with 300 ml of 0.1% digitonin/20mM KPB/0.15 M NaCl. The column effluent was monitored for absorbance at 280 nm with Thermo Scientific NanoDrop™ Spectrophotometers. Then connect a small polypropylene column of hydroxyapatite (Bio-Rad) (1 ml, 0.75 x 2.3 cm) to one end of the ABT-gel column and then apply 150 ml of 0.1 mM atropine/0.1% digitonin/20mM KPB/0.15 M NaCl. After disconnecting the hydroxyapatite column from ABT-gel column, the specifically bound receptor proteins were eluted apply the 15 ml of 0.5 M KPB/ 0.1% digitonin/10 mM carbachol. The collected purified fraction was concentrated 100-fold by ultrafiltration discs using Amicon Centricon® centrifugal filter YM-30 with 30,000 kDa of cut-offs, and frozen in liquid $N_2$ and stored at –80°C.

**HA Immunoaffinity chromatography purification**

We have used Monoclonal antibody anti-HA covalently linked to agarose that recognizes native as well as denatured-reduced forms of HA-tag proteins. All steps were performed at 4°C. Briefly, in each purification a solubilized-3x HA-$M_3R$ from ten 175 $cm^2$ COS-7 culture flask was incubated with 5 ml of equilibrate HA-agarose (wash the resin with three sequential 5 ml aliquots of glycine-HCl, pH 2.5

followed by three sequential 5 ml aliquots of 1xPBS, pH 7.4), for 18 hours, at 4°C with gentle mixing. The 3xHA-$M_3$R bead suspension was transferred to the appropriate chromatography column (1 x 10 cm column), the flow though under gravity was collected and column was rinsed (0.5 ml/min) with 10 volumes of column buffer (50 mM Tris–HCl, and pH 7.5, 0.05% dodecyl maltoside, 150 mM NaCl, 1 mM $CaCl_2$, 1 mM $MgCl_2$, protease inhibitors cocktail, and 5% glycerol). The column effluent was monitored for absorbance at 280 with Thermo Scientific NanoDrop™ Spectrophotometers until $A_{280}$=0.01. Fractions were collected at 5 min intervals, and 50 µl aliquots of each fraction were assayed by western blotting using the anti-HA antibody to detect 3x HA-$M_3$R. At a flow rate of 1.5 ml/min eluted the bound fusion protein with 5 x 1 column volume aliquots of a solution containing 50 mM Tris–HCl, pH 7.5, 100 µg/µl of HA peptide, 0.05% dodecyl maltoside, 150 mM NaCl, 10 mM EDTA, 1 mM $CaCl_2$, protease inhibitors cocktail and 5% glycerol. Sometime we eluted HA-tagged $M_3$R with 10 x 1 ml aliquots of 0.1 M glycine-HCl, pH 2.5 buffer into vials containing 30-50 ml of 1 M Tris buffer, pH 8.0 for neutralization.

**Immobilized metal affinitty chromatograhphy**

We have used HIS-Select® High Flow Nickel Affinity Gel for purification of Flag-$M_3$R-His10 with a capacity to bind about 10-20 mg histidines tagged protein per mL of packed gel. All steps were performed at 4°C. Briefly, HIS-Select HF affinity gel (5 ml) was transfer to the appropriate chromatography column. Wash the affinity gel with 2 volumes of deionized water to remove ethanol and then 3 volumes of equilibration buffer (50 mM sodium phosphate, pH 8.0, 10 mM imidazole and 0.5 M sodium chloride). Membrane homogenates prepared from COS-7 cells (10 ml, 1 mg/ml) was incubate in solubilization buffer containing 50 mM sodium phosphate, pH 7.5, 10 mM imidazole, 0.5 M sodium chloride and protease inhibitors cocktail with n-dodecyl-β-D-maltoside/NP40 1% (0.8 + 0.2 % w/v, respectively) during 1 h at 4°C with mild agitation. Following, ultracentrifugation at 100,000 x g 30 minutes at 4°C, the clarified sample was diluted 5-fold with pH 8.0, 10 mM imidazole, 5% glycerol and 0.5 M sodium chloride and loaded onto the metal immobilized affinity gel at a rate of 10 ml/h.

After all of the extract is loaded, washing the column with 50 ml of the column-washing buffer (50 mM sodium phosphate, pH 7.5, 10 mM imidazole, 0.3 M sodium chloride and 5% glycerol) at a rate of 50 ml/h. The column washed until the A280 of the eluate from the column is stable and near that of the wash buffer. The bound receptor was eluted with 15 ml of eluate buffer (50 mM sodium phosphate, pH 8.0, 250 mM imidazole, 0.3 M sodium chloride and 5% glycerol) with flow rate of 10 ml/h.

### ANTI-Flag affinitty chromatograhphy

We have used ANTI-FLAG®M1 Affinity Gel (monoclonal antibody covalently attached to agarose by hydrazide linkage) for purification of Flag-$M_3R$-His10 with a capacity to bind top 0.6 mg/ml Flag tagged protein. All steps were performed at room temperature. Briefly, the buffer of collected fraction from HIS-Select® High Flow Nickel Affinity Gel was exchange to TBS/Ca buffer (50 mM Tris, pH 7.4, 0.15 NaCl, 10 mM $CaCl_2$) using a Sephadex G-25 desalting column. ANTI-FLAG® affinity gel (1 ml) was resuspended in 5 ml TBS (50 mM Tris, pH 7.4, 150 mM NaCl) to make a uniform suspension of the gel beads, transfer to the appropriate chromatography column and drain buffer TBS completely. We wash column by loading 3 x 5 ml of 0.1 M glycine HCl, pH 3.5, and followed by 3 x 5 ml of TBS buffer. The sample was loaded onto the column under gravity flow and three passes over column to increase the binding efficiency. The column was washed three times with 10 ml of TBS/Ca. The bound receptor was eluted with 5 ml of eluate buffer (0.1 M glycine HCl, pH 3.5) under gravity flow collecting the eluate in 1 M Tris, pH 8.0. Some time, competitive elution was performed using 5 ml of TBS buffer containing 100 µg/ml of Flag peptide.

### Reconstitution of purified $M_3R$ into phospholipid vesicles

Lipids phosphatidylcholine (PC) and phosphatidylinositol (PI), cholesterol hemissuccinate 12:12:12 (w:w:w) were mixed in chloroform and dried under a stream of nitrogen gas. The dried lipid film was suspended in 20 mM HEPES (pH 7.5), 150 mM NaCl, and 5 mM EDTA. Liposomes were obtained by bath sonication for 1 h at 10-20°C under nitrogen gas and satured with a detergent

mixture of n-dodecyl-β-D-maltoside/NP40 measuring the A540 of the lipid-detergent suspension until translucent. The pooled from affinity chromatography fractions containing purified $M_3$ muscarinic receptor and purified G-protein (1:1000 pmol) were incubated with the detergent-saturated liposomes for 1 h at 4°C. Excess detergent was removed by overnight batch adsorption to 0.5 ml of moist Bio-Beads SM-2 (Bio-Rad) per ml of total suspension at 4°C. The resulting suspension of protein-lipid vesicles were separated from the Bio-Beads and then collected by centrifugation at 200,000 × g for 1 h. Pellet was washed with the Hepes-buffered solution before resuspension and use in radioligand binding assays.

**Sodium dodecyl sulfate polyacrylamide gel electrophoresis and Western blot**

Proteins resolved on 12% SDS-PAGE were subjected to immunoblotting onto Immobilon P polyvinylidene difluoride membranes (PVDF, Millipore, Bedford, MA, USA) using a semidry transfer system (Bio-Rad). Membranes were blocked for 1 h in 5% BSA, Tris-buffered saline, pH 7.4 with 0,1% Tween-20 (TBST) prior to overnight incubation with primary antibody under mild agitation at 4°C. Proteins were detected with the following primary rabbit anti-$M_3$R antibody (1:1000, Santa Cruz Biotechnology, Santa Cruz, CA, USA): horseradish-peroxidase conjugated goat anti-rabbit IgG (1:2000, Santa Cruz Biotechnology). Membranes were washed and developed, using the enhanced Super Signal chemiluminescence's detection kit (Pierce Biotechnology, Rockford, IL, USA), and HyBlot CL autoradiography film (Denville Scientific, Metuchen, NJ, USA) using ChemiDocTM XRS (Bio-Rad).

**Biotin-BMCC labelling**

The acylation of $M_3$R expressed in COS-7 cells was detected by the biotin-switch method [17]. The receptor was then incubated overnight with denaturalization buffer containing 1% Triton X-100 and 40 mM *N*-ethylmaleimide (NEM, Sigma-Aldrich), at 4°C to quench free cysteines. The excess of NEM was removed for desalting column (Pierce Biotechnology). The sample was treated with 1 M hydroxylamine ($NH_2OH$) pH 7.4 (Sigma-Aldrich) to cleave the acyl-thioester bond 2 h at 4°C, thereby generating a free sulfhydryl group. As a control, hydroxylamine

was replaced by PBS. The excess of hydroxylamine was removed by a desalting column (Pierce Biotechnology). The sample was incubated for 2 h, at room temperature with 100 µM of the sulfhydryl-specific reagent biotin-conjugated, 1-biotinamido-4-[4'-(maleimidomethyl)cyclohexanecarboxamido] butane (Btn-BMCC, Pierce Biotechnology), which recognizes free sulfhydryl groups, and washed again. The bound protein was resuspended in 20 µl of 5 x SDS-PAGE loading buffer, and run on SDS-PAGE. Labelled proteins were detected by Western blotting as described before using streptavidin-HRP-conjugated.

## Enzymatic receptor deglycosylation

COS-7 membrane homogenates expressing $M_3R$ and purified receptor (10 µl, 0.5 µl, respectively) were digested with N-Glycosidase F (PNGase F, New England Biolabs, Beverly, USA). The $M_3R$ is combined with glycoprotein denaturing buffer (0.5 % SDS, 40 mM dithiothreitol, DTT) and denatured by heating reaction at 100°C for 10 minutes. After the addition of 1% NP-40 and 10 µl of reaction buffer (50 mM sodium phosphate pH 7.5), two-fold dilutions of PNGase F are added, and the reaction mix is incubated for 2 hours at 37°C, according to the manufacturer's protocol. Separation of reaction products are visualized by SDS-PAGE and Western Blotting analysis as described before.

## Muscarinic receptor radioligand binding assay

The binding of [$^3$H]-N-methylscopolamine ([$^3$H]-NMS, 81 Ci/mmol, Perkin-Elmer Life Sciences) was performed on membrane homogenated expressing $M_3R$ and purified receptor in phospholipid vesicles (5 µg/ml and 2 nmol, respectively in 200 µl of assay buffer). In brief, receptors were incubated with different concentrations of [$^3$H]-NMS (ranging from 0.25 pM to 3200 pM) in assay buffer (20 mM Hepes, pH 7.4, 100 mM NaCl, 10 mM $MgCl_2$) at 30°C for 2 h. Non-specific binding was assessed in the presence of 10 µM atropine. Binding reactions were terminated by rapid filtration through Whatman GF/B filters (Maidstone, Kent, UK) using a MultiScreen™ Vacuum Manifold 96-well (Millipore Corp, Bedford, MA), followed by three washes (~250µl per wash) with ice-cold milliQ

water. Filters were dried, 4 ml of scintillation cocktail was added and the bound ligand was determined by scintillation counting.

### Guanosine 5'-[γ-$^{35}$S]-thiotriphosphate binding assays

The guanosine 5'-[γ-$^{35}$S]-thiotriphosphate ([$^{35}$S]-GTPγS), 1250 Ci/mmol Perkin-Elmer Life Sciences) binding assays were conducted as a modification of the described previously method [18]. Briefly, membrane homogenate fractions (100 μg protein/ml) were incubated with 0.3 nM [$^{35}$S]-GTPγS and 1 μM guanosine-5'-diphosphate (GDP, Sigma Aldrich), in the absence or in the presence of carbamoylcholine chloride (Cch, from 1 nM to 1 mM) in 1 ml of 10 mM Hepes, pH 7.4, 10 mM $MgCl_2$, 1 mM EGTA, 100 mM NaCl, 0,2% BSA and 10 μg/ml saponin. Reactions were incubated at 30°C for 1 h. Non-specific binding was determined by incubation of samples in the presence of 10 μM unlabeled GTPγS. Reactions were stopped by addition of 5 ml of ice-cold assay buffer, immediately followed by rapid filtration through Whatman GF/C filters presoaked in the same buffer containing 0.5% polyethyleneimine. The washed filters were dry and resuspended in 4 ml scintillation cocktail, vortex mixed and radioactivity was detected by liquid scintillation counting.

### Statistical analysis

All binding data were analyzed using the commercial program GraphPad PRISM 5.0 (GraphPad Prism). Statistical analyses were performed using unpaired Student's *t*-test or two-way ANOVA. The number of samples in each experimental condition is indicated in figure legends. Differences were considered statistically significant when $P$ values were $<0.05$. Values are expressed as means ± S.E.M.

## Results

### 3.1 Solubilization of $M_3$R expressed in COS-7 cells

**Total protein concentration in solubilized fractions:** We initiated the study of the $M_3$R solubilization by determining the total proteins in solubilizing fractions

using Bradford assays. Cells were collected and membrane homogenates were prepared as described under *Materials and Methods*. Equal concentrations of membrane fractions were solubilized with different detergents according to the detailed description in the same section. We determined the total protein concentration in the supernatant by measuring the absorbance at 595 nm according to the Bradford assays (Fig. 1). Although this increase in protein concentration may be due to other proteins, we expect a greater amount of soluble $M_3R$ by receptor overexpression *(Romero-Fernandez et al., in press)*.

The results show that almost all detergents resulted in increased solubilization when compared with the soluble fraction of an untreated sample (Fig. 1). Nonetheless, the total protein found in the control sample, was about 0.15 ± 0.07 mg/ml; this may be due to the ultracentrifugation extract peripheral proteins that are weakly attached to the membrane. According to the results, the order of detergents that could efficiently solubilize the homogenate membranes was: Triton X-100 > SDS > CTAB > DG > NP40 > DDM > CHAPS > Tween-80 > OG. Of the detergents that had a higher amount of total soluble proteins, we investigated those that could preserve a functional $M_3R$ using [$^3$H]-N-methylscopolamine binding assay.

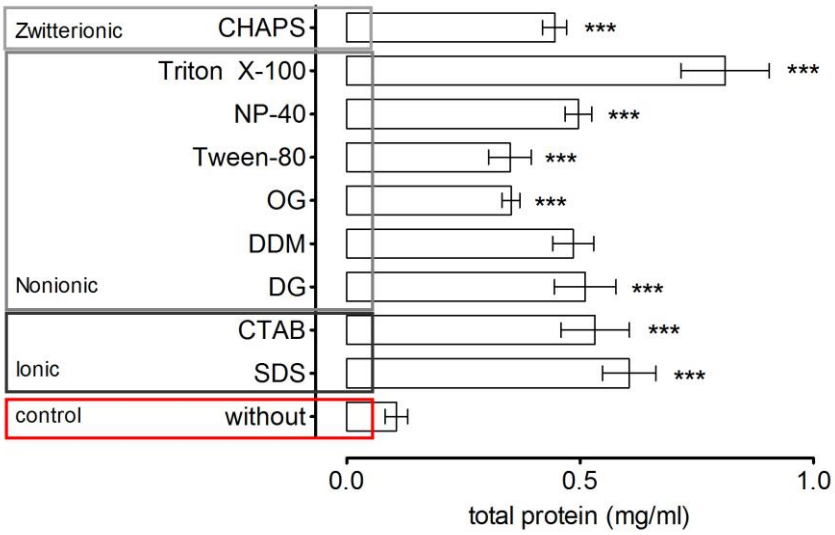

**Figure 1.** Membrane homogenates prepared from COS-7 cells (500 µl, 1 mg/ml) were incubated in a solubilization buffer containing 50 mM Tris–HCl, pH 7.5, 150 mM NaCl, 1 mM $CaCl_2$, 1 mM $MgCl_2$, 1% of glycerol, a cocktail of protease inhibitors, and mixed with detergent (1%) during 1 h at 4°C with mild agitation. Bars represent the mean ± S.E.M of total protein concentration calculated from three separate experiments by Bradford method, *(n=3)* performed in triplicate. All data obtained are significantly different when compared to an untreated sample (one-way, ANOVA****P<0.001*). SDS, sodium dodecyl sulfate, CTAB, Cetyl trimethyl-ammonium bromide; DG, digitonin; DDM; n-dodecyl-β-D-maltoside; OG, β-D-glucopyranoside; NP-40, Nonited P40; Chaps, 3-[(3-Cholamidopropyl) dimethylammoniol-1-propane-sulfonate].

**Measure of $M_3R$-$GFP_2$:** We generated a construct that contains the entire $M_3R$ sequence with a green fluorescence protein fused to the C-terminus of the receptor. In previous work, we checked that adding $GFP_2$ had no influence on the membrane localization or the level expression of $M_3R$ Moreover, binding experiments performed using [$^3$H]-NMS on crude membrane fractions from COS-7 cells expressing $M_3R$-$GFP_2$ revealed specific ligand interactions.

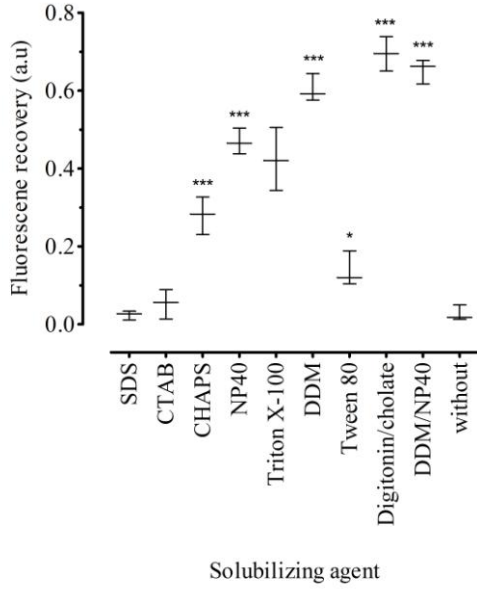


**Figure 2.** Crude Membrane fractions expressing $M_3R$-$GFP_2$ (0.5 ml) were incubated with the solubilization buffers containing detergent during 1 h at 4°C with gentle agitation. Samples were then centrifuged at 100,000 x g for 30 minutes at 4°C. The efficiency was determined by excitation with wavelength of 395 nm and measuring the emission fluorescence at 509 nm, before and after ultracentrifugation in a fluorescence spectrophotometer. Data are presented as means ± S.E.M of three independent experiments, each one performed in triplicate. Data obtained are significantly different from untreated sample values (one-way ANOVA: **P<0.05*, ****P<0.001*).

In this study, we analyze the level of receptors in the soluble fraction of each solubilizing agent exploiting GFP2 fusion protein properties [19]. Briefly, after the cell breakage expressing the construct, a series of centrifugation steps was performed and the analysis of each fraction revealed the construct was mainly found in the 100,000 x g fraction. Fluorescent membrane homogenates were incubated in the different surfactants as it had been previously described. The ratio between the fluorescence in the soluble fraction and the initial fluorescence in the crude solubilized fraction was used as a measurement of the efficiency of each solubilizing agent (Fig. 2). As a control measure, a soluble fraction obtained from an untreated sample was used. Autofluorescence and the absorbance of solubilization buffer were taken into account.

**Stable form and native conformation of solubilized $M_3R$:** Different detergents solubilized membrane homogenates expressing $M_3R$. The soluble fractions were obtained by centrifugation to 100,000g x for 30 min at 4°C and the pharmacological properties were determined by saturation binding assays, as described in *Materials and Methods* (Table 1). We used Western blot to detect $M_3R$ in the soluble fraction (Fig. 3).

**Table 1.** Pharmacological properties of solubilized-$M_3R$ from COS-7 cells

| Detergent | **Binding studies** [$^3$H]-NMS | |
|---|---|---|
| | $K_D$ *(nM)* | $B_{max}$ *(pmol/mg protein)* |
| Chaps | 0.94 ± 0.02 | 0.21 ± 0.03 |
| Sucrose monolaurate | 0.82 ± 0.05 | 0.10 ± 0.04 |
| SDS | 0.37 ± 0.02 | 0.05 ± 0.01 |
| Triton X-100 | 0.76 ± 0.01 | 0.58 ± 0.05 |
| Digitonin/Sodium cholate | 0.51 ± 0.03 | 0.86 ± 0.06 |
| DDM/NP40/CHS | 0.43 ± 0.04 | 0.81 ± 0.07 |

Membranes transfected COS-7 cells expressing $M_3R$ were solubilized using different detergents and detergent mixtures. Each soluble fraction was incubated with [$^3$H]-NMS in Hepes at 30°C for 2 h. Non-specific binding was measured using 10 µM atropine. To analyze the saturation binding data, the nonlinear curve-fitting program Prism 5.0 was used. Data are presented as means ± S.E.M, *(n=2)*, performed in triplicate.

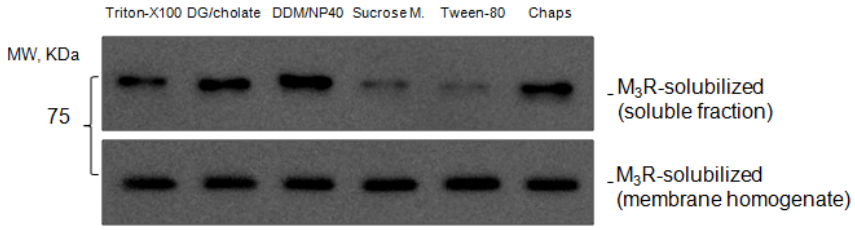


**Figure 3.** Expression level of $M_3R$ in solubilized fraction from different solubilizing agent. Proteins were resolved on 12% SDS-PAGE, and Western blot was performed with antibody against $M_3$ and HRP-conjugated goat anti-rabbit IgG as a secondary antibody as described under *Material and Methods*. Blots were normalized by the level of membrane-bound $M_3R$, and are representative of two independent experiments.

**Stability time course of DDM/NP40-receptor:** The stability of the solubilized DDM/NP40 $M_3R$ was examined by storage of the extracted sample at 4°C and periodical measurement of the [$^3$H]-NMS binding capacity for 1 month. Storage of the solubilized receptor at 4°C resulted in a time-dependent loss of binding capacity that could be fit to a single phase decay process (Fig. 4).

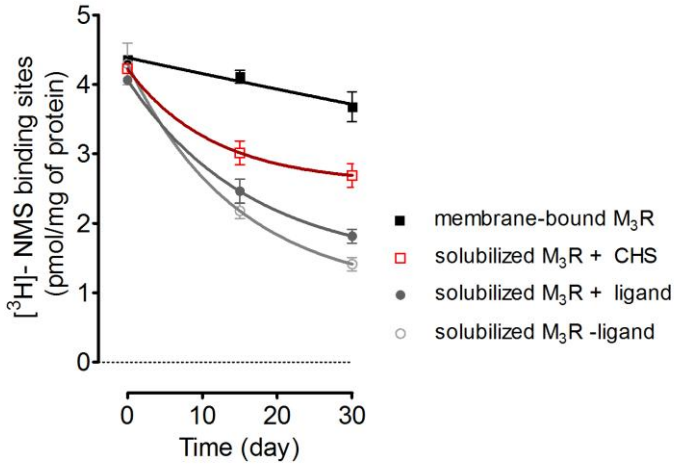


**Figure 4.** Membranes (1 mg/ml) were incubated in Hepes buffer and mixed with 1% of DDM/NP40 with or without CHS for 1 h at 4°C with mild agitation. Samples were subject to subsequent ultracentrifugation at 100,000 x g for 30 minutes at 4°C, the extracted sample was stored at 4°C and the [$^3$H]-NMS binding capacity was measured over a period of one month. Data are presented as mean ± S.E.M. *(n=3)*, performed in triplicate.

The results show that membrane-bound $M_3R$ have around 4.27 ± 0.06 pmol/mg of [$^3$H]-NMS binding sites, which remain practically constant throughout time tested (87%). The solubilization of membrane-bound $M_3R$ with DDM/NP40 without CCh decrease over 60% (1.03 ± 0.09 pmol/mg) with a receptor stability of the t ½ ≈ 27 days. The specific activity achieved was about 1.2-fold higher than that of the starting membrane and decreased only 37% of [$^3$H]-NMS putative binding sites with CCh incubation. Furthermore, membrane pre-incubation with 100 µM of CHS (agonist smaller increase) and the presence during the solubilization process resulted in a rise in half-life of the receptor up to 35 days, which represents an increase of approximately 23% for the stability of the solubilized receptor.

### 3.2 Affinity purification of $M_3R$

**ABT-agarose affnitty chomatography purification:** Solubilized mAChRs prepared from rat brain was subjected to affinity chromatography using 3-(2'-aminobenzhydryloxy)-tropane (ABT) agarose gel (kindly provided by Dr. T. Haga, University of Tokyo, Japan, essentially as described by Haga and Haga. 1985 [9]). The protein concentration and [$^3$H]-NMS binding activity of the rat brain membrane preparation was 3.74 mg/ml and 6.25 pmol/ml (1.67 ± 0.04 pmol/mg of protein), measured by Bradford method and saturation assay, respectively. The membrane preparation contained approximately 3.12 nmol of [$^3$H]-NMS binding sites in 500 ml is obtained from 100 g of tissue. Concentration protein in soluble fraction was 1.8 mg/ml, while [$^3$H]-NMS binding sites was 2.1 pmol/ml. The recoveries of protein and the [$^3$H]-NMS binding activity from the membrane preparations were 49% and 32%, respectively.

In brief, the supernatants containing digitonin/cholate solubilized rat mAChRs were loading to the ABT-agarose gel column. Non-specifically bound proteins were washed out. The column effluent was monitored for absorbance at 280 nm with Thermo Scientific NanoDrop™ Spectrophotometers. Followed, the hydroxyapatite column was connecting to one end of the ABT-gel column and washed and mAChRs was eluate from ABT-gel column applying 0.1 M of atropine. The specifically bound mAChRs were eluted from hydroxyapatite column

(HA). The eluate was pooled and concentrated 50-100 fold using ultrafiltration discs YM-30 and frozen in liquid $N_2$ and stored at –80°C *(see Materials and Methods section)*. The amount of purified mAChRs from ABT-agarose affinity chromatography purification is approximately 0.58 nmol/l. Amicon concentrated elute proteins were separated by one-dimensional gel electrophoresis, and proteins were visualized by silver staining, then $M_3R$ was detected by Western blot analysis (Fig. 5).

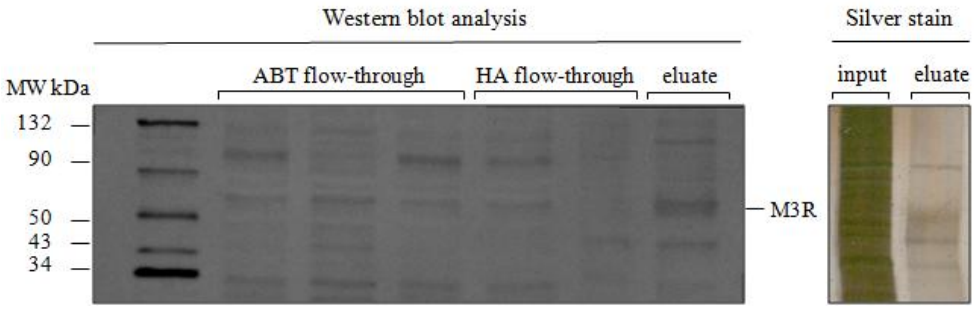


**Figure 5.** Aliquots (0.05% v/v) of the ABT flow-through, HA flow-through and eluate fraction of ABT-HA affinity chromatography was subjected to 12% SDS-PAGE and Western blot using the anti-$M_3R$ antibody as described under *Materials and Methods*. Amicon concentrated eluate receptor from ABT-HA affinity chromatography was separated by 12% SDS-PAGE gel and proteins were detected by silver staining.

**Immobilized metal affinitty chromatograhphy:** We enginered 10xHis-tag into the C-terminus of construct Flag-$M_3R$ to facilitate the purification using nickel affinity chromatography, also called immobilized metal affinitty chromatograhphy (IMAC). Hexahistidine tagged protein for purification by means IMAC has been widely used in purification many GPCRs [14,20]. We have used HIS-Select® High Flow Nickel Affinity Gel for immobilized metal affinitty chromatograhphy (IMAC) of Flag-$M_3R$-His10. The protein concentration and [$^3$H]-NMS binding activity of the COS-7 membrane preparation was 3.94 mg/ml and 28.56 pmol/ml (7.25 ± 0.04 pmol/mg of protein), measured by Bradford method and saturation assay, respectively. The membrane preparation contained approximately 14.28 nmol of [$^3$H]-NMS binding sites in 500 ml of culture cells. Concentration protein in soluble fraction was 3.09 mg/ml, while [$^3$H]-NMS binding sites was 18.43 pmol/ml. The recoveries of protein and the [$^3$H]-NMS binding activity from the

membrane preparations were 77% and 64%, respectively. The eluted fractions from IMAC were concentrated by ultracentrifugation using Amicon Centricon® centrifugal filter YM-30 and a sample of each steps were resolved on SDS-PAGE, and immunoblotted for $M_3R$ using an anti-$M_3R$ antibody (Fig. 6). The amount of purified $M_3R$ from IMAC was approximately 14129.84 pmol/l, as suggested the [$^3$H]-NMS binding. Some time, in order to obtain $M_3R$ of sufficient purity was performed using anti-FLAG®M1 agarose affinity gel.

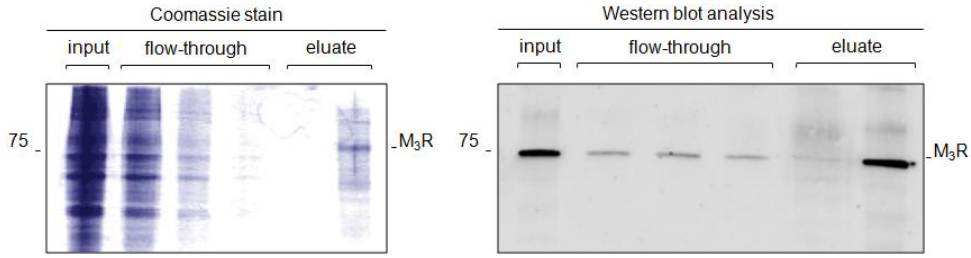


**Figure 6.** Immobilized nickel affinity chromatography purification of $M_3R$. Pooled aliquots (0.05% v/v) of the input, flow-through and eluate fraction of IMAC were subjected to 12% SDS-PAGE and proteins were detected by Coomassie blue staining. Resolved proteins were analyzed by Western blot using the anti-$M_3R$ antibody. Blots are representative of five independent experiments.

**HA-immunoaffinity purification:** In addition, we have used monoclonal antibody anti-HA covalently linked to agarose that recognizes native forms of $M_3R$-tagged. Briefly, a solubilized-3xHA-$M_3R$ obtained from COS-7 cells, with similar protein concentration and [$^3$H]-NMS binding activity that used for IMAC purification, was incubated with equilibrate HA-agarose for 18 h at 4°C with gentle mixing according manufactures instruction described under *Material and Methods*. The column effluent was monitored for A280 with Thermo Scientific NanoDrop™ Spectrophotometers. Fractions were collected at 5 min intervals, and 20 µl aliquots of each fraction were assayed by Western blot using the anti-HA antibody to detect 3x HA-$M_3R$ (Fig. 7). The bound fusion receptor was eluted with elution buffer containing 100 µg/ml of HA peptide or 0.1 M glycine-HCl, pH 2.5 buffer.The eluted fractions from HA-immunoaffinity chromatography was pooled, concentrated, and subsequently subjected to SDS-PAGE followed of

immunoblotting with an anti-HA antibody (Fig. 7). The HA-immunoaffinity chromatography of purified $M_3R$ yield rising up to 8497.31 pmol/l.

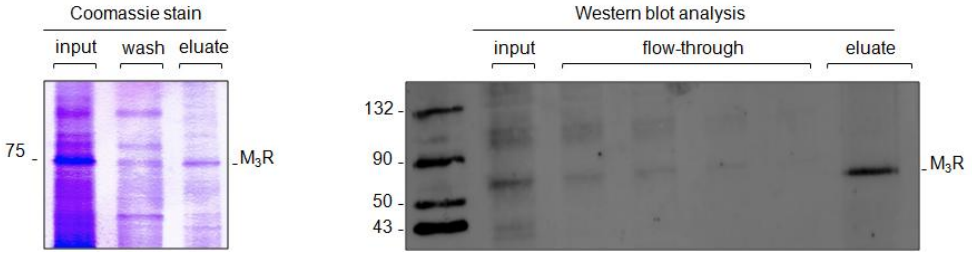


**Figure 7.** HA-immunoaffinity chromatography purification of $M_3R$. Pooled aliquots (0.05% v/v) of the input, flow-through and eluate fraction of HA-purification were subjected to 12% SDS-PAGE and proteins were detected by Coomassie blue staining. Resolved proteins were analyzed by Western blot using the anti-$M_3R$ antibody. Blots are representative of three independent experiments.

**Enzymatic digestion and mass spectrometry of purified $M_3R$:** The ~75-kDa band from IMAC was excised from the gel and enzymatic digested with trypsin for 18 h. Following digestion, the extracted peptides were analyzed by MALDI-TOF *(Barcelona Scientific Park service)*. A theoretical digest of muscarinic receptor using the Find Mod tool available from the ExPASy Proteomics Server (http://www.expasy.org/), was performed and compared with the spectra obtained. Five peptides from the trypsin digestion were detected; agree to 10% coverage of the receptor (Table. 2).

**Table 2.** Peptides identified in enzymatic digests of the purified-$M_3R$ by MALDI-TOF

| Observed mass (Da) | Predicted mass (Da) | Amino acid (sequence) | Amino acid (number, location*) |
|---|---|---|---|
| 1416.7629 | 1416.7634 | YFSITRPLTYR | 194-204, TM |
| 0906.5413 | 0906.5658 | AIYSIVLK | 390-397, ICL |
| 0584.0940 | 0587.3511 | LQAQK | 435-439, ICL |

*Receptor location: N-term, amino-terminal domain; ICL, intracellular loop; TM, transmembrane domain; ECL, extracellular loop; C-term, carboxyl terminal domain.

**Modelling of the M3R using I-TASSER algorithm:** Prediction of 3-dimensional protein structures from amino acid sequences represents one of the most important challenges of the computational structural biology. We have generated automated full-length 3D M3R structural predictions using I-TASSER computer algorithms [21]. The community-wide Critical Assessment of Structure Prediction (CASP) has considered I-TASSER models one of the best methods for structure modeling. In the CASP experiments, human experts use their biochemical knowledge (function, family characteristics, mutagenesis, catalytic residues, etc.), helping template recognition, structural assembly, and final model selection. Recently, has been described CASP8, where both human (as‘‘Zhang’’) and server (as ‘‘Zhang-Server’’) predictions are include [22], enabling non-experts can be generate structural models on their own or through internet services (Fig. 8).

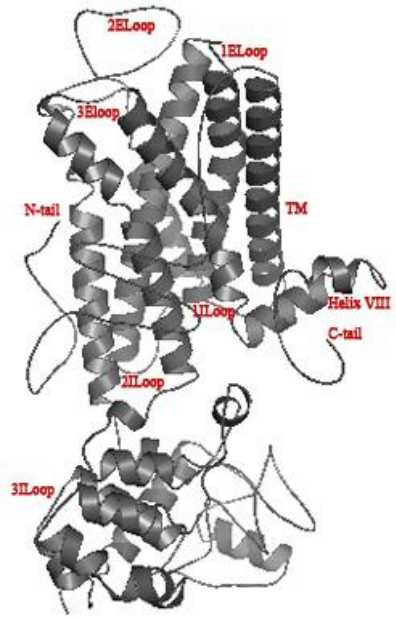


**Figure 8.** Prediction of 3-dimensional structure from amino acid sequences of $M_3R$ using I-TASSER computer algorithms. I-TASSER server is freely available at http://zhang.bioinformatics.ku.edu/I-TASSER.

**Purified $M_3R$ from COS-7 cell maintained the full biological properties:** The ligand binding properties of purified $M_3R$ (0.5-2 nmol of NMS-binding sites/mg of protein) was determined by [$^3$H]-NMS binding. The purified receptor showed high affinity for [$^3$H]-NMS. The $K_D$ values of purified receptor for [$^3$H]-NMS was similar for solubilized receptor and membrane-bound receptor ($K_D$= 485 ± 120 pM) (Fig. 9), suggesting that functional properties of the receptor were retained throughout the purification process. In addition, the purified receptor was reconstituted with purified Gαq protein in lipid vesicles consisting of phosphatidylcholine (PC), phosphatidylinositol (PI), and CHS, and then examined its ability to activate Gαq my measuring the carbachol-dependent [$^{35}$S]-GTPγS binding activity for the reconstituted lipid vesicles. Purified receptor could activate $G\alpha_q$ ($pEC_{50}$= 4.31 ± 0.24 µM) (Fig. 10), results consistent with the previous data obtained on reconstitution of G protein with other purified muscarinic receptor subtype [14,23,24].

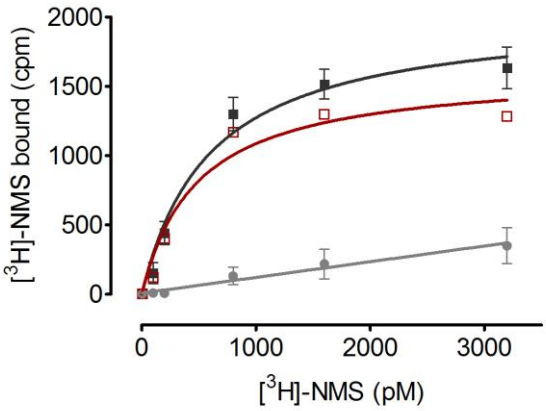


**Figure 9.** Saturation binding of [$^3$H]-NMS to purified $M_3R$. Purified-$M_3R$ (2 nmol/ml) was incubated with [$^3$H]-NMS (6.25-3200 pM) in Hepes buffer at 30ºC for 2 h. Non-specific binding was measured using 5 µM atropine. To analyze the saturation binding data, the nonlinear curve-fitting program Prism 5.0 was used. Data are presented as means ± S.E.M of two independent experiments, each performed in duplicate. Binding data suggest that the functional properties of the receptor were retained throughout the purification process.

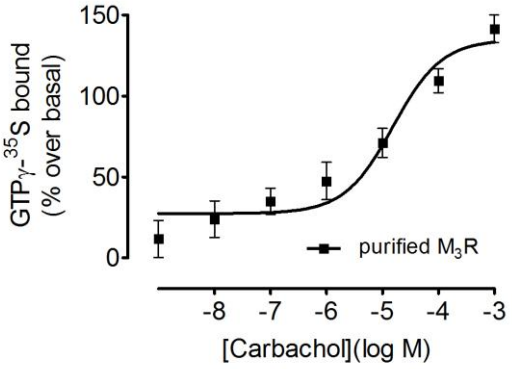


**Figure 10.** Stimulation of [$^{35}$S]-GTPγS binding to Gq protein reconstituted with purified $M_3R$. Gq protein and purified $M_3R$ were reconstituted into lipids as described previously [23]. The reconstituted vesicles containing 2 nmol of purified receptor were incubate with 5 nM [$^{35}$S]-GTPγS and 5 μM GDP in absence (basal) or presence of 10 μM carbachol for 2 h at 30°C, and [$^{35}$S]-GTPγS binding to $G\alpha_q$ proteins was measured. [$^{35}$S]-GTPγS binding in the presence of 5 μM of unlabeled GTPγS was defined as nonspecific binding. Data are presented as means ± S.E.M of two independent experiments, each one performed in duplicate.

### 3.3 Post-translational modifications of purified $M_3R$

**$M_3R$ expressed on COS-7 was strongly glycosylated:** The $M_3R$ contains five potential asparagine-linked glycosylation sites. Enzymatic digestion with Glycosidase F (PNGaseF) was use to examine putative N-glycosylation of the $M_3R$. Solubilized $M_3R$ and purified receptor from COS-7 cells were deglycosylated with PNGaseF, separated on SDS-PAGE followed by Western blot analysis using an anti-$M_3$ antibody (Fig. 11). Consistent with the lack of N-glycosylation, immunoblots showed a decrease in the apparent molecular mass of the $M_3R$ band, in both the solubilized $M_3R$ and purified receptor, suggesting that the uppermost band represent the fully glycosylated form (Fig. 11). Followed, to investigate the $M_3R$ N-glycosylation map, we substituted the asparagine residues at positions Asn5, Asn6, Asn15, Asn41 and Asn48 of the potential N-glycosylation sites to glutamine generating simple mutants. Solubilized membrane proteins from COS-7 cells expressing $M_3R^{WT}$ or specific mutant were subject to SDS-PAGE following Western blot analysis. N-glycosylation mutants migrate at lower molecular weights

than their $M_3R^{WT}$ counterpart, except the $M_3R^{N6Q}$ mutant (Fig. 12), suggesting that four sites (N5, N15, N41 and N48) of $M_3R$ would be glycosylated. In addition, the presence of a higher molecular weight band in the $M_3R^{WT}$ and mutants, presumably corresponding to dimer species, suggesting that simple point of glycosylation is not required for the formations of this molecular species (Fig. 12).

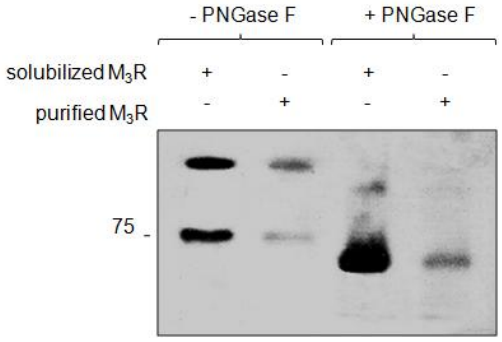


**Figure 11.** Deletion of potential N-terminal N-glycosylation sites in $M_3R$. Solubilized membrane protein and purified receptor was enzymatic digested with/without N-Glycosidase F, resolved on SDS-PAGE, and visualized by Western blot analysis using a primary anti-$M_3R$ antibody and horseradish-peroxidase conjugated goat anti-rabbit IgG as a secondary antibody. Western blot analysis showing the receptor it is glycosylated. Blots are representative of two independent experiments.

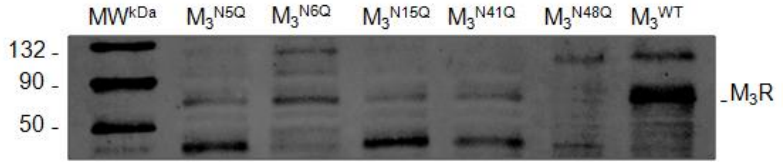


**Figure 12.** A possible $M_3R$ N-glycosylation map is suggested. COS-7 cells transiently expressing $M_3R^{WT}$, $M_3R^{N5Q}$, $M_3R^{N6Q}$, $M_3R^{N15Q}$, $M_3R^{N41Q}$ or $M_3R^{N48Q}$ were lysed in CelLytic™ buffer. Solubilized proteins were then resolved on SDS-PAGE, and immunoblotted for $M_3R$ using anti-$M_3R$ antibody and HRP-conjugated goat anti-rabbit IgG as a secondary antibody. Blots are representative of three independent experiments.

In addition, membrane homogenates prepared from COS-7 cells expressing $M_3R^{WT}$ or specific mutants was use for saturation binding assay using [$^3$H]-NMS. We found differences in receptor density ($B_{max}$) by means of [$^3$H]-NMS binding

measurements when compared mutants with native receptor levels (Fig 13). Also, [$^3$H]-NMS binding data showed that the TM-treated $M_3R$, used as non-glycosylation receptor control, decrease significantly receptor expression at the cell surface at over 40% lower levels ($B_{max}$) as compared with $M_3R^{WT}$ (Fig. 13). In addition, TM-treated $M_3R$ displayed slight change on binding affinity ($K_D$) for the [$^3$H]-NMS as compared to $M_3R^{WT}$. However, in the mutants showed not significant change $K_D$ for [$^3$H]-NMS (Fig. 13).

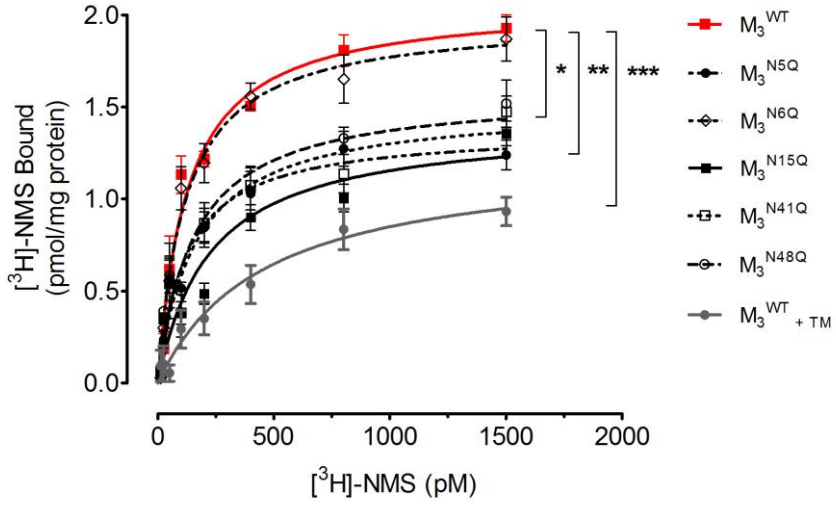


**Figure 13**. COS-7 cells transiently expressing $M_3R^{WT}$, $M_3R^{N5Q}$, $M_3R^{N6Q}$, $M_3R^{N15Q}$, $M_3R^{N41Q}$ or $M_3R^{N48Q}$ were lysed in CelLytic$^{TM}$ buffer. Membrane preparations were incubated with [$^3$H]-NMS in Hepes buffer at 30ºC for 2 h. Non-specific binding was measured using 10 µM atropine. Saturation binding data were analyzed using nonlinear curve-fitting using Prism 5.0. Data are presented as means ± S.E.M of three independent experiments, each one performed in duplicate. Chemical blockage of $M_3R$ N-glycosylation by tunicamycin (TM) was used as a control. ***: Significantly different compared to TM-treated cells (two-way ANOVA ***$P$<0.001, ** $P<0.01$, *$P<0.05$).

In fact, that TM-treated receptor clearly affects the receptor expression levels; cells with/without TM-treated expressing $M_3R$ were use to determine receptor cellular distribution by immunohistochemistry and confocal microscopy. In non-treated cells, the $M_3R$ showed mainly immunoreactivity at plasma membrane. However, TM-treated cells showed strong intracellular receptor signal (Fig. 14).

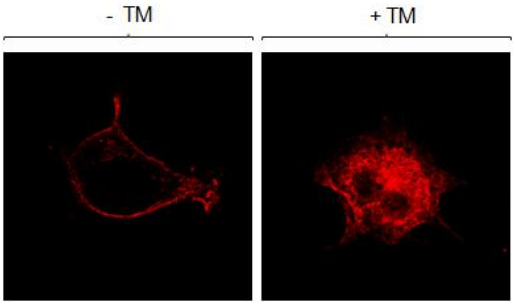


**Figure 14.** Subcellular localization of the $M_3R$ expressed in COS-7 cells with/without TM treatment. After fixation and permeabilization, the cells were immunostained with rabbit anti-$M_3R$ antibody followed Texas Red-conjugated goat anti-rabbit IgG *(red)*. Images are representative of two separate indirect immunofluorescence experiments acquired by confocal microscope.

**Cross-linking palmitoylation study of the $M_3R$:** The $M_3R$ contains two potential sites for palmitoylation within their carboxyl tail. The acylation of purified $M_3R$ was detected by nonradioactive biotin-switch means [17]. Briefly, after blocking of the free sulfhydryl groups in the $M_3R$ and make ones by hydroxylamine removes the fatty acid chains, the labeled with sulfhydryl-specific reagent was used to determined the occurrence of palmitoylation. The specific non-radiolabel Btn-BMCC cross-linking to the $M_3R$ shows that receptor contains covalently bound palmitic acid (Fig 15). In order to determine potential acylation site of $M_3R$, we constructed a series of mutant receptors where the cysteine residues at position $Cys^{561}$ and $Cys^{563}$ were substituted to alanine using the QuickChange Site-Directed Mutagenesis. COS-7 cells expressing $M_3R^{WT}$ or palmitoylation deficient receptor mutants were labelled with [$^3$H]-palmitate, followed by receptor immunoprecipitation, SDS-PAGE and autoradiography. The autoradiogram demonstrated that the receptor incorporated [$^3$H]-palmitate. Substitution of $Cys^{561}$ residue with alanine, resulted in a significantly decreased, but not complete abolish $M_3R$ palmitoylation as compared with the $M_3R^{WT}$. A measurable incorporation of [$^3$H]-palmitate into $Cys^{563}$ was shown, suggesting that $Cys^{563}$ was weakly palmitoylated in COS-7 cells. Thus, results reveal $Cys^{561}$ and $Cys^{563}$ of $M_3R$ as the preferred palmitoylation sites (Fig. 16).

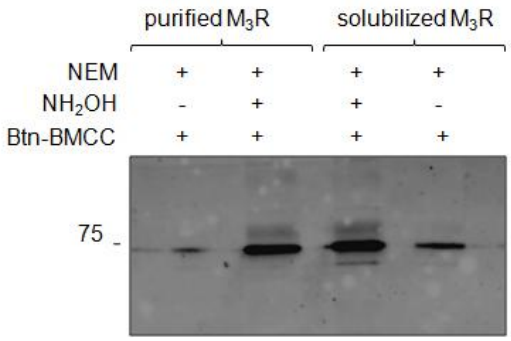


**Figure 15.** $M_3R$ expressed in COS-7 cells is palmitoylated. Both, solubilized and purified fractions, free cysteines in $M_3R$ were quenched by *N*-ethylmaleimide, and $M_3R$ was subjected to Btn-switch procedure by using hydroxylamine hydrolysis and Btn-BMCC as a crosslinker. Proteins were run on SDS-PAGE and transferred to nitrocellulose membranes. Blots were probed using streptavidin-conjugated horseradish peroxidase, and the labeled proteins were detected with ECL.

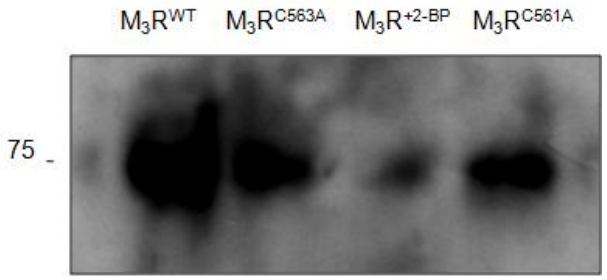


**Figure 16.** [$^3$H]-palmitate incorporation into $M_3R^{WT}$ and palmitoylation deficient mutants. Cells expressing $M_3R^{WT}$, $M_3R^{C561A}$ or $M_3R^{C563A}$ were metabolically labeled with [$^3$H]-palmitate. Immunoprecipitated receptors using an anti-$M_3R$ antibody were resolved on SDS-PAGE. [$^3$H]-Palmitate incorporation was revealed by autoradiography, and band intensity of autoradiogram on the gel corresponded to the degree of palmitoylation. Chemical blockage of $M_3R$ palmitoylation by 2-bromopalmitate (2-BP) was used as a control. Blots shown are representative of three experiments.

Also, saturation-binding assays were performed to determine the $M_3R^{WT}$ and $M_3R$ palmitoylation deficient mutant's expression levels and pharmacological properties (Fig. 17). No significant differences in receptor density ($B_{max}$) were observed by means of [$^3$H]-NMS binding measurements. [$^3$H]-NMS binding data showed that mutants were expressed at the cell surface at similar levels ($B_{max}$) as compared with

$M_3R^{WT}$. In addition, mutants displayed no significantly changes in binding affinity ($K_D$) for the [$^3$H]-NMS as compared to $M_3R^{WT}$ (Fig. 17). Furthermore, confocal microscopy showed that cells expressing $M_3R^{WT}$ with/without 2-bromopalmitate treatment, blocking receptor palmitoylation, the receptor was mainly localized to the plasma membrane (Fig. 18).

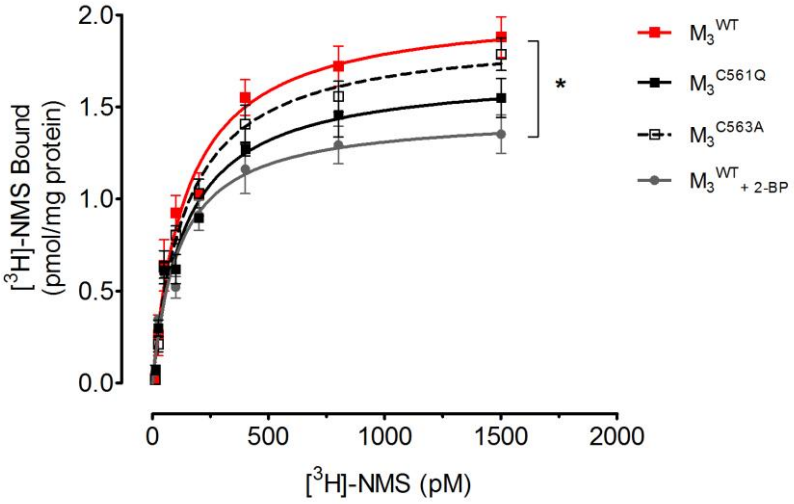


**Figure 17**. COS-7 cells transiently expressing $M_3R^{WT}$, $M_3R^{C561AQ}$ or $M_3R^{C563A}$ were lysed in CelLytic$^{TM}$ buffer. Membrane preparations were incubated with [$^3$H]-NMS in Hepes buffer at 30ºC for 2 h. Non-specific binding was measured using 10 µM atropine. Saturation binding data were analyzed using nonlinear curve-fitting using Prism 5.0. Data are presented as means ± S.E.M of three independent experiments, each one performed in duplicate. Chemical blockage of $M_3R$ palmitoylation by 2-bromopalmitate (2-BP) was used as a control. *: Significantly different compared to 2-bromopalmitate treated cells (two-way ANOVA *$P$<0.05).

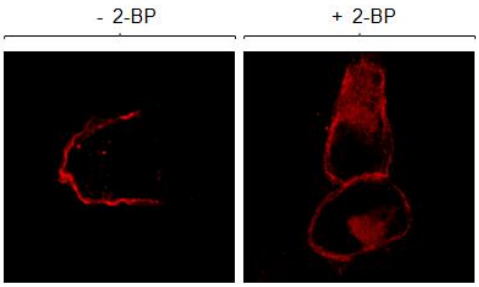

**Figure 18.** Subcellular localization of the $M_3R$ expressed in COS-7 cells with/without 2-bromopalmitated (2-BP) treatment. After fixation and permeabilization, the cells were immunostained with rabbit anti-$M_3R$ antibody followed Texas Red-conjugated goat anti-rabbit IgG *(red)*. Images are representative of two separate indirect immunofluorescence experiments acquired by confocal microscope.

## Discussion

In this study, we describe solubilization and affinity purification of M3R from transiently transfected COS-7 cells; characterize aspects of the biochemistry of the purified receptor demonstrating that receptor is decorated by N-linked glycosylation and palmitoylation.

The complex relationship between a membrane protein and the lipids in lipid bilayer makes the choice of a proper detergent for a particular GPCR solubilization a complicate process, and solubilizing agent selection depend of particular receptor and cell type [25,26]. We examined some critical parameters for effective muscarinic receptor solubilization previously analyzed [27,28] and starting with different detergents and combinations taking into consideration previous results [3]. Triton X-100 results in a large increase of total protein concentration in the soluble fraction. Triton X-100 has conjugated aromatic rings capable of absorbing light in the ultra-violet region, interfering with monitoring of protein at 280 nm. In addition, moderate receptor recovery in the soluble fraction was obtained with Triton X-100. Also, OG showed low solubilization percentage and small [$^3$H]-NMS binding site recovery in soluble fractions. A similar behavior was observed for Tween-80 and sucrose monolaurate. For these reasons these detergents were discarded in future assays.

SDS completely abolishes the fluorescence of the protein. SDS acts by disrupting hydrogen bonds and hydrophobic interactions of proteins, leading to their unfolding. These strong denaturing properties could explain the results obtained. Although in our study, the total protein concentration assay showed a good solubilization of membrane homogenates, we have limited its use to SDS-PAGE electrophoresis. The use of CTAB yields a relatively good COS-7 membrane

homogenate solubilization; however, it results in a low level of functional M3R. This effect is perhaps not as dramatic as SDS-induced denaturation, but it apparently affects the native conformation of the receptor leading to low receptor recovery in comparison to what is obtained by other solubilizing agents. Nevertheless, data reported suggest that some GPCRs can be renatured after SDS solubilization by transferring the membrane protein to a renaturing detergent or lipid environment near the host lipid bilayer [29]. Due to the high $M_3R$ solubilization efficiency by SDS, we may explore the use of this aggressive treatment and receptor renaturation in future works.

Among the many types of detergents used in solubilization of membrane proteins, CHAPS together with DG and DDM are usually used for the GPCR solubilization and have been appropriate options in many solubilization and purification experiments [3,4]. Regarding mAChRs, it has been described that CHAPS solubilizes the receptor from rat brain of neonatal and adult [30] and bovine cerebral cortex [31], Although previous reports showed that CHAPS efficiently solubilizes mAChRs [32], in our case CHAPS has demonstrated a satisfactory extraction ability of total protein from COS-7 membrane homogenates, but the soluble fraction resulted in a low recovery of [$^3$H]-NMS binding sites. The solubilization of five different mAChRs produced in insect *Sf9* cells using CHAPS was found to be ineffective, which could support the results obtained [33]. Also, other studies had reported lower percentage of mAChRs solubilization with CHAPS as solubilizing agent [34]. Previous studies have shown that the receptor solubilization efficiency depends on the specific membrane environment of the protein. Lipid membranes of different structures cause variations in the solubilizing agent efficiency, and experimental conditions, from the same receptor expressed in different cellular systems, affect the resulting solubilization yield [35]. Differences in host membrane lipid composition of these cell types probably account for this discrepancy [36]. In fact, CHAPS is able to solubilized DR from rat brain, but it was not efficient for extracting this same receptor from *P. pastoris* [37]. Something similar was reported by Sarramegna et al. in the same host to describe which of the little numbers of detergents, such as CHAPS, digitonin, and deoxycholate can

solubilize the hμOPR from the rat brain membranes, none of these detergents have been able to solubilize the receptor expressed in *P. pastoris* [19].

Digitonin/sodium cholate solubilized 51% of $M_1R$, 36% of $M_2R$, 3% of $M_3R$, 28% of $M_4R$ and 17% of $M_5R$ from insect *Sf9* cells with retention of the [$^3$H]-NMS binding activity. Optimization of solubilizing concentrations using cholate, resulted in solubilization of up to 50-60% for $M_1R$, $M_2R$ and $M_4R$, but only to 25% for $M_5R$ and 7% for $M_3R$ [33]. Although these differences may be due to their cellular membrane composition, these authors suggest that solubility and stability of mAChRs in detergents differ among the subtypes. Similar results have been reported previously [38]. Our results showed that COS-7 cell-expressing $M_3R$ could be solubilized to similar levels as previously reported [39]. In all experiments, the receptor recovery was over 70% of protein bound membrane homogenates. However, fluorescence measurements for $M_3R$-GFP$^2$ and [$^3$H]-NMS binding site recovery in the soluble fraction from a mixture of digitonin/sodium cholate 1% does not significantly differ from those obtained with some of the detergents tested as DDM/NP40. The digitonin concentrations employed to ensure the complete solubilize of $M_3R$ complicates the spectra, and disrupt further $M_3R$ biochemical characterizations, as SDS-PAGE protein migration and mass spectrometry. The low CMC and high micelle molecular weight of digitonin cause that various detergent removal methods are unsuitable for this detergent. In addition, the use of digitonin was ruled out in view of its high price, and the small solubilization rate difference obtained with regard to other detergents or detergent mixtures assayed.

DDM has effectively been used in the solubilization of various GPCRs [3]. In comparison with other detergents used, DDM has excellent stability and spectral properties which makes it quite useful for assessing the protein stability and concentration during the purification process. Additionally, this detergent can be removed by dialysis or size exclusion chromatography. Our results show that it is possible to reach over 60 % recovery of $M_3R$-GFP$^2$ in the soluble fraction. [$^3$H]-NMS binding data suggest that receptor levels in the solubilized fraction are close to those obtained with digitonin/cholate, becoming similar even when using a

mixture of DDM/NP40 1%. Maybe the relatively long alkyl chains of DDM provide $M_3R$ stability through interactions between the hydrophobic chains and the receptor environment, since its micelles would cover most of the hydrophobic regions of the receptor creating an environment close to that of the lipid bilayer. NP40 with a shorter alkyl chain can be more effective in delipidating membrane proteins than other detergents used causing high total protein extraction. DDM longer aliphatic tails avoid excessive disruptions to membrane homogenates, which can lead to form aggregates and loss of functional activity. It is likely that both detergent properties together made some experimental favorable conditions for a good recovery of the receptor from COS-7 membrane homogenates. These results obtained are supported by previous studies, which demonstrated that the combination of several detergents causes a good efficiency of solubilization and stability of GPCRs [40]. Indeed, some GPCRs need the simultaneous use of various detergents for solubilization, for example, the combination of CHAPS/DM/CHS permitted solubilization of the NTS1 receptor with an efficiency of 85%, whereas solubilization with CHAPS/CHS resulted in an efficiency of 35% against 30% with DDM alone [41]. Furthermore, for purification and spectroscopic characterization of functional hAR2A receptor in *S. cerevisiae*, a combination of added CHS/CHAPS -after initial solubilization with DDM- was required to stabilize the functional state of the protein [42].

Pre-incubation with specific ligands has been used to increase the stability of the protein during GPCR solubilization [43]. The stability of rat $M_3R$ expressed in insect and solubilized with digitonin was increased by the specific ligand propylbenzylcholine incubation prior to receptor solubilization [44]. Nevertheless, the functional solubilization by a mixture of digitonin/CHS of different mAChRs is independent of pre-stabilization by any ligand [33]. We observed that the presence of $M_3R$ ligand improve receptor stability. In addition, adding 100 µM of CHS causes a rise in half-life of the solubilized receptor up to 35 days. This increase on receptor stability can be interpreted as the agonist binding helps to stabilize the folded conformation of the receptor and CHS stabilize the receptor conformation in soluble fraction.

In this study, we provided an efficient way to produce significant amount of functional $M_3R$ respect to receptor level of star preparation. IMAC have been widely used with good results in GPCR purification [20], and previously have been reported that the introduction of epitope tag to N-terminal or C-terminal no affect $M_3R$ functionality [12-15]. In this study, using IMAC and HA affinity purification we obtained clear specific band corresponding to $M_3R$ in SDS-PAGE analysis, confirmed by MALDI-TOF mass spectrometric analysis and producing 14129.84 and 8497.31 pmol/ml respectively that represent an 56 and 33% respect membrane-bound $M_3R$ preparation, and 86% and 51% respect to $M_3R$ at solubilized fraction. However, we did not produced great amount of $M_3R$ for structural studies, only just produced $M_3R$ in level that permitted make functional assays. Maybe great amounts of $M_3R$ could be produced in another expression system using our purifications strategy. COS-7 cells grow only as adherent monolayers on cell culture dishes and for large-scale $M_3R$ production purposes, many dishes of cells would be needed. This implies a time-consuming and expensive process. Recently development describing transient transfection of suspension grown HEK293 cells [53] and CHO-K1-S cells [45], as well as codon optimization for increased of $M_3R$ expression, should be considered. Those advances should permit easy large-scale $M_3R$ production in mammalians cells, guaranteeing proper post-translational modifications. Our findings, three peptides were detected using MALDI-TOF mass spectrometry analysis confirming specificity of $M_3R$ band obtained. Trypsin digestion produces large hydrophobic peptides that do not ionize well using MALDI mass spectrometry. Chemical digestion, for example cyanogen bromide, can replace enzymatic digestion [46]. However, $M_3R$ not have enough number of methionines sufficiently spaced allowing cyanogen bromide cleavage generating properly peptides for MS analysis. Large yield of appropriate size peptides for MS analysis is likely to occur using a combination of trypsin and cyanogen bromide cleavage [47].

N-linked glycosylation is the most common post-translational modification of GPCRs with approximately 70-90% of occurrence in the consensus sequences [48]. Increasing amounts of evidence support that core N-glycan contributes to

important roles in GPCRs expression, structure and/or function [48-51]. Although all mAChRs contain putative N-glycosylation sites only few reports with differing results, which have been published for N-glycosylation of mAChRs [52]. Currently, no investigation has been reported regarding N-linked glycosylation of human $M_3R$. In our current study, by Western blot analysis, comparing enzymatic deglycosylation of solubilized and purified receptor with the same sample without treatment, we provide evidence that $M_3R$ is glycosylated in some or all potential N-glycosylation sites. In addition, comparing electrophoretic migration of five putative sites for asparagine-linked glycosylation with the wild-type receptor we suggest a possible map for N-glycosylation in this cell type. Also, our data showed the presence of a higher molecular weight band in the wild-type and N-glycosylation deficient mutants, presumably corresponding to dimer species, suggesting that simple point of glycosylation is not required for the formations of this molecular species. In agree with previous results [53], our finding suggest that TM-treated cells clearly affects the receptor expression levels at membrane plasmatic and slightly change on binding affinity for [$^3$H]-NMS. Confocal microscopy confirmed this observation, showing a $M_3R$ expressed in TM-treated cells mainly at intracellular compartments. However, TM can affect indirectly receptor expression [54], so the specific role of N-glycan chain in receptor expression/function would need further research.

Similarly, to other posttranslational modifications, the acylation of $M_3R$ is poorly known. With this aim, by specific non-radiolabel Btn-BMCC cross-linking to the M3R we provide evidence that receptor contains covalently bound palmitic acid. The labelled with [$^3$H]-palmitate, followed by receptor immunoprecipitation, SDS-PAGE and autoradiography of wild-type receptor and simple palmitoylation deficient mutants confirmed this observation. Our autoradiogram finding suggests $Cys^{561}$ and $Cys^{563}$ of $M_3R$ as the preferred palmitoylation sites. In addition, 2-BP treatment, blocking receptor palmitoylation not has significant effect on pharmacological properties and subcellular distribution of $M_3R$. Palmitoylation was no required for interaction of $M_2R$ with Gi proteins, but enhances the ability of the receptor to interact with Gi proteins and was induced by agonist binding [55].

The muscarinic subtype signaling cascade difference suggests that these results may not be extrapolated to $M_3R$, needing clarifies the role of palmitoylation affecting the interaction with Gq protein.

Collectively, our results showed that a combination of DDM/NP40/CHS is able to keep the $M_3R$ stable in solution, and allowed the tagged receptor to be purified in a functional form by a combination of purifications methods, such as IMAC followed Flag affinity chromatography as judged by Western blot, radioligand-binding experiments and MALDI-TOP analysis. In addition, we provide evidences for $M_3R$ suffers higher post-translational modifications and suggest a possible map site for N-glycosylation and palmytoilation occurrence in COS-7 cells.

## References

[1] Eglen, R.M. (2006). Muscarinic receptor subtypes in neuronal and non-neuronal cholinergic function. Auton Autacoid Pharmacol 26, 219-33.

[2] Peretto, I., Petrillo, P. and Imbimbo, B.P. (2009). Medicinal chemistry and therapeutic potential of muscarinic M3 antagonists. Med Res Rev 29, 867-902.

[3] Sarramegn, V., Muller, I., Milon, A. and Talmont, F. (2006). Recombinant G protein-coupled receptors from expression to renaturation: a challenge towards structure. Cell Mol Life Sci 63, 1149-64.

[4] Sarramegna, V., Talmont, F., Demange, P. and Milon, A. (2003). Heterologous expression of G-protein-coupled receptors: comparison of expression systems fron the standpoint of large-scale production and purification. Cell Mol Life Sci 60, 1529-46.

[5] Massotte, D. (2003). G protein-coupled receptor overexpression with the baculovirus-insect cell system: a tool for structural and functional studies. Biochim Biophys Acta 1610, 77-89.

[6] Andre, C., De Backer, J.P., Guillet, J.C., Vanderheyden, P., Vauquelin, G. and Strosberg, A.D. (1983). Purification of muscarinic acetylcholine receptors by affinity chromatography. EMBO J 2, 499-504.

[7] Peterson, G.L., Herron, G.S., Yamaki, M., Fullerton, D.S. and Schimerlik, M.I. (1984). Purification of the muscarinic acetylcholine receptor from porcine atria. Proc Natl Acad Sci U S A 81, 4993-7.

[8] Ma, A.W., Pawagi, A.B. and Wells, J.W. (2008). Heterooligomers of the muscarinic receptor and G proteins purified from porcine atria. Biochem Biophys Res Commun 374, 128-33.

[9] Haga, K. and Haga, T. (1985). Purification of the muscarinic acetylcholine receptor from porcine brain. J Biol Chem 260, 7927-35.

[10] Alberts, P. and Bartfai, T. (1976). Muscarinic acetylcholine receptor from rat brain. Partial purification and characterization. J Biol Chem 251, 1543-7.

[11] Peterson, G.L., Toumadje, A., Johnson, W.C., Jr. and Schimerlik, M.I. (1995). Purification of recombinant porcine m2 muscarinic acetylcholine receptor from Chinese hamster ovary cells. Circular dichroism spectra and ligand binding properties. J Biol Chem 270, 17808-14.

[12] Park, P.S. and Wells, J.W. (2003). Monomers and oligomers of the M2 muscarinic cholinergic receptor purified from Sf9 cells. Biochemistry 42, 12960-71.

[13] Parker, E.M., Kameyama, K., Higashijima, T. and Ross, E.M. (1991). Reconstitutively active G protein-coupled receptors purified from baculovirus-infected insect cells. J Biol Chem 266, 519-27.

[14] Hayashi, M.K. and Haga, T. (1996). Purification and functional reconstitution with GTP-binding regulatory proteins of hexahistidine-tagged muscarinic acetylcholine receptors (m2 subtype). J Biochem 120, 1232-8.

[15] Zeng, F.Y. and Wess, J. (1999). Identification and molecular characterization of m3 muscarinic receptor dimers. J Biol Chem 274, 19487-97.

[16] Haga, K. and Haga, T. (1983). Affinity chromatography of the muscarinic acetylcholine receptor. J Biol Chem 258, 13575-9.

[17] Drisdel, R.C., Alexander, J.K., Sayeed, A. and Green, W.N. (2006). Assays of protein palmitoylation. Methods 40, 127-34.

[18] Borroto-Escuela, D.O., Correia, P.A., Perez Alea, M., Narvaez, M., Garriga, P., Fuxe, K. and Ciruela, F. Impaired M(3) muscarinic acetylcholine receptor signal transduction through blockade of binding of multiple proteins to its third intracellular loop. Cell Physiol Biochem 25, 397-408.

[19] Sarramegna, V., Muller, I., Mousseau, G., Froment, C., Monsarrat, B., Milon, A. and Talmont, F. (2005). Solubilization, purification, and mass spectrometry analysis of the human mu-opioid receptor expressed in Pichia pastoris. Protein Expr Purif 43, 85-93.

[20] Grisshammer, R. and Tucker, J. (1997). Quantitative evaluation of neurotensin receptor purification by immobilized metal affinity chromatography. Protein Expr Purif 11, 53-60.

[21] Zhang, Y. (2008). I-TASSER server for protein 3D structure prediction. BMC Bioinformatics 9, 40.

[22] Zhang, Y. (2009). I-TASSER: fully automated protein structure prediction in CASP8. Proteins 77 Suppl 9, 100-13.

[23] Furukawa, H. and Haga, T. (2000). Expression of functional M2 muscarinic acetylcholine receptor in Escherichia coli. J Biochem 127, 151-61.

[24] Tota, M.R., Kahler, K.R. and Schimerlik, M.I. (1987). Reconstitution of the purified porcine atrial muscarinic acetylcholine receptor with purified porcine atrial inhibitory guanine nucleotide binding protein. Biochemistry 26, 8175-82.

[25] Prive, G.G. (2007). Detergents for the stabilization and crystallization of membrane proteins. Methods 41, 388-97.

[26] Seddon, A.M., Curnow, P. and Booth, P.J. (2004). Membrane proteins, lipids and detergents: not just a soap opera. Biochim Biophys Acta 1666, 105-17.

[27] Peterson, G.L., Rosenbaum, L.C. and Schimerlik, M.I. (1988). Solubilization and hydrodynamic properties of pig atrial muscarinic acetylcholine receptor in dodecyl beta-D-maltoside. Biochem J 255, 553-60.

[28] Baron, B. and Abood, L.G. (1984). Solubilization and characterization of muscarinic receptors from bovine brain. Life Sci 35, 2407-14.

[29] Dong, M., Baggetto, L.G., Falson, P., Le Maire, M. and Penin, F. (1997). Complete removal and exchange of sodium dodecyl sulfate bound to soluble and membrane proteins and restoration of their activities, using ceramic hydroxyapatite chromatography. Anal Biochem 247, 333-41.

[30] Singh, A.K. (1994). Regulation of the CHAPS-solubilized muscarinic receptors by an inhibitory GTP binding protein (Gi) in the brain of neonatal and adult rats. Comp Biochem Physiol Physiol 109, 255-67.

[31] Shirakawa, O. and Tanaka, C. (1985). Molecular characterization of muscarinic receptor subtypes in bovine cerebral cortex by radiation inactivation and molecular exclusion h.p.l.c. Br J Pharmacol 86, 375-83.

[32] Baron, B., Gavish, M. and Sokolovsky, M. (1985). Heterogeneity of solubilized muscarinic cholinergic receptors: binding and hydrodynamic properties. Arch Biochem Biophys 240, 281-96.

[33] Rinken, A., Kameyama, K., Haga, T. and Engstrom, L. (1994). Solubilization of muscarinic receptor subtypes from baculovirus infected Sf9 insect cells. Biochem Pharmacol 48, 1245-51.

[34] Rinken, A. (1996). Formation of the functional complexes of m2 muscarinic acetylcholine receptors with GTP-binding regulatory proteins in solution. J Biochem 120, 193-200.

[35] Babcock, G.J., Mirzabekov, T., Wojtowicz, W. and Sodroski, J. (2001). Ligand binding characteristics of CXCR4 incorporated into paramagnetic proteoliposomes. J Biol Chem 276, 38433-40.

[36] Staudinger, R. and Bandres, J.C. (2000). Solubilization of the chemokine receptor CXCR4. Biochem Biophys Res Commun 274, 153-6.

[37] de Jong, L.A., Grunewald, S., Franke, J.P., Uges, D.R. and Bischoff, R. (2004). Purification and characterization of the recombinant human dopamine D2S receptor from Pichia pastoris. Protein Expr Purif 33, 176-84.

[38] Rinken, A. and Haga, T. (1993). Solubilization and characterization of atrial muscarinic acetylcholine receptors in sucrose monolaurate. Arch Biochem Biophys 301, 158-64.

[39] Han, S.J., Hamdan, F.F., Kim, S.K., Jacobson, K.A., Bloodworth, L.M., Li, B. and Wess, J. (2005). Identification of an agonist-induced conformational change occurring adjacent to the ligand-binding pocket of the M(3) muscarinic acetylcholine receptor. J Biol Chem 280, 34849-58.

[40] le Maire, M., Champeil, P. and Moller, J.V. (2000). Interaction of membrane proteins and lipids with solubilizing detergents. Biochim Biophys Acta 1508, 86-111.

[41] Tucker, J. and Grisshammer, R. (1996). Purification of a rat neurotensin receptor expressed in Escherichia coli. Biochem J 317 ( Pt 3), 891-9.

[42] O'Malley, M.A., Lazarova, T., Britton, Z.T. and Robinson, A.S. (2007). High-level expression in Saccharomyces cerevisiae enables isolation and spectroscopic characterization of functional human adenosine A2a receptor. J Struct Biol 159, 166-78.

[43] Liitti, S., Matikainen, M.T., Scheinin, M., Glumoff, T. and Goldman, A. (2001). Immunoaffinity purification and reconstitution of human alpha(2)-adrenergic receptor subtype C2 into phospholipid vesicles. Protein Expr Purif 22, 1-10.

[44] Vasudevan, S., Hulme, E.C., Bach, M., Haase, W., Pavia, J. and Reilander, H. (1995). Characterization of the rat m3 muscarinic acetylcholine receptor produced in insect cells infected with recombinant baculovirus. Eur J Biochem 227, 466-75.

[45] Rosser, M.P. et al. (2005). Transient transfection of CHO-K1-S using serum-free medium in suspension: a rapid mammalian protein expression system. Protein Expr Purif 40, 237-43.

[46] Kraft, P., Mills, J. and Dratz, E. (2001). Mass spectrometric analysis of cyanogen bromide fragments of integral membrane proteins at the picomole level: application to rhodopsin. Anal Biochem 292, 76-86.

[47] Quach, T.T., Li, N., Richards, D.P., Zheng, J., Keller, B.O. and Li, L. (2003). Development and applications of in-gel CNBr/tryptic digestion combined with mass spectrometry for the analysis of membrane proteins. J Proteome Res 2, 543-52.

[48] Markkanen, P.M. and Petaja-Repo, U.E. (2008). N-glycan-mediated quality control in the endoplasmic reticulum is required for the expression of correctly folded delta-opioid receptors at the cell surface. J Biol Chem 283, 29086-98.

[49] Lanctot, P.M., Leclerc, P.C., Escher, E., Guillemette, G. and Leduc, R. (2006). Role of N-glycan-dependent quality control in the cell-surface expression of the AT1 receptor. Biochem Biophys Res Commun 340, 395-402.

[50] Roy, S., Perron, B. and Gallo-Payet, N. Role of asparagine-linked glycosylation in cell surface expression and function of the human adrenocorticotropin receptor (melanocortin 2 receptor) in 293/FRT cells. Endocrinology 151, 660-70.

[51] Duvernay, M.T., Filipeanu, C.M. and Wu, G. (2005). The regulatory mechanisms of export trafficking of G protein-coupled receptors. Cell Signal 17, 1457-65.

[52] Nathanson, N.M. (2008). Synthesis, trafficking, and localization of muscarinic acetylcholine receptors. Pharmacol Ther 119, 33-43.

[53] Liles, W.C. and Nathanson, N.M. (1986). Regulation of neuronal muscarinic acetylcholine receptor number by protein glycosylation. J Neurochem 46, 89-95.

[54] van Koppen, C.J. and Nathanson, N.M. (1990). Site-directed mutagenesis of the m2 muscarinic acetylcholine receptor. Analysis of the role of N-glycosylation in receptor expression and function. J Biol Chem 265, 20887-92.

[55] Hayashi, M.K. and Haga, T. (1997). Palmitoylation of muscarinic acetylcholine receptor m2 subtypes: reduction in their ability to activate G proteins by mutation of a putative palmitoylation site, cysteine 457, in the carboxyl-terminal tail. Arch Biochem Biophys 340, 376-82.

# CHAPTER 4

## ALTERED TRAFFICKING AND UNFOLDED PROTEIN RESPONSE INDUCTION AS A RESULT OF $M_3$ MUSCARINIC RECEPTOR IMPAIRED N-GLYCOSYLATION

(contents of this chapter is a manuscript submitted for publications in Glycobiology Journal)

## Altered trafficking and unfolded protein response induction as a result of $M_3$ muscarinic receptor impaired N-glycosylation


### Abstract

The human $M_3$ muscarinic acetylcholine receptor is present in both the central and peripheral nervous system, and it is involved in the pathophysiology of several neurodegenerative and autoimmune diseases. We previously suggested a possible N-glycosylation map for $M_3$ muscarinic receptor expressed in COS-7 cells. Here, we examined the role that N-linked glycans play in the folding and cell surface trafficking of this receptor. The five potential asparagine-linked glycosylation sites in muscarinic receptor were mutated and expressed in COS-7 cells. The elimination of N-glycan attachment sites did not affect the cellular expression levels of the receptor. However, proper receptor localization to the plasma membrane was affected as suggested by reduced [$^3$H]-N-methylscopolamine binding. Confocal microscopy confirmed this observation, and showed that the non-glycosylated receptor was primarily localized in the intracellular compartments. The mutant variant showed an increase in phosphorylation of the α-subunit of eukaryote initiation factor 2, and other well-know endoplasmic reticulum stress-markers of the unfolded protein response pathway, which further supports the proposal of the improper intracellular accumulation of the non-glycosylated receptor. The receptor devoid of glycans showed more susceptibility to apoptosis and reduced cell viability. Our findings suggest up-regulation of pro-apoptotic Bax protein, down-regulation of anti-apoptotic Bcl-2, and cleavage of caspase-3 effectors. Collectively, our data provide the first experimental evidence of the critical role that N-glycan chains play in determining muscarinic receptor distribution and localization, as well as in cell integrity.

## Introduction

The human $M_3$ muscarinic acetylcholine receptor ($M_3R$) is a member of the G-protein-coupled receptor (GPCR) superfamily and is present in the central and peripheral nervous system. This receptor is one of the five muscarinic subtypes ($M_1$-$M_5$) which mediate important cellular functions, and it has been linked to several neurodegenerative and autoimmune diseases including diabetes type 2, Sjögren's syndrome, chronic obstructive pulmonary disease, overactive bladder, obesity, irritable bowel syndrome, gastrointestinal spasms, wound healing and cancer [1].

As a membrane receptor protein, newly synthesized $M_3R$ undergoes important modifications such as N-glycosylation and disulfide bond formation during its biosynthesis and translational processes to the endoplasmic reticulum (ER) membrane [2]. Only receptors properly folded and assembled are transported from the ER to the *cis*-Golgi complex in a process termed 'quality control' [3]. This surveillance mechanism ensures that unfolded or misfolded proteins are retained in the ER lumen by molecular chaperones or carried to 26S proteasome for degradation through either ER-associated degradation or autophagy [4,5].

The excessive accumulation of unfolded proteins or misfolded protein aggregates into insoluble structures causes ER-stress and it is associated with various human diseases such as metabolic alterations, atherosclerosis, neurodegenerative diseases, and ischemia [6-8]. When the survival and adaptative mechanism to overcome the ER stress is not sufficient to restore ER homeostasis, a persistent unfolded protein response (UPR) signalling occurs and the cell could enters into programmed cell death [9]. Multiple UPR pathways have been proposed to contribute to ER stress-induced cell apoptosis, although the mechanism remains mostly unknown [10,11]. Recently, this apoptotic process has been reported to be mediated by factors, including C/EBP homologous protein (CHOP)/GADD153, apoptosis signal-regulating kinase 1 (ASK1) and caspase-12 [12].

Although N-linked glycosylation is the most common post-translational modification of GPCRs with approximately 70-90% of occurrence in the consensus

sequences, only few studies, with differing results, have been reported to date for their role in muscarinic acetylcholine receptors (mAChRs) [13]. The molecular mechanism underlying the role of N-glycosylation in maturation and transport to the plasma membrane of muscarinic receptors remains to be clarified. With this aim, we previously expressed the five potential N-glycosylation-site-deficient mutants of $M_3R$ in COS-7 cells. Western blot analysis suggested that four of them were glycosylated. In addition, non-significant changes in receptor level and [$^3$H]-N-methylscopolamine binding at the cell surface -determined by a saturation assay- were detected when point mutations were introduce into the receptor sequence at the N-glycosylation sites. However, both the binding assay and confocal microcopy showed that the lack of all glycosylation sites -produced by the treatment with tunicamycin- caused a significant decrease in the transport of the receptor to the plasma membrane, showing intracellular perinuclear localization *(Romero-Fernandez et al., in preparation)*. Here, we have studied a mutant receptor where the five putative glycosylation sites have been mutated (N-glycosylation deficient mutant receptor, nGly-$M_3R$). We have determined relevant features of the role of N-linked glycosylation in human $M_3R$ expressed in COS-7 cells by means of biochemical, ligand-binding and cellular approaches. Our findings suggest a role of N-glycan chains in the correct cellular processing of M3R. Furthermore, lack of glycosylation would make the receptor more prone to intracellular accumulation and could trigger cell apoptosis.

## Materials and Methods

### Generation of $M_3R$ N-glycosylation deficient mutant

To generate cDNA constructs encoding nGly-$M_3R$, asparagine residues in each glycosylation consensus sequence of WT-$M_3R$ were replaced with glutamine residues using the Quick-Change site-directed mutagenesis kit (Stratagene, La Jolla, CA, USA). Mutations were confirmed by DNA sequencing. The primers (from Sigma Aldrich, St. Louis, MO, USA) used for mutagenesis (5'→3') were as follows: $M_3R^{N5Q}$: 5'-gAgAgTCACAATgACCTTgCACCAgAACAgTACAACCTCgCCTTTg-3'.

$M_3R^{N6Q}$: 5'-gAgAgTCACAATgACCTTgCACAATCAgAgTACAACCTCgCCTTTg-3'. $M_3R^{N15Q}$: 5'-CCTCgCCTTTgTTTCCACAgATCAgCTCCTCCTgg-3'. $M_3R^{N41Q}$: 5'-CATTTCggCAgCTACCAggTTTCTCgAgCAgCTggC-3'. $M_3R^{N48Q}$: 5'-CTCgAgCAgCTggCCAgTTCTCCTCTCCAgACgg-3'.

## Cell culture and transfection

COS-7 cells (American Type Culture Collection) were grown in Dulbecco's modified Eagle's medium (DMEM), supplemented with 2 mM of L-glutamine, 100 units/ml penicillin, 100 µg/ml streptomycin, and 10% (v/v) fetal bovine serum (Invitrogen, Carlsbad, CA, USA) at 37°C and in an atmosphere of 5% $CO_2$. For transfection, cells were grown in 6-well dishes at a concentration of $1\times10^6$ cells/well or in 75cm$^2$ flasks and cultured overnight before transfection. Cells were transiently transfected either using linear Polyethylenimine transfection reagent (Polysciences Inc., Warrington PA, USA) or Fugene® HD transfection reagent (Roche Applied Science, Indianapolis, USA), according to the manufacturer's protocol. As an ER-stress control, cells were incubated, at 4 h post-transfection, in the absence or presence of 5 µg/ml tunicamycin (Sigma Aldrich) and cells were harvested after 48 h. Apoptosis was induced in grown COS-7 cells by the addition of hydrogen peroxide at a concentration of 100 µM for 15 h before assays.

## Cell membrane preparation and solubilization

About 48 h after transfection, COS-7 cells were washed twice with ice-cold phosphate buffered saline (PBS), scraped in ice-cold buffer containing 50 mM Tris-HCl, pH 7.4, 5 mM $MgCl_2$ and protease inhibitor cocktail (Roche Diagnostics, Mannheim, Germany). Samples were subjected to centrifugation for 5 min at 500 × g, and pellets were homogenized using a Polytron tissue homogenizer (for 30 s, five times each 30 seconds on ice) followed by centrifugation at 1000 x g for 5 min at 4°C to remove unbroken cells and nuclei. The supernatant fraction was removed and passed through a 25-gauge needle 10 times before being transferred to ultracentrifuge tubes and subjected to centrifugation at 40,000 x g for 30 min at 4°C. The resulting membrane pellets were resuspended in buffer containing 10 mM

Tris-HCl, pH 7.4, 5 mM $MgCl_2$. In some cases, membrane pellets were incubated in solubilization buffer containing 50 mM Tris–HCl, pH 7.4, 150 mM NaCl, 1 mM $CaCl_2$, 1 mM $MgCl_2$, 1% of glycerol, protease inhibitor cocktail, and a mixture of n-dodecyl-β-D-maltoside and Nonited P40 (1%) during 1 h at 4°C. Solubilized membrane proteins were recovered by collection of the supernatant, after ultra-centrifugation at 100,000 x g for 30 min at 4°C. Membrane homogenates and solubilized membrane protein concentrations were determined by means of a Bradford protein assay kit (Bio-Rad, Hercules, CA, USA), using bovine serum albumin (BSA) as standard. Samples were immediately used or stored at -80°C until required.

For p-eIF2α blocking experiments, used as a control, twice the volume of blocking peptide (10 µg/ml) was incubated with one volume of an antibody against p-eIF2α (Cell Signaling Technology). After 45 min at room temperature, p-eIF2α was subjected to immunoblotting as described below.

## Sodium dodecyl sulfate polyacrylamide gel electrophoresis and Western blotting

Proteins resolved by 12% sodium dodecyl sulfate polyacrylamide **(**SDS-PAGE) were subjected to immunoblotting onto PVDF membranes (Millipore, Bedford, MA, USA) using a semidry transfer system. Membranes were blocked for 1 h in 5% BSA or nonfat dry milk, Tris-buffered saline, pH 7.4 with 0,1% Tween-20 (TBST) prior to overnight incubation with primary antibody under mild agitation at 4°C. Proteins were detected with the following primary antibody: horseradish-peroxidase conjugated goat anti-rabbit IgG (HRP) (Cell Signaling Technology, USA). Membranes were washed and developed, using the enhanced Super Signal chemiluminescence's detection kit (ECL) (Pierce Biotechnology, Rockford, IL, USA), and HyBlot CL autoradiography film (Denville Scientific, Metuchen, NJ, USA) using ChemiDocTM XRS (Bio-Rad). The primary antibodies used were as follows: rabbit anti-$M_3$ (Santa Cruz Biotechnology, Santa Cruz, CA, USA); GRP78/Bip, phosphorylated-eIF2α and total eIF2α, Bax, Bcl-2 and caspase-3, were all from Cell Signaling Technology.

## Immunoblotting for total and phosphorylated ERK1/2

COS-7 cells transiently expressing WT-$M_3R$ and nGly-$M_3R$ were rendered quiescent by serum starvation overnight prior to ERK phosphorylation. Subsequently, an additional 2 h pre-incubation step, in fresh serum-free medium, was performed to minimize basal activity before cells were challenged with the muscarinic agonist carbachol for the time and concentration indicated (100 µM for 5 min). Next, a rapid rinsing with ice-cold PBS was performed in order to finish stimulation, and before cells were lysed with 500 µl ice-cold lysis buffer (50 mM Tris–HCl, pH 7.4, 150 mM NaCl, 1% Triton X-100, protease and phosphatase inhibitor cocktail) during 10 min. The cellular debris was removed by centrifugation at 10,000 × *g* for 5 min at 4°C, and the total protein content was measured using BCA Protein Assay Reagent (Pierce Biotechnology). Aliquots corresponding to 20 µg of protein were mixed with SDS-PAGE sample buffer, separated by 12% SDS-PAGE and analyzed by immunobloting. Membranes were blotted for total-44/42 MAPK (Erk1/2) and phosphorylated-44/42 MAPK (p-Erk1/2) using polyclonal antibodies, followed HRP-conjugated goat anti-rabbit IgG as a secondary antibody as described, all from Cell Signalling Technology. Immunoreactivity bands were visualized as described above and then measured by quantitative densitometry.

## In-Cell Western immuno-fluorescent assay

The CHOP level was measured by In Cell-Western blot. COS-7 cells were seeded onto poly-D-lysine-coated 96-well plates (Corning, Corning, NY, USA) in DMEM, and were transiently transfected as described above with WT-$M_3R$ or nGly-$M_3R$. Cells treated with tunicamycin 4 h after transfection, and harvested 48 h post-transfection, were used as an ER-inducer control. Following fixation, permeabilization, and blocking with LI-COR Odyssey Blocking Buffer® (LI-COR Bioscience, UK), cells were incubated overnight at 4°C with polyclonal antibody against CHOP (Cell Signaling Technology). After further washing, cells were incubated with an infrared secondary antibody (goat anti-mouse, 1:1500 dilution, LI-COR Bioscience) in LI-COR Odyssey Blocking Buffer® and plates were

scanned by Odyssey infrared scanner. Total number was normalized using DRAQ5/Sapphire 700 staining agents. Results are presented as arbitrary units.

### Immunocytochemistry Staining

Cells were cultured on 35-mm glass coverslips coated with 0.1 mg/ml poly-D-lysine (Sigma Aldrich) in 6-well dishes as described above. Cells were grown at a concentration of $1\times10^6$ cells/well and transfected as described. After 48 h cells were washed in PBS and fixed with 3.7% formaldehyde solution for 20 min at room temperature followed by two washes with PBS containing 20 mM glycine (buffer A). Then, after permeabilization with buffer A containing 0.2% (v/v) Triton X-100/PBS for 5 min at room temperature, cells were treated with buffer A containing 5% BSA. After 1 h, cells were labelled with rabbit anti-$M_3$R antibody (Santa Cruz Biotechnology) for 1 h at 37°C, extensively washed, and stained with goat anti-rabbit IgG-fluorescein isothiocyanate-conjugated (FITC) (Santa Cruz Biotechnology) in the same manner. Washed samples were rinsed and mounted onto glass slides using fluorescent mounting medium (Dako). Microscope observations were performed with a Leica TCS-SL confocal microscope (Leica).

### Muscarinic receptor radioligand binding assay

The binding of [$^3$H]-NMS (81 Ci/mmol, Perkin-Elmer Life Sciences) and [$^3$H]-QNB (42 Ci/mmol, Amersham Life Biosciences) were performed according to a few modification of the methodologies described previously [14,15]. In brief, COS-7 cells expressing WT-$M_3$R or nGly-$M_3$R were harvested by trypsinization followed by centrifugation and resuspension in iso-osmotic Hepes buffer. Cells (100,000 cells/1 ml assay by hemocytometer counting) were then incubated with different concentrations of [$^3$H]-NMS or [$^3$H]-QNB (ranging from 0.25 pM to 1500 pM) in DMEM buffered with Hepes at 4°C, overnight. Non-specific binding was assessed in the presence of 10 µM atropine. Only for [$^3$H]-QNB ligand dissociation from cell-surface, a stringent wash after ligand incubation was use (acid wash buffer: 10 mM MES, pH 5.0 (2-[N-morpholino] ethane sulfonic acid), 120 mM NaC1, 0.9 mM $CaC1_2$, and 0.5 mM $MgC1_2$). Bound ligand was separated from free ligand by vacuum filtration over Whatman GF/B filters that had been pretreated

with 0.5% polyethyleneimine for 3 h using a Brandel cell harvester (Brandel Inc., Gaithersburg, MD, USA). The filters were washed three times with 5 ml of ice-$H_2O$. Cells were incubate in 0.5% (v/v) Triton-X 100/PBS for 1 h, add 4 ml scintillant and the bound ligand was estimated by scintillation counting.

## [$^{35}$S]-GTPγS binding assays

The guanosine 5'-[γ-$^{35}$S]-thiotriphosphate ([$^{35}$S]-GTPγS, 1250 Ci/mmol Perkin-Elmer Life Sciences) binding assays were conducted as a modification of the described previously method [16]. Briefly, membrane homogenate fractions (100 μg protein/ml) were incubated with 0.3 nM [$^{35}$S]-GTPγS and 1 μM guanosine-5'-diphosphate (GDP, Sigma Aldrich), in the absence or in the presence of carbamoylcholine chloride (Cch, from 1 nM to 1 mM) in 1 ml of 10 mM Hepes, pH 7.4, 10 mM $MgCl_2$, 1 mM EGTA, 100 mM NaCl, 0,2% BSA and 10 μg/ml saponin. Reactions were incubated at 30°C for 1 h. Non-specific binding was determined by incubation of samples in the presence of 10 μM unlabeled GTPγS. Reactions were stopped by addition of 5 ml of ice-cold assay buffer, immediately followed by rapid filtration through Whatman GF/C filters presoaked in the same buffer containing 0.5% polyethyleneimine. The washed filters were dry and resuspended in 4 ml scintillation cocktail, vortex mixed and radioactivity was detected by liquid scintillation counting.

## Cell viability assay

To estimate cell viability, COS-7 cells expressing wild-type or N-glycosylation deficient receptors were seeded ($5\times10^3$) into 96-well plates (BD Biosciences) in 200 μl of DMEM and incubated at 37°C, 5% $CO_2$. After culturing for 24 h, 20 μl of the CellTiter 96® Aqueous One Solution (3-(4,5-dimethylthiazol-2-yl)-5-(3-carboxymethoxyphenyl)-2-(4-sulfophenyl)-2H-tetrazolium (MTS), Promega, Madison, WI, USA) (MTS) were added to each well and cells were then incubated for 1 h in a 37°C, 5% $CO_2$. 25 μl of 10% SDS were added to stop the reaction, and absorbance was measured at 492 nm using POLARstar Optima plate reader (BMG Labtechnologies, Offenburg, Germany).

## Statistical analysis

All binding data were analyzed using the commercial program GraphPad PRISM 5.0 (GraphPad Prism). Statistical analyses were performed using unpaired Student's *t*-test or one/two-way ANOVA. The number of samples in each experimental condition is indicated in figure legends. Differences were considered statistically significant when *P* values were <0.05. Values are expressed as means ± S.E.M.

## Results

### 4.1 $M_3R$ expressed in COS-7 cells is glycosylated and loss of N-glycan chains promotes intracellular receptor accumulation

$M_3R$ contain five-consensus sequence for N-linked glycosylation as deduced from the amino acid sequence. We previously showed by Western blot analysis of point N-glycosylation mutants that four sites (N5, N15, N41 and N48) were glycosylated *(Romero-Fernandez et al., in preparation)*. Here, the role of the $M_3R$ putative N-glycosylation sites on receptor structure and function was investigated by mutating all potential N-glycosylation sites. The asparagine residues at positions N5, N6, N15, N41 and N48 of wild-type receptor (WT-$M_3R$), were replaced by glutamine generating nGly-$M_3R$. Chemical blockage of $M_3R$ N-glycosylation by tunicamycin was used as a control.

Solubilized membrane proteins from tunicamycin treated-COS-7 cells expressing WT-$M_3R$ and cells expressing nGly-$M_3R$ without tunicamycin treatment were separated by SDS-PAGE followed by Western blot analysis using an anti-$M_3R$ antibody. Solubilized $M_3R$, with presumed native N-glycosylation yielded a band at approximately 80 kDa. Immunoblots showed a decrease in the apparent molecular mass of the $M_3R$ band, in both the tunicamycin-treated WT-$M_3R$ and the nGly-$M_3R$, consistent with the lack of N-glycosylation, and suggesting that the uppermost band represents the fully glycosylated form (Fig. 1).

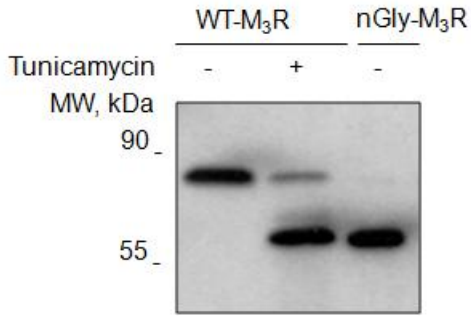


**Figure 1.** $M_3R$ receptor is glycosylated. COS-7 cells transiently expressing $M_3R^{WT}$ with/without tunicamycin-treatment or cells expressing nGly-$M_3R$ without tunicamycin treatment were lysed in CelLytic™ buffer. Solubilized proteins were then resolved on SDS-PAGE, and immunoblotted for $M_3R$ using anti-$M_3R$ antibody and HRP-conjugated goat anti-rabbit IgG as a secondary antibody. Deglycosylated receptor from tunicamycin-treated cells was used as a control. Blots are representative of two independent experiments.

In addition, WT-$M_3R$ and nGly-$M_3R$ were expressed in COS-7 cells, and the cellular distribution was analyzed by immunocytochemistry and confocal microscopy. Different staining patterns were observed in cells expressing the nGly-$M_3R$ compared to WT-$M_3R$ (Fig. 2). nGly-$M_3R$ showed a predominantly intracellular signal; in contrast, the WT-$M_3R$ was mainly localized to the plasma membrane (Fig. 2).

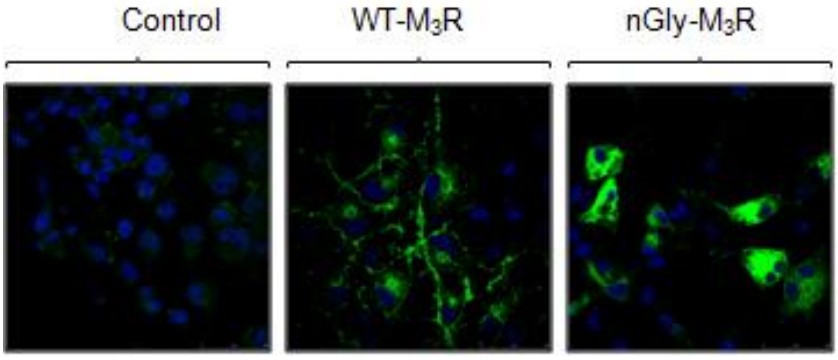


**Figure 2.** Subcellular localization of WT-$M_3R$ and nGly-$M_3R$ transiently expressed in COS-7 cells. After fixation and permeabilization, the cells were immunostained with rabbit anti-$M_3R$ polyclonal antibody followed fluorescein-isothiocyanate-conjugated goat anti-rabbit *(green)*. Nucleis were stained with Hoechst 33342 *(blue)*. Images for indirect immunofluorescence were acquired with confocal microscope. The background signal obtained from non-transfected cells stained with secondary antibody (absence of the primary antibody) was used as a control. Images are representative of three separate experiments. Scale bar equals 10 μm.

Saturation binding assays were performed in order to determine the WT-$M_3$R and nGly-$M_3$R expression levels and pharmacological properties. Radioligand binding experiments were carried out with intact COS-7 cells expressing WT-$M_3$R or nGly-$M_3$R. The total $M_3$R expression level (both surface and internal) was measured using the membrane-permeant antagonist [$^3$H]-quinuclidinyl benzilate ([$^3$H]-QNB) and the intracellular level was determined by [$^3$H]-QNB binding dissociation from the cell-surface with a stringent wash buffer. $M_3$R at the cell surface was measured using the membrane-impermeable antagonist [$^3$H]-N-methylscopolamine, ([$^3$H]-NMS).

The [$^3$H]-QNB binding studies without stringent wash after incubation showed non-significant differences in the total number of nGly-$M_3$R when compared to the number of WT-$M_3$R *(data not shown)*. However, upon [$^3$H]-QNB ligand dissociation from the cell-surface, different receptor expression levels were detected. The mutant showed 3-fold higher receptor level at intracellular compartments as compared to WT-$M_3$R, suggesting intracellular accumulation (Table 1). Furthermore, clear differences in receptor density ($B_{max}$) were observed by means of [$^3$H]-NMS binding measurements. [$^3$H]-NMS binding data showed that nGly-$M_3$R was expressed at the cell surface at over 60% lower levels ($B_{max}$) as compared with WT-$M_3$R (Table 1). The nGly-$M_3$R displayed unchanged binding affinity ($K_D$) for the [$^3$H]-NMS antagonist as compared to WT-$M_3$R receptor. However, a slight effect on $K_D$ for [$^3$H]-QNB could be observed (Table 1).

**Table 1.** Ligand binding data of WT-$M_3$R and nGly-$M_3$R transiently expressed COS-7 cells.

| Receptor | **Binding assay data** | | | |
|---|---|---|---|---|
| | [$^3$H]-NMS | | [$^3$H]-QNB $_{intracellular}$ | |
| | $K_d$ *(pM)* | $B_{max}$ *(fmol/mg)* | $K_d$ *(pM)* | $B_{max}$ *(fmol/mg)* |
| WT-$M_3$R | 180 ± 42 | 1658 ± 214 | 320 ± 43 | 573 ± 88 |
| nGly-$M_3$R | 491 ± 35 | 452 ± 129 | 2897 ± 27 | 1964 ± 155 |

[$^3$H]-NMS and [$^3$H]-QNB binding was performed on intact COS-7 cells. Receptor expression levels were checked after COS-7 cells transfection with variable amount of cDNA up to 2 µg (Table 1 show data for 2 µg cDNA) as indicated. Nonlinear curve-fitting using GraphPad PRISM 5.0 determined dissociation constants ($K_D$) and maximal binding capacities ($B_{max}$). Data are presented as means ± S.E.M of six independent experiments, each one performed in triplicate.

### 4.2 N-glycosylation deficient mutant was able to activate the G protein

We decided to examine two classical steps in the signalling pathway of activated $M_3R$; activation of the G protein and triggering of mitogen-activated protein kinase ERK1/2 pathway. Membrane homogenates were prepared from COS-7 cells expressing WT-$M_3R$ or nGly-$M_3R$, and [$^3$H]-NMS binding was performed to guarantee equal pmol receptor/mg of protein in all samples. G-protein activation was carried out by a using a [$^{35}$S]-GTPγS filter-binding assay [16].

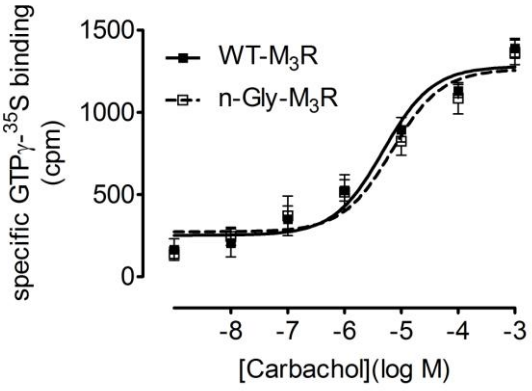


**Figure 3.** Carbachol-induced stimulated [$^{35}$S]-GTPγS binding to G proteins on COS-7 cells transiently expressing WT-$M_3R$ or nGly-$M_3R$ in the presence of 1 µM GDP. Binding of [$^{35}$S]-GTPγS (0.3 nM) to G proteins onto membrane homogenates were measured in absence or presence of different concentrations of carbachol as shown for 1 h at 30°C. After reaction stopped by rapid filtration, the filters were washed, dry and the radioactivity was detected by scintillation counting. [$^{35}$S]-GTPγS binding in the presence of 10 µM of unlabeled GTPγS was defined as nonspecific binding. Data, presented as counts per minute (cpm), are mean ± S.E.M values of three independent experiments, each assayed in triplicate (Carbachol $EC_{50}$ values: WT-$M_3R$, 4.80 ± 0.17 µM and nGly-$M_3R$, 6.55 ± 0.27 µM).

Carbachol stimulated WT-$M_3$R and nGly-$M_3$R with similar potency ($EC_{50}$ values: WT-$M_3$R, 4.80 ± 0.17 μM and nGly-$M_3$R, 6.55 ± 0.27 μM, n=3). We found that nGly-$M_3$R could activate the G protein with the same ability than the WT-$M_3$R (Fig. 3). In addition, COS-7 cells expressing nGly-$M_3$R mutant receptor -activated upon agonist stimulation- were able to increase the p-ERK1/2 level to a similar extent to that of WT-$M_3$R. Interestingly, non-stimulated cells expressing nGly-$M_3$R showed a high level of p-ERK1/2 (Fig. 4). This finding can be linked with the previous report that this activation pathway may be associated with up-regulation of ER-resident molecular chaperones [17].

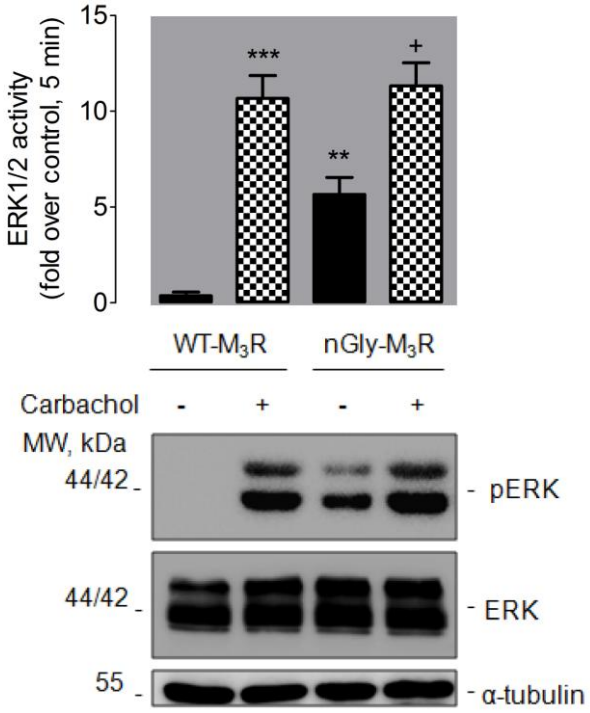


**Figure 4.** Upon carbachol-stimulated cells expressing WT-$M_3$R or nGly-$M_3$R, the levels of the phosphorylated ERK 1/2 protein and total ERK 1/2 were determined by Western blot analysis. Immunoreactivity bands were measured by quantitative densitometry.

### 4.3 Unfolded protein response occurred in cells expressing non-glycosylated mutant $M_3R$

Our previous findings led to the hypothesis that the nGly-$M_3R$ is associated to ER-stress. In eukaryotic cells, UPR consists of three distinct signalling pathways. In the last decade, numerous studies have described in detail the inositol-requiring kinase 1 (IRE-1), double-stranded RNA-activated protein kinase-like ER kinase (PERK), and activating transcription factor 6 (ATF6) signalling cascades [3-5]. In order to determine if abnormal accumulation of the nGly-M3R is able to induce UPR in COS-7 cells, we performed Western blot (Fig. 5 and 6) and In-Cell Western immuno-fluorescent assays to detect the expression of ER-stress-markers (Fig. 7).

We found evidence for activation of UPR, marked by elevated levels of phosphorylated α-subunit of eukaryote initiation factor 2 (eIF2α) and an increased expression of ER-localized chaperone proteins, which were consistent with our earlier proposal. Phosphorylated eIF2α (p-eIF2α) was detected at lower level in cells expressing WT-$M_3R$ and completely abolished by cell incubation with a p-eIF2α inhibitor peptide used as a control (Fig. 5). However, cells expressing nGly-$M_3R$ showed an increased level of p-eIF2α compared with cells expressing WT-$M_3R$. A similar result was observed in tunicamycin-treated cells, an ER-stress inductor used as a control (Fig. 5).

Furthermore, nGly-$M_3R$ was able to significantly increase GRP78/Bip levels in COS-7 cells and to a lower extent in cells expressing WT-$M_3R$. Also, calnexin and calreticulin levels were found to be increased (Fig. 6). Similar results were observed when compared to those obtained for the ER-stress inducer, tunicamycin (Fig. 6). In addition, CHOP expression level was minimal in cells expressing WT-$M_3R$ and up-regulated in cells expressing nGly-$M_3R$ similarly to what could be observed for cells treated with tunicamycin (Fig. 7). These results agree with the idea that CHOP is induced at the transcription level in response to ER stress.

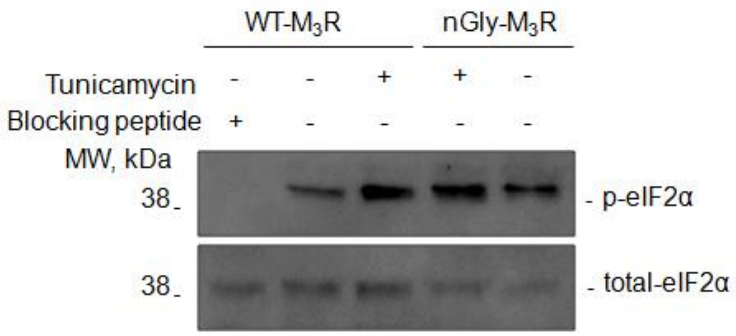


**Figure 5.** Up-regulation of eIF2α phosphorylation in cells that undergo ER stress. Whole-cell lysates expressing WT-$M_3$R or nGly-$M_3$R were analyzed for total eIF2α and a blocking peptide was used as a control by Western blot using a antibody for eIF2α and horseradish-peroxidase conjugated goat anti-rabbit IgG as a secondary antibody. Tunicamycin-treated cell was used as an ER-inducer control. Blots are representative of two independent experiments.

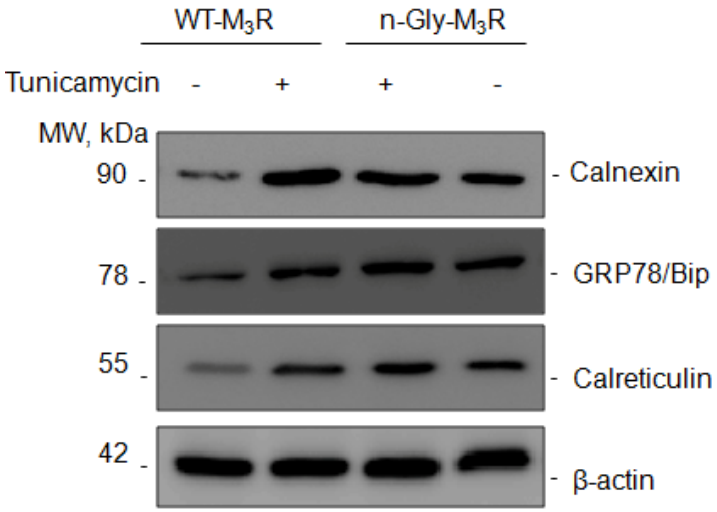


**Figure 6.** Increase levels of ER-localized chaperone proteins were determined. Cells expressing WT-$M_3$R or nGly-M3R were lysed in CelLytic™ M buffer and resolved by 12% SDS-PAGE followed by immunoblotted using antibodies for multiple chaperone proteins and HRP-conjugated goat anti-rabbit IgG as a secondary antibody. Tunicamycin-treated cell was used as an ER-inducer control. β-actin was detected as a loading control. Blots are representative of two independent experiments.

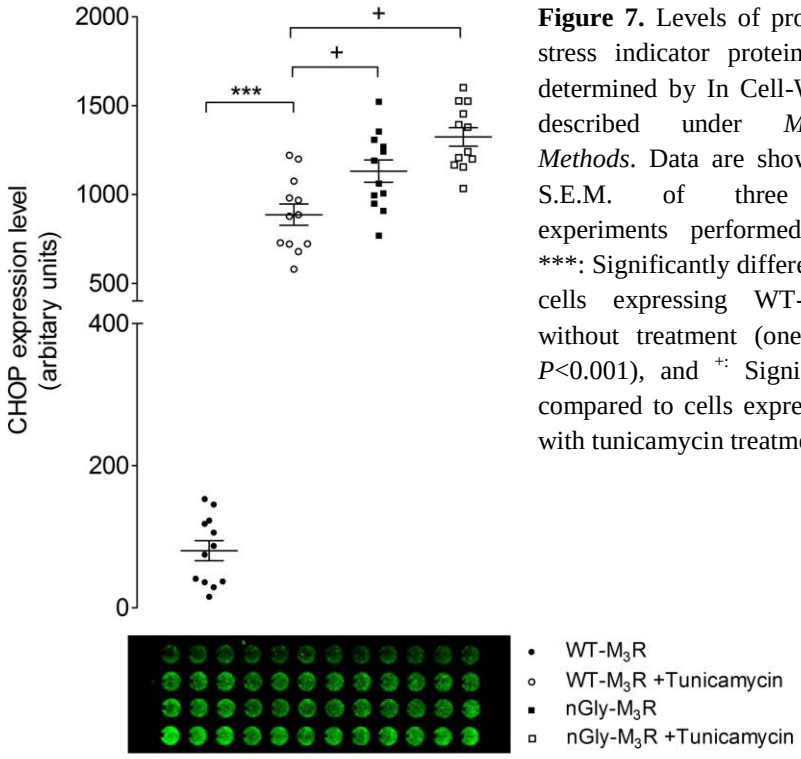


**Figure 7.** Levels of pro-apoptotic ER-stress indicator protein CHOP, were determined by In Cell-Western blot as described under *Materials and Methods*. Data are shown as means ± S.E.M. of three independent experiments performed in triplicate. ***: Significantly different compared to cells expressing WT-$M_3R$ receptor without treatment (one-way ANOVA $P<0.001$), and $^{+:}$ Significant different compared to cells expressing WT-$M_3R$ with tunicamycin treatment, $P<0.05$).

## 4.4. Prolonged unfolded protein response by mutant $M_3R$ induces ER-stress and promotes cell apoptosis

It has been previously shown that cells accumulating misfolded non-glycosylated proteins are unable to restore homeostasis through UPR, leading to cell death, basically via apoptosis [18]. Multiple UPR pathways can contribute to ER stress-induced cell apoptosis and autophagy [9-11]. Recently, it has been reported that apoptosis is mediated by factors including, CHOP/GADD153, apoptosis signal-regulating kinase 1 (ASK1) and caspase-12 [19-21]. The occurrence of ER-stress in COS-7 cells expressing nGly-$M_3R$ led us to investigate the possibility that mutated cells could have an increased susceptibility to undergo apoptosis. Apoptosis was assessed by measuring protein levels of anti-apoptotic or pro-apoptotic regulators of the Bcl-2 family, by means of Western blot analysis (Fig. 8), and by activation

of caspase-3, which was determined by the appearance of cleaved fragments of caspase-3 (Fig. 9).

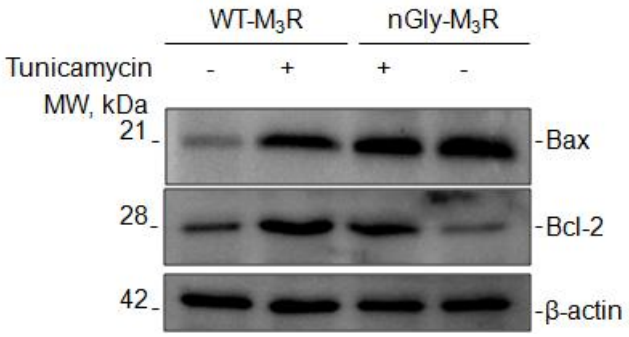


**Figure 8.** $M_3R$ N-glycosylation deficient induces ER-stress promotes cell apoptosis in COS-7 cells. Cells expressing WT-$M_3R$ or nGly-$M_3R$ were treated with/without the indicated concentration of tunicamycin; cell lysates were lysed and Bcl-2 family protein level were determined by Western blot. Immunoblotting shows alters levels for pro-apoptotic Bax and anti-apoptotic Bcl-2; significant up-regulation of Bax expression is evident in tunicamycin treated cells and cells expressing nGly-$M_3R$, but not in cells without treatment. β-actin levels served as loading control. Blots are representative of two independent experiments.

Our results showed non-signalling apoptosis in cells transfected with WT-$M_3R$. In contrast, apoptosis seemed to be ellicited in cells expressing nGly-$M_3R$. Furthermore, a robust increase in activated caspase-3 level was achieved in the case of nGly-$M_3R$ when the classical apoptosis-inducer hydrogen peroxide was used (Fig. 9). The increased expression level of pro-apoptotic Bax corroborates the above results (Fig. 8). Similarly, Bcl-2 levels were significantly down-regulated by deglycosylated mutant suggesting a loss of the survival response by a persistent UPR (Fig. 8). These findings suggest that nGly-$M_3R$ predisposes cells to apoptosis through caspase-3 activation counter-balanced with an early marked anti-apoptotic signal of Bcl-2 family proteins. This signalling would be unbalanced with time, by a chronic UPR, making cells expressing nGly-$M_3R$ more susceptible to cell disruption. In addition, cell growth was measured by MTS assay using CellTiter 96® AQueous One Solution Cell Proliferation Assay kit according manufactures instructions. We found a significant decrease in cell viability for COS-7 cells expressing the mutated receptor compared to cells expressing WT-$M_3R$ (Fig. 10).

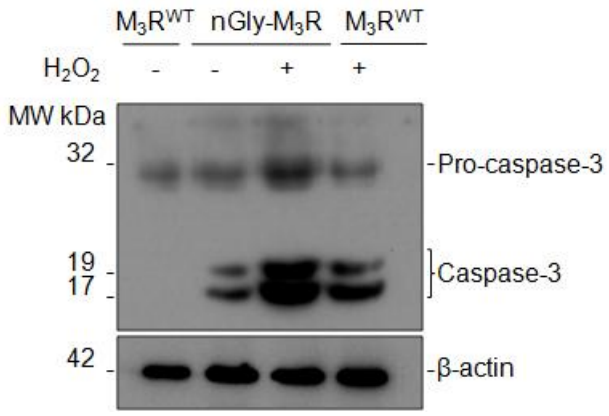


**Figure 9.** Cells expressing WT-$M_3R$ or nGly-$M_3R$ were treated with/without the indicated concentration of hydrogen peroxide ($H_2O_2$); cell lysates were lysed and activation of caspase-3 was determined by Western blot. Levels of active caspase-3 were measured in cell expressing nGly-$M_3R$ and markedly and persistently higher in apoptosis-induced cells expressing nGly-$M_3R$, suggesting that persistent ER-stress induce apoptosis is mediated by caspase-3. Blots are representative of two independent experiments.

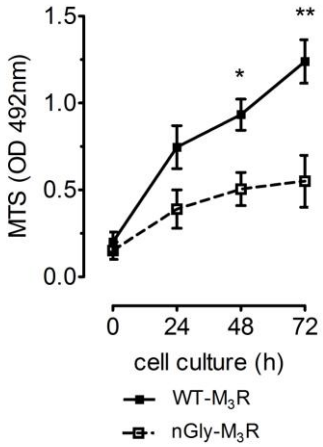


**Figure 10.** COS-7 cells were transiently transfected with the WT-$M_3R$ or nGly-$M_3R$ ($5\times10^3$) were seeded into 96-well plates and cultured overnight. Cell viability was measured at the indicated time point using CellTiter 96® Aqueous One Solution assay according manufactures instructions. Data are expressed as means ± S.D. and significant differences were determined using the two-way ANOVA *(*P<0.05; **P<0.01)*.

## Discussion

The presence of consensus sequences for N-glycosylation in most members of the GPCR family suggests that this post-translational modification may play important roles in receptor expression, structure and/or function. Increasing evidence supports the notion that core N-glycan contributes not only to receptor folding, but also to the cell surface transport [2,22-24]. All muscarinic acetylcholine receptors contain putative asparagine-linked glycosylation sites but only scarce reports, with differing results, have been published for N-glycosylation of muscarinic acetylcholine receptors [13]. In our current study, we analyzed, for the first time, the role of N-glycan chains of the human $M_3R$ transiently expressed on COS-7 cells, in both receptor folding and cell-surface trafficking. Western blot analysis (using samples treated with the N-glycosylation blocking agent tunicamycin as a control) of a receptor with of all five sites for asparagine-linked glycosylation in WT-M*3*R mutated, provides compelling evidence that $M_3R$ is glycosylated at these potential N-glycosylation sites. In addition, we found that N-glycan chains are required for proper receptor cell surface trafficking. [$^3$H]-NMS binding results together with confocal microcopy observations showed that lack of N-glycosylation resulted in altered cell surface receptor expression. Simultaneously, [$^3$H]-QNB binding suggested intracellular accumulation of nGly-$M_3R$.

In a coherent view, it is known that improperly folded proteins are recognized by UDP-glucose: glycoprotein glucosyltransferase that catalyzes the re-glucosylation of immaturely processed glycoprotein with ER retention prompting another round of calnexin/calreticulin assisted folding [25], which could be associated with ER stress. On the other side, our [$^3$H]-QNB data could be interpreted as reflecting partially impaired receptor folding. Indeed, calnexin/calreticulin binds to specific lectin-structure, during glycoprotein maturation promoting proper protein folding and disulfide bond formation by interacting with the protein disulfide isomerase ERp57 [2,24,26]. Proper $M_3R$ conformation is important for receptor cell-surface transport [27]. However, mutating the glycosylation sites did not drastically affect the pharmacological properties of the receptor, as shown by unchanged dissociation constant for [$^3$H]-NMS in membrane homogenates (data not shown).

$M_3R$ association in dimeric/oligomeric complexes [28] may allow other receptors to act as scaffold proteins helping receptor transport to the plasma membrane [29], ant this could explain the presence of functional receptor at the cell surface. Collectively, our findings suggest that preventing attachment of oligosaccharides to $M_3R$ results in decreased receptor level at the cell surface probably due to defects in the trafficking process -by which glycan structures contribute to receptor transport through the secretory pathway- without drastic conformational changes.

At some point in the ER-stress mechanism, cells activate UPR in an effort to maintain ER-homeostasis [4]. Phosphorylation of eIF2α is a well-characterized mechanism for down-regulation of protein synthesis under ER-stress [3], whereas up-regulation of ER-resident chaperones and induction of transcriptional factors has been previously reported in ER-stress [5]. The unexpected activation of ERK1/2 in non agonist-stimulated cells expressing nGly-$M_3R$, suggests that this pathway is associated to nGly-$M_3R$-induced ER stress by intracellular mutant accumulation. This view is in agreement with previous reports showing that this is associated with GRP78 up-regulation [17]. We therefore determined the levels of phosphorylated-elF2α by immunoblotting. To further validate ER-stress induction, we assessed the levels of GRP78/Bip [30], calnexin [10], and calreticulin [31], three well-known ER-stress markers. The results showed strong intracellular localization of nGly-$M_3R$ compared to WT-$M_3R$, and concomitant induction of the ER-stress markers GRP78/Bip and p-eIF2α. Furthermore, a slight increased expression level of ER resident molecular chaperones, that facilitate proper glycoprotein folding during biosynthesis like calnexin and calreticulin, was detected. Thus, our results suggest that UPR is activated in the case of the expression of nGly-$M_3R$.

CHOP is also known to be induced at the transcriptional level in response to ER-stress [20]. We found CHOP induction, in tunicamycin-treated COS-7 cells expressing WT-$M_3R$ or nGly-$M_3R$, to a similar extent than in cells expressing nGly-$M_3R$ without tunicamycin treatment. It had been previously shown that the ER stress-CHOP apoptosis signal is transmitted to mitochondria through Bax translocation [21], presumably mediated by Bim, a pro-apoptotic BH3-only type

Bcl-2 family member [32]. This early evidence could sustain our observed Bax increased levels. In addition, Bcl-2 levels were promoted in tunicamycin-treated cells suggesting survival response. This is consistent with previous results that propose the importance of Blc-2 not only at the mitochondria but also at the ER [33]. However, Bcl-2 levels were appreciably down-regulated during nGly-$M_3$R induced ER-stress suggesting loss of the survival response by a persistent UPR.

Our results reveal that prolonged UPR in COS-7 cells expressing nGly-$M_3$R resulted in measurable activation of caspase-3. These cells were more susceptible to disruption, indicated by strong apoptosis signal response to hydrogen peroxide treatment. Our findings, including hypothetical cytochrome *c* release by $Ca^{2+}$ increase resulting from ER-stress [34], can be interpreted as reflecting that nGly-$M_3$R promotes ER stress-induced cell apoptosis by caspase activation through a mitochondrial-dependent pathway. However, it was previously shown that, in ER stress-induced apoptosis, caspase-12 was able to activate caspase-9 thus promoting cleavage of procaspase-3 by a non-dependent cytochrome *c* pathway [19]. The possibility that nGly-$M_3$R may also use this pathway to active caspase-3 should also been considered and would need further research. Our results suggest that nGly-$M_3$R can promote apoptotic cell death, which is consistent with previous evidence supporting this possibility [18].

Overall, our findings, taken together, suggest the $M_3$R N-glycosylation-deficient mutant promotes impairment of receptor trafficking, and elicits ER-stress, and increased susceptibility to cell disruption.

## References

[1] Peretto, I., Petrillo, P. and Imbimbo, B.P. (2009). Medicinal chemistry and therapeutic potential of muscarinic M3 antagonists. Med Res Rev 29, 867-902.

[2] Markkanen, P.M. and Petaja-Repo, U.E. (2008). N-glycan-mediated quality control in the endoplasmic reticulum is required for the expression of correctly folded delta-opioid receptors at the cell surface. J Biol Chem 283, 29086-98.

[3] Schroder, M. and Kaufman, R.J. (2005). The mammalian unfolded protein response. Annu Rev Biochem 74, 739-89.

[4] Malhotra, J.D. and Kaufman, R.J. (2007). The endoplasmic reticulum and the unfolded protein response. Semin Cell Dev Biol 18, 716-31.

[5] Ron, D. and Walter, P. (2007). Signal integration in the endoplasmic reticulum unfolded protein response. Nat Rev Mol Cell Biol 8, 519-29.
[6] Rasheva, V.I. and Domingos, P.M. (2009). Cellular responses to endoplasmic reticulum stress and apoptosis. Apoptosis 14, 996-1007.
[7] Rao, R.V. and Bredesen, D.E. (2004). Misfolded proteins, endoplasmic reticulum stress and neurodegeneration. Curr Opin Cell Biol 16, 653-62.
[8] Kaufman, R.J. (2002). Orchestrating the unfolded protein response in health and disease. J Clin Invest 110, 1389-98.
[9] Zhang, K. and Kaufman, R.J. (2008). Identification and characterization of endoplasmic reticulum stress-induced apoptosis in vivo. Methods Enzymol 442, 395-419.
[10] Zuppini, A., Groenendyk, J., Cormack, L.A., Shore, G., Opas, M., Bleackley, R.C. and Michalak, M. (2002). Calnexin deficiency and endoplasmic reticulum stress-induced apoptosis. Biochemistry 41, 2850-8.
[11] Takizawa, T., Tatematsu, C., Watanabe, K., Kato, K. and Nakanishi, Y. (2004). Cleavage of calnexin caused by apoptotic stimuli: implication for the regulation of apoptosis. J Biochem 136, 399-405.
[12] Oyadomari, S. and Mori, M. (2004). Roles of CHOP/GADD153 in endoplasmic reticulum stress. Cell Death Differ 11, 381-9.
[13] Nathanson, N.M. (2008). Synthesis, trafficking, and localization of muscarinic acetylcholine receptors. Pharmacol Ther 119, 33-43.
[14] Schmidt, M., Fasselt, B., Rumenapp, U., Bienek, C., Wieland, T., van Koppen, C.J. and Jakobs, K.H. (1995). Rapid and persistent desensitization of m3 muscarinic acetylcholine receptor-stimulated phospholipase D. Concomitant sensitization of phospholipase C. J Biol Chem 270, 19949-56.
[15] Hoover, R.K. and Toews, M.L. (1989). Evidence for an agonist-induced, ATP-dependent change in muscarinic receptors of intact 1321N1 cells. J Pharmacol Exp Ther 251, 63-70.
[16] Borroto-Escuela, D.O., Correia, P.A., Perez Alea, M., Narvaez, M., Garriga, P., Fuxe, K. and Ciruela, F. Impaired M(3) muscarinic acetylcholine receptor signal transduction through blockade of binding of multiple proteins to its third intracellular loop. Cell Physiol Biochem 25, 397-408.
[17] Zhang, L.J., Chen, S., Wu, P., Hu, C.S., Thorne, R.F., Luo, C.M., Hersey, P. and Zhang, X.D. (2009). Inhibition of MEK blocks GRP78 up-regulation and enhances apoptosis induced by ER stress in gastric cancer cells. Cancer Lett 274, 40-6.
[18] Hauptmann, P., Riel, C., Kunz-Schughart, L.A., Frohlich, K.U., Madeo, F. and Lehle, L. (2006). Defects in N-glycosylation induce apoptosis in yeast. Mol Microbiol 59, 765-78.
[19] Morishima, N., Nakanishi, K., Takenouchi, H., Shibata, T. and Yasuhiko, Y. (2002). An endoplasmic reticulum stress-specific caspase cascade in apoptosis. Cytochrome c-independent activation of caspase-9 by caspase-12. J Biol Chem 277, 34287-94.
[20] Nakayama, Y., Endo, M., Tsukano, H., Mori, M., Oike, Y. and Gotoh, T. Molecular mechanisms of the LPS-induced non-apoptotic ER stress-CHOP pathway. J Biochem 147, 471-83.

[21] Gotoh, T., Terada, K., Oyadomari, S. and Mori, M. (2004). hsp70-DnaJ chaperone pair prevents nitric oxide- and CHOP-induced apoptosis by inhibiting translocation of Bax to mitochondria. Cell Death Differ 11, 390-402.

[22] Duvernay, M.T., Filipeanu, C.M. and Wu, G. (2005). The regulatory mechanisms of export trafficking of G protein-coupled receptors. Cell Signal 17, 1457-65.

[23] Roy, S., Perron, B. and Gallo-Payet, N. Role of asparagine-linked glycosylation in cell surface expression and function of the human adrenocorticotropin receptor (melanocortin 2 receptor) in 293/FRT cells. Endocrinology 151, 660-70.

[24] Lanctot, P.M., Leclerc, P.C., Escher, E., Guillemette, G. and Leduc, R. (2006). Role of N-glycan-dependent quality control in the cell-surface expression of the AT1 receptor. Biochem Biophys Res Commun 340, 395-402.

[25] Pearse, B.R., Tamura, T., Sunryd, J.C., Grabowski, G.A., Kaufman, R.J. and Hebert, D.N. The role of UDP-Glc:glycoprotein glucosyltransferase 1 in the maturation of an obligate substrate prosaposin. J Cell Biol 189, 829-41.

[26] Zapun, A., Darby, N.J., Tessier, D.C., Michalak, M., Bergeron, J.J. and Thomas, D.Y. (1998). Enhanced catalysis of ribonuclease B folding by the interaction of calnexin or calreticulin with ERp57. J Biol Chem 273, 6009-12.

[27] Zeng, F.Y., Soldner, A., Schoneberg, T. and Wess, J. (1999). Conserved extracellular cysteine pair in the M3 muscarinic acetylcholine receptor is essential for proper receptor cell surface localization but not for G protein coupling. J Neurochem 72, 2404-14.

[28] Alvarez-Curto, E., Ward, R.J., Pediani, J.D. and Milligan, G. Ligand regulation of the quaternary organization of cell surface M3 muscarinic acetylcholine receptors analyzed by fluorescence resonance energy transfer (FRET) imaging and homogeneous time-resolved FRET. J Biol Chem 285, 23318-30.

[29] Van Craenenbroeck, K. et al. Dopamine D(4) receptor oligomerization - contribution to receptor biogenesis. FEBS J

[30] Zhang, Y., Liu, R., Ni, M., Gill, P. and Lee, A.S. Cell surface relocalization of the endoplasmic reticulum chaperone and unfolded protein response regulator GRP78/BiP. J Biol Chem 285, 15065-75.

[31] Gelebart, P., Opas, M. and Michalak, M. (2005). Calreticulin, a Ca2+-binding chaperone of the endoplasmic reticulum. Int J Biochem Cell Biol 37, 260-6.

[32] Puthalakath, H. et al. (2007). ER stress triggers apoptosis by activating BH3-only protein Bim. Cell 129, 1337-49.

[33] Schinzel, A., Kaufmann, T. and Borner, C. (2004). Bcl-2 family members: integrators of survival and death signals in physiology and pathology [corrected]. Biochim Biophys Acta 1644, 95-105.

[34] Boya, P., Cohen, I., Zamzami, N., Vieira, H.L. and Kroemer, G. (2002). Endoplasmic reticulum stress-induced cell death requires mitochondrial membrane permeabilization. Cell Death Differ 9, 465-7.

# CHAPTER 5

## ENHANCED CONSTITUTIVE ACTIVITY AND RECEPTOR DESENSITIZATION CHANGES IN NON-PALMITOYLATED $M_3$ MUSCARINIC RECEPTOR

(contents of this chapter is a manuscript submitted for publications in Journal Cell Biology)

## Enhanced constitutive activity and receptor desensitization changes in non-palmitoylated $M_3$ muscarinic receptor

### Abstract

Human $M_3$ muscarinic acetylcholine receptor regulates many main physiological roles in the central and peripheral nervous system and it is involved in the pathophysiology of several neurodegenerative and autoimmune diseases. We have undertaken the study of post-translational palmitoylation in order to elucidate the potential roles of these fatty-acid chains in receptor expression and function. Two cysteine residues, located in the C-terminal receptor domain, which are putative fatty acid-linked palmitoylation sites were mutated to alanine and the mutants transiently expressed in COS-7 cells. The elimination of fatty acid chains attachment sites did not affect significantly the cellular expression level and cellular localization of the receptor, as suggested by [$^3$H]-N-methylscopolamine binding measurements. This observation was consistent with the confocal microscopy analysis, which showed that the palmitoylation-deficient receptor was primarily localized to the plasma membrane within detergent-resistant domains. However, mutated receptor showed a significantly lower level of receptor associated to detergent-resistant domains. In addition, although mutant receptor exhibited a slight increase in [$^3$H]-N-methylscopolamine binding affinities, it did not differ significantly from the wild-type receptor in its ability to stimulate carbachol-dependent G-protein coupling and to increase inositol phosphate production. We found, however, significant inositol phosphate levels in non-stimulated cells expressing the mutated receptor, pointing to an increase in agonist-independent receptor constitutive $G_{\alpha q11}$ activation. This proposal was confirmed by means of nuclear transcriptional factor reporter gene assays. Collectively, our data provide experimental evidence for the potential role of palmitoylation in determining $M_3$ muscarinic receptor residence within lipid raft, as well as receptor internalization.

## Introduction

The human $M_3$ muscarinic acetylcholine receptor ($M_3R$) is a member of the G-protein-coupled receptor (GPCR) superfamily which is present in the central and peripheral nervous system [1]. This receptor mediates important cellular functions, and it has been linked to several neurodegenerative and autoimmune diseases including diabetes type-2, Sjögren's syndrome, chronic obstructive pulmonary disease, overactive bladder, obesity, irritable bowel syndrome, gastrointestinal spasms and cancer [2]. Although increasing evidence suggests an important role for post-translational modifications in GPCR structure and function [3-5], only few studies have been reported to date for muscarinic acetylcholine receptors [6]. Therefore, the occurrence and the molecular mechanism(s) underlying the role of these post-translational modifications in human $M_3R$ remain to be clarified. One of these modifications is reversible covalent lipid modifications, involving the attachment of the fatty acyl chain through a thioester bond to cysteine residues located in the carboxyl-terminal tail of the receptor [7]. Even though no reliable consensus sequence for palmitoylation has been identified to date, about 80% of known GPCRs contain one or more modified cysteine residues in the region of the C-terminal tail -some of them highly conserved- where it is accepted that covalent linkage of palmitic acid occurs [3]. Palmitoylated carboxyl-cysteine tail residues are likely attached to the cell membrane thereby creating an additional intracellular loop in GPCRs, like in the case of bovine rhodopsin where cysteines 322 and 323 form a fourth cytoplasmic loop that is thought to be anchored to the plasma membrane [8]. This loop may be involved in mediating protein-membrane and/or protein-protein interactions in GPCRs [9].

In addition, palmitoylation has been proposed to be involved in receptor targeting to the membrane lipid microdomains affecting receptor-mediated signaling [10]. It has been recently established that palmitoylation is a dynamic process encompassing cycles of palmitoylation and depalmitoylation that may play a role in regulating signaling processes in cells [11]. Increasing supporting evidence suggests that fatty acyl chains may contribute to the efficiency and selectivity of G-

protein coupling, receptor phosphorylation and desensitization, endocytosis and transport to the plasma membrane [3,12].

$M_3R$ contains two potential cysteine residues for lipid modification within its cytoplasmic carboxyl-terminal domain, and its signaling cascade -triggered by agonist binding to the receptor- is well established and involves signaling by Gq family of G-proteins, activation of phosphoinositide-specific phospholipase C (PLC) and subsequent increase of intracellular [Ca2+] [13]. In spite of this knowledge, the existence and role of palmitoylation in $M_3R$ function had not been previously investigated. In this study, we show that $M_3R$ is post-translationally modified with covalently bound palmitic acid and that $M_3R$ palmitoylation is dynamically regulated upon agonist stimulation of the receptor. In addition, we have identified the potential $M_3R$ palmitoylation sites in COS-7 cells and we demonstrate, by using acylation-deficient mutants, the functional significance of $M_3R$ palmitoylation for the regulation of receptor constitutive activity, receptor anchorage within lipid rafts and receptor internalization.

## Materials and Methods

### Generation of acylation-deficient mutant $M_3R$

To generate cDNA constructs encoding acylation-deficient mutant receptors, cysteine residues in the carboxyl-tail of the wild-type receptor were replaced by alanine residues using the Quick-Change site-directed mutagenesis kit (Stratagene, La Jolla, CA, USA). Mutation was subsequently verified by automated DNA sequencing. The 5'-3' primers used are as follows: $M_3$RC561A: 5'-CAAgATgCTgCTgCTggCCCAgTgTgACAAAAAAAAAgAggCgC-3', $M_3$RC563A: 5'-CAAgATgCTgCTgCTgTgCCAggCTgACAAAAAAAAAgAggCgC-3'.

### Cell culture, transfection and membrane preparation

African green monkey kidney cells (COS-7 cells, American Type Culture Collection) were cultured in Dulbecco's modified Eagle's medium (Lonza Ibérica,

SA, Spain) supplemented with 2 mM of L-glutamine, 100 units/ml penicillin, 100 µg/ml streptomycin sulfate, and 10% (v/v) fetal bovine serum (Invitrogen, Carlsbad, CA, USA) at 37°C and in an humidified atmosphere of 5% $CO_2$. For transfection, cells were grown in 6-well dishes at a concentration of $1\times10^6$ cells/well or in 175cm2 flasks (70% confluence) and cultured 24 h before transfection. Cells were transiently transfected using linear polyethylenimine transfection reagent (PEI, Polysciences Inc., Warrenton PA, USA) or Fugene® HD transfection reagent (Roche Applied Science, Indianapolis, USA), according to the manufacturer's protocol. In some case, cells cultured to almost confluent condition were incubated with 100 µM of 2-bromopalmitate (2-BP) (Sigma Aldrich, St. Louis, MO) 4 h after transfection and harvested 48 h post-transfection.

About 48 h after transfection, COS-7 cells were washed twice with cold phosphate buffered saline (PBS), harvested and homogenized in 20 mM Hepes, pH 7.4, 5 mM $MgCl_2$, 1 mM EDTA, using a Polytron tissue homogeniser and cell membranes or solubilized membrane proteins were prepared as previously described [13]. Protein concentrations were determined by means of a Bradford protein assay (Bio-Rad, Hercules, CA, USA), using bovine serum albumin (BSA) as a standard. Both, membrane preparations and solubilized proteins were either used immediately or frozen in liquid nitrogen, and stored at -80°C until needed.

**Isolation of raft fractions by sucrose gradient**

Cos-7 cells grown on 175-$mm^2$ flask were suspended, washed twice, and suspended in modified tyrode's solution. Cells were lysed with 1 ml of ice-cold lysis buffer (0.1% (v/v) triton x-100, 50 mm Tris-HCl pH 7.6, 50 mm NaCl, 5 mm EDTA, 50 mM NaF, 1 mm $Na_3VO_4$, 5 mM $Na_4P_2O_7$ containing a protease inhibitors cocktail. Lysates were sonicated on ice and incubated with constant rotation at 4°C for 1 h. Lysates (1 ml) were mixed with 3 ml of 60% (w/v) sucrose in STE buffer (50 mM Tris-HCl, pH 7.6, 50 mM NaCl, 5 mM EDTA, and 1 mM $Na_3VO_4$ and overlaid with 4 ml of 35% (w/v) sucrose and 4 ml of 5% (w/v) sucrose. centrifugation was performed at 200,000g for 15 h at 4°c with a Beckman

rotor. Fractions of 0.5 ml were collected from the top of the gradients, quantified by the BCA assay, separated bySDS-PAGE and analyzed by immunoblotting.

**Sodium dodecyl sulfate polyacrylamide gel electrophoresis and Western blot**

Proteins resolved onto 12% sodium dodecyl sulfate (SDS) polyacrylamide gel electrophoresis (PAGE) were subject to immunoblotting onto Immobilon P polyvinylidene difluoride membranes (PVDF, Millipore, Bedford, MA) using a semidry transfer system (Bio-Rad, USA). Membranes were blocked for 1 h in 5% BSA, Tris-buffered saline, pH 7.5 with 0,1% Tween-20 (TBST) prior to overnight incubation with the primary antibody under mild agitation at 4°C. Proteins were detected with a rabbit anti-$M_3$R (1:50, Santa Cruz Biotechnology, USA) and the following: horseradish-peroxidase (HRP)-conjugated goat anti-rabbit IgG (Santa Cruz Biotechnology) or streptavidin-HRP conjugated when the receptor was labeled with biotin-BMCC. The membrane was washed, and developed using the enhanced Super Signal chemiluminescence's detection system (ECL, Pierce Biotechnology, Rockford, CA, USA), and HyBlot CL autoradiography film (Denville Scientific, Metuchen, NJ) using ChemiDocTM XRS (Bio-Rad).

**Biotin-BMCC labelling**

The acylation of $M_3$R expressed in COS-7 cells was detected by the biotin-switch method [14]. The receptor was incubated overnight with denaturalization buffer containing 1% Triton X-100 and 40 mM *N*-ethylmaleimide (NEM, Sigma Aldrich, St. Louis, MO, USA), at 4°C, to quench free cysteines. The excess of NEM was removed with a desalting column (Pierce Biotechnology, Rockford, IL, USA). The sample was treated 2 h at 4°C with 1 M hydroxylamine ($NH_2OH$) pH 7.4 (Sigma-Aldrich) to cleave the acyl-thioester bond thereby generating free sulfhydryl groups. As a control, hydroxylamine was replaced by PBS. The excess of hydroxylamine was removed by a desalting column (Pierce Biotechnology). The sample was incubated for 2 h, at room temperature, with 100 μM of the sulfhydryl-specific biotin-conjugated reagent, 1-biotinamido-4-[4'-(maleimidomethyl)cyclohexanecarboxamido] butane (Btn-BMCC, Pierce Biotechnology), which recognizes free sulfhydryl groups, and washed again. The

bound protein was resuspended in 20 µl of 5x SDS-PAGE loading buffer, and subject to SDS-PAGE. Labelled proteins were detected by Western blotting as described before using streptavidin conjugated horseradish peroxidase (Pierce Biotechnology).

## Immunocytochemistry Staining

Cells were cultured onto 35-mm glass coverslips coated with 0.1 mg/ml poly-D-lysine (Sigma Aldrich) in 6-well dishes as described above. Cells were grown at a concentration of $1\times10^6$ cells/well and transfected with Fugene® HD transfection reagent (Roche Applied Science, Indianapolis, USA). Cells were washed, after 48 h, in PBS and fixed with 3.7% formaldehyde solution for 10 min at room temperature followed by two washes with PBS buffer containing 20 mM glycine (buffer A). Then, after permeabilization with buffer A containing 0.2% Triton X-100 for 5 min at room temperature, cells were treated with buffer A containing 1% BSA for 1 h. Cells were subsequently labelled with rabbit anti-$M_3R$ polyclonal antibody (1:50, Santa Cruz Biotechnology, USA) for 1 h at 37°C, extensively washed, and stained with goat anti-rabbit IgG-fluorescein isothiocyanate (FITC)-conjugated (1:100, Santa Cruz Biotechnology) in the same manner. Washed samples were rinsed and mounted onto glass slides using fluorescent mounting medium (Dako Glostrup Denmark). Microscope observations were performed with a Leica TCS-SL confocal microscope (Leica, Bannockburn, IL, USA).

## Muscarinic radioligand binding assay

The binding of [3H]-N-methyl scopolamine ([3H]-NMS, 81 Ci/mmol, Perkin-Elmer Life Sciences, USA) was conducted as variant of described previously [15]. In brief, membrane homogenates (5 µg/ml) were incubated different concentrations of [3H]-NMS (ranging from 0.25 pM to 1500 pM) for 2 h at 30°C in assay buffer (20 mM Hepes, pH 7.4, 100 mM NaCl, 10 mM $MgCl_2$). Non-specific binding was assessed in the presence of 5 µM atropine. Binding reactions were stopped by rapid filtration through Whatman GF/B filters (Maidstone, Kent, UK) used Brandel cell harvester (Brandel Inc., Gaithersburg, MD), and filters was washed extensively

with ice-cold milliQ water before remained bound was determined by scintillation counting.

### Immunoprecipitation of [35S]-GTPγS bound Gαq11 subunits

The [35S]-GTPγS (1250 Ci/mmol Perkin-Elmer Life Sciences) binding assay was conducted in membrane homogenate fractions using a method modified from that described previously [16,17]. In brief, membranes prepared from COS-7 cells were incubated with 0.3 nM [$^{35}$S]-GTPγS and 1 μM guanosine-5'-diphosphate (GDP, Sigma Aldrich), in the absence (basal) or in the presence of 100 μM carbamoylcholine chloride (carbachol, Sigma-Aldrich) in 200 μl of 10 mM Hepes, pH 7.4, 10 mM MgCl2, 1 mM EGTA, 100 mM NaCl, 0,2% BSA and 10 μg/ml saponin. Reactions were incubated at 30°C for 2 h. Nonspecific binding was determined by incubation of samples in the presence of 5 μM unlabeled GTPγS. Reactions were terminated by addition of 1 ml of ice-cold assays buffer, centrifuged and solubilized with 0.2% SDS. The supernatants were treated by vortex and incubated overnight at 4°C with heterotrimeric Gαq11 protein polyclonal antibody (Santa Cruz Biotechnology), followed by incubation with protein-A sepharose suspension 1 h at room temperature. The washed protein-A beads were resuspended in 1 ml cocktail, vortex mixed and radioactivity was detected by liquid scintillation counting.

### Inositol Phosphate Determination

COS- 7 cells were grown in 12-well plates at 37°C, 5% $CO_2$ and 2 μCi/ml *myo*-[$^{3}$H-]inositol (Amersham Biosciences, Germnay) for 18 h at 3,0 Ci/ml in DMEM (high glucose, w/o inositol (Invitrogen) . After labelling, cells were washed and incubated for 30 min in Krebs-bicarbonate solution (120 mM NaCl, 3.1 mM KCl, 1.2 mM $MgSO_4$, 2.6 mM $CaCl_2$, 10 mM glucose and 25 mM $NaHCO_3$, pH 7.4) and subsequently incubated in FCS free medium with 10 μM of carbachol -or without carbachol- in the presence of 10 mM LiCl for 5 min. Reactions were terminated removal of the agonist containing medium, the addition of 5% ice-cold perchloric acid and incubation at 4°C for 20 minutes. 0.4 ml of the lysate was then added to

0.1 ml of 10 mM EDTA and 0.5 ml of a 1:1 ratio (v/v) of tri-n-octylamine and 1,1,2 trichlorotrifluoroethane (Freon) solution. The samples were then vortexed and centrifuged at 4,000 rpm for 10 minutes in a Heraeus Megafuge to separate aqueous phase containing the inositol phosphates from the non-aqueous phase. Then, 0.3 ml of the aqueous upper phase was added to columns containing Dowex AG 1 x 8 resin. The columns were washed with 10 ml milliQ $H_2O$, then 25 mM ammonium formate, and finally the $^3$H-inositol phosphates were eluted with 1 M ammonium formate, 0.1 M formic acid. 1 ml of the eluted sample was collected and 10 ml scintillation fluid was added and counting.

**Luciferase reporter gene assay**

For luciferase assays, 24 hours before transfection, cells were seeded at a density of $1 \times 10^6$cells/well in six-well dishes and transfected with PEI. Cells were co-transfected with plasmids corresponding to three constructs as follows (per six-well): 1 μg firefly luciferase-encoding experimental plasmid pGL4-NFAT-luc2p (Promega, Stockholm, Sweden), 1 μg of wild-type or mutant receptor expression vectors and 50 ng *R*luc-encoding internal control plasmid (phRG-B; Promega). Approximately 24 h after post transfection the cells were transferred to 96-white-well plates (PerkinElmer Life, Waltham, MA). After 36 hours the cells were incubated with appropriate ligands (typically 20 h, at 37°C) and harvested with passive lysis buffer (Promega), the luciferase activity of cell extracts was determined using a luciferase assay system according to the manufacturer's protocol (Reporter Gene Kit, Promega) in a POLARstar Optima plate reader (BMG Labtechnologies, Offenburg, Germany) using a 535 nm excitation filter with a 30-nm bandwidth. Firefly luciferase was measured as firefly luciferase luminescence over a 15 s reaction period. The luciferase values were normalized against *R*luc luminescence values.

**In-Cell Western immuno-fluorescent assay**

Cell surface expression of receptor was evaluated by *on cell western* analysis experiments performed in transiently transfected $M_3R^{WT}$ or $M_3R^{C561/563A}$ in COS-7 cells [18]. Cells were seeded onto poly-D-lysine-coated 96-well plates (Corning,

Corning, NY), grown for 48 hours and then treated/no-treated for 10 min (carbachol 100 □M). After the drug treatment, cells were fixed with 3.7% paraformaldehyde for 10 min at room temperature, washed (without detergent to avoid membrane permeabilization), blocked for 90 min in LI-COR Odyssey Blocking Buffer® (LI-COR Biosciences, UK) and then incubated overnight at 4°C with a monoclonal anti-$M_3$R antibody (1:1000; Santa Cruz Biotechnology). Then, cell were washed and incubated with an infrared secondary antibody (goat anti-rabbit, 1:1500, LI-COR Biosciences, UK) in LI-COR Odyssey Blocking Buffer® and plates were scanned by the Odyssey infrared scanner. The integrity of the plasma membrane was evaluated with and without the addition of detergent (0.1% Triton X-100). Total cell number was normalized using DRAQ5/Sapphire 700 staining agents. Results are presented as the percentage of total protein detected at the cell surface.

### Statistical analysis

All binding data were analyzed using the commercial program GraphPad PRISM 5.0 (GraphPad Prism, San Diego, CA, USA). The number of samples (*n*) in each experimental condition is indicated in figure legends. When two experimental conditions were compared, statistical analysis was performed using an unpaired Student's *t*-test. Otherwise, statistical analysis was performed by one-way analysis of variance (ANOVA) followed by Tukey's Multiple Comparison post-test. The *P* value 0.05 and lower was considered significant.

## Results

### 5.1 Palmitoylation of $M_3$R on Cys561 and Cys563 and agonist-mediated changes of receptor palmitoylation

The $M_3$R contains two potential cysteine residues for lipid modification within their cytoplasmic carboxyl-terminal domain. A non-radioactive biotin-switch assay can detect $M_3$R acylation [14]. We blocked free sulfhydryl groups in $M_3$R, treated the sample with hydroxylamine in order to remove palmitoylation, and labeled with a sulfhydryl-specific reagent to determine the occurrence of palmitoylation. The

specific non-radiolabel Btn-BMCC cross-linking to $M_3R$ showed that the receptor contains covalently bound palmitic acid (Fig. 1). Palmitoylation occurred via a thioester type linkage because palmitate was cleaved by hydroxylamine [11]. In order to determine the potential acylation site of $M_3R$, we constructed a mutant receptor where the cysteine residues at position Cys561 and $Cys^{563}$ were substituted to alanine and chemical blockage of $M_3R$ palmitoylation by 2-BP was used as a control.

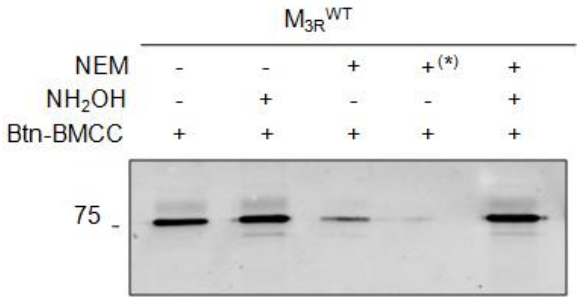


**Figure 1.** $M_3R$, expressed in COS-7 cells, is palmitoylated at two different sites (Cys561 and Cys563). After blocking the free sulfhydryl groups of the immunoprecipitated receptors, from COS-7 cells, these were subject to hydroxylamine treatment which removes palmitoylation, and the receptors were labeled with Btn-BMCC. Proteins were run on SDS-PAGE and transferred to nitrocellulose membranes. Blots were probed using streptavidin-HRP conjugated, and the labeled proteins were detected with ECL. * higher concentration of NEM was used (50 mM).

Palmitoylation occurrence at $M_3R$ and the potential acylation sites were confirmed by metabolic labeling of COS-7 cell samples with [$^3$H]-palmitate binding followed by receptor immunoprecipitation. One of the two-cysteine residues in the carboxyl tail of $M_3R$, $Cys^{561}$, is highly conserved among GPCRs, and consequently it could be a good candidate to be the palmitoylation site of $M_3R$. COS-7 cells expressing $M_3R^{WT}$ or acylation-deficient mutant were labelled with [$^3$H]-palmitate, followed by receptor immunoprecipitation, SDS-PAGE and autoradiography. Replacement of $Cys^{561}$ residue with alanine, resulted in significantly decreased, but not complete abolished $M_3R$ palmitoylation as compared with the WT receptor (Fig. 2). A measurable incorporation of [$^3$H]-palmitate into $Cys^{563}$ was inferred, suggesting that $Cys^{563}$ was weakly palmitoylated (Fig. 2). Moreover, double substitution of

$Cys^{561/563}$ resulted in undetectable [$^3$H]-palmitate incorporation (Fig. 2). Thus, we show, under the experimental conditions used, that $Cys^{561}$ and $Cys^{563}$ are the preferential palmitoylation sites of $M_3R$.

We also examined whether palmitoylation of $M_3R^{WT}$ may be affected by its agonist carbachol. Cells expressing $M_3R^{WT}$ were metabolically labelled with [$^3$H]-palmitate for one hour in the absence or in the presence of increasing concentrations of carbachol followed by immunoprecipitation, SDS-PAGE and fluorography (Fig. 3). Our data suggest that treatment with agonist results in a dose-dependent increase of [$^3$H]-palmitate incorporation into the receptor. Western blot analysis, carried out in parallel, of samples used as a control revealed that receptor synthesis was not significantly affected by agonist incubation (Fig. 3).

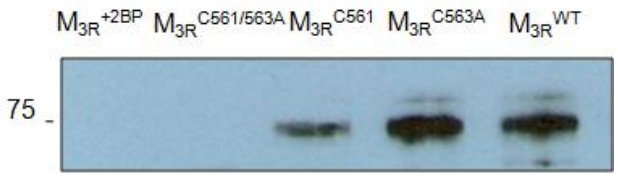


**Figure 2.** [$^3$H]-palmitate incorporation into WT and mutant receptors. COS-7 cells transiently expressing $M_3R^{WT}$, $M_3R^{C561}$, $M_3R^{C563A}$ or $M_3R^{C561/563A}$ were metabolically labeled with [$^3$H]-palmitate as described. Immunoprecipitated receptors using an anti-$M_3R$ antibody were resolved on SDS-PAGE. [$^3$H]-Palmitate incorporation was revealed by autoradiography, and band intensity of autoradiogram on the gel corresponded to the degree of palmitoylation. As a negative control, immunoprecipitated $M_3R$ from 2BP-treated cells was used. Blots are representative of three independents experiments.

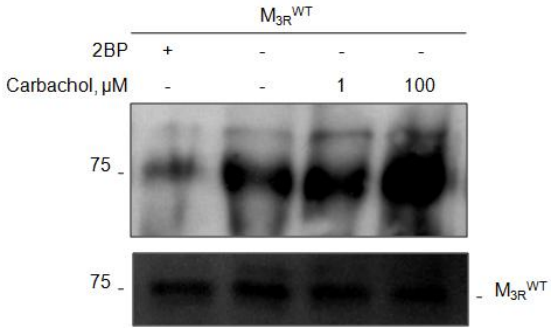

**Figure 3.** Carbachol induces increase in receptor palmitoylation by an agonist-dependent manner. Cells expressing $M_3R^{WT}$ were metabolically labelled with [$^3$H]-palmitate for 1 h in the absence or presence of increase concentrations of carbachol followed by immunoprecipitation, SDS-PAGE and fluorography. After exposure time of 25 day for [$^3$H]-palmitate labeling we showed the effect of agonist treatment on level of receptor palmitoylation (upper panel). Expression of the $M_3R$ was analyzed by immunobloting (lower panel) used as control for level receptor synthesis by agonist incubation. Blots are representative of two independent experiments.

## 5.2 Palmitoylation-deficient $M_3R$ is properly expressed at the plasma membrane

$M_3R^{WT}$ and $M_3R^{C561/563A}$ were transiently expressed in COS-7 cells, and the cellular distribution was analyzed by immunocytochemistry and confocal microscopy. Unchanged staining patterns were observed in cells expressing the mutated receptor when compared to the $M_3R^{WT}$ pattern. Both $M_3R^{WT}$ and mutant receptor showed clear cell membrane immunoreactivity (Fig. 4), suggesting that lack of palmitoylation did not affect receptor trafficking or cell surface localization.

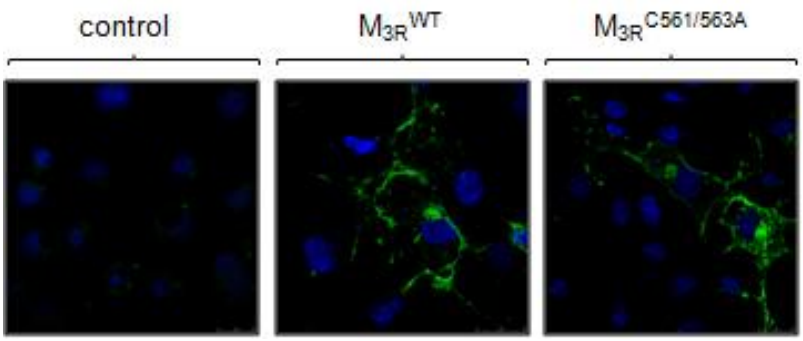


**Figure 4.** Subcellular localization of WT receptor and acylation-deficient mutant receptors in COS-7 cells. Cells transiently expressing $M_3$RWT or $M_3$RC561/563A were immunostained, after fixation and permeabilization, with rabbit anti-$M_3R$ antibody followed by fluorescein-isothiocyanate-conjugated goat anti-rabbit *(green)*. Nuclei were stained with Hoechst 33342 *(blue)*. Images for indirect immunofluorescence were acquired with a confocal microscope and the background signal obtained from non-transfected cells stained with the secondary antibody (in the absence of the primary antibody), was used as a control. Images are representative of three separate experiments. Scale bar equals 10 μm.

$M_3R$ has been previously localized to detergent-resistant membranes (DRMs), showing that lipid microdomains are required for efficient receptor function [19]. In addition, previous studies proposed a role for palmitate anchoring of the protein to the membrane [10]. Thus, we examined the acylation-deficient mutant within DRMs in COS-7 cells. Cells expressing $M_3R^{WT}$ or $M_3R^{C561/563A}$ with or without 2-BP treatment were lysed and extracted with Triton X-100 as described under *Material and Methods*. Lysates were layered on the bottom of a sucrose gradient and subject to ultracentrifugation. Representative fractions corresponding to Triton soluble fraction (fraction 9) and to DRMs (fraction 2), collected from a 35%/5% sucrose interface, were analyzed by immunoblotting. Results revealed that the majority of $M_3R$ was found in the DRMs, whereas cells expressing the mutated receptor showed a significantly lower level of receptor associated to DRMs. Chemical blockage with 2-BP used as a control, was able to slightly block association of $M_3R$ with lipid rafts (Fig. 5). In some cases, before Triton X-100 extraction, $M_3R$ was activated with carbachol and a slight increase in the presence of $M_3R$ in DRMs was observed compared with non-stimulated cells *(data not shown)*.

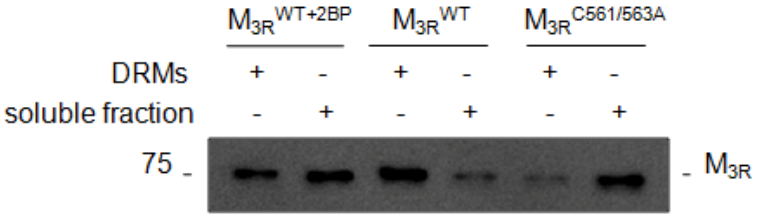


**Figure 5.** Distribution of $M_3R^{C561/563A}$ within DRMs. Cells expressing $M_3R^{WT}$ with/without 2-bromopalmitate treatment or $M_3R^{C561/563A}$ were lysated and extracted with Triton X-100 (1% (w/v) at 4ºC and lysate was subjected to sucrose density gradient centrifugation. Twelve fractions of the gradient were collected from the top to the bottom and a representative fraction of insoluble rafts fractions (fraction 2) and soluble fractions (fraction 9) were subjected to SDS–PAGE and analysed by immunoblotting. Chemical blockage with 2-BP was as a control. Blots are representative of two independents experiments.

In addition, saturation assays were performed to determine the $M_3R^{WT}$ and mutant receptor expression level and pharmacological properties. [$^3$H]-NMS binding assays were carried out with membrane homogenates from COS-7 cells expressing

$M_3R^{WT}$ or the mutated receptor. Binding data from assays performed in intact cells showed that the receptor density ($B_{max}$) of the mutated receptor at the cell surface was comparable with that of $M_3R^{WT}$ *(data not shown)*. In addition, mutant receptor displayed no significant expression levels as compared with $M_3R^{WT}$ both assayed in membrane homogenates (Table 1). However, acylation-deficient mutant displayed a slight increase in [$^3$H]-NMS binding affinity. [$^3$H]-NMS binding measurements indicate that mutant showed approximately 2- to 2.5-fold $K_D$ values with regard to $M_3R^{WT}$ (Table 1). The level of $M_3R$ expression was confirmed by Western blot analysis (Fig. 6). Interestingly, the mutant receptor showed a significant decrease in the intensity of the high molecular weight band, presumably corresponding to homodimer species, suggesting that lack of palmitoylation could affect formation of this molecular species (Fig. 6). More extensive investigations would be required to unambiguously prove this point.

**Table 1.** Ligand binding data of WT and $M_3R^{C561/563A}$ transiently expressed COS-7 cells

| | **Binding assay data** | |
|---|---|---|
| Receptor | [$^3$H]-NMS | |
| | *$K_D$ (pM)* | *Bmax (pmol/mg protein)* |
| $M_3R^{WT}$ | 191.5 ± 24.5 | 2.193 ± 0.12 |
| $M_3R^{C561/563A}$ | 75.8 ± 12.7* | 1.855 ± 0.09 |

Membrane homogenates from PEI transfected COS-7 cells (5 µg) transiently expressing $M_3R^{WT}$ or $M_3R^{C561/563A}$ were incubated with [$^3$H]-NMS (6.25-1500 pM) in Hepes at 30°C for 2 h. Non-specific binding was measured using 5 µM atropine. Nonlinear curve-fitting using GraphPad PRISM 5.0 determined dissociation constants ($K_D$) and maximal binding capacities ($B_{max}$). Data are presented as means ± S.E.M of two independent experiments, each one performed in triplicate. *: significant difference Student´s *t* test, ($P$<0.05).

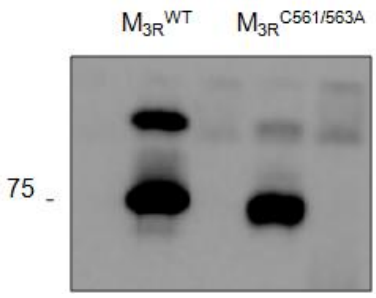


**Figure 6.** COS-7 cells expressing $M_3R^{WT}$ and the $M_3R^{C561/563A}$ were lysed in CelLytic™ M buffer and the level was determined by Western blot. Proteins were resolved on 12% SDS-PAGE followed by electro-blotting using the anti-$M_3R$ antibody and HRP-conjugated goat anti-rabbit IgG, as a secondary antibody. Blots are representative of two independent experiments.

## 5.3 Carbachol stimulation elicits similar levels of inositol phosphate accumulation for non-palmitoylated $M_3R$ mutant and wild-type receptor

Different studies have proposed that the attachment of palmitate would be associated with the regulation of receptor G protein coupling and subsequent downstream signalling cascades [12]. In order to investigate the functional significance of palmitoylation upon G protein-mediated signalling events, we determined the ability of $M_3R^{C561/563A}$ for coupling to $G\alpha_q$ protein and increasing intracellular inositol phosphate levels in COS-7 cells. G protein activation was carried out by a using a [$^{35}$S]-GTPγS binding/immunocapture assay [16,17]. Carbachol-induced [$^{35}$S]-GTPγS binding to $G\alpha_q$, on membrane homogenates expressing WT or mutant receptor, was determined by radioactivity counting after $G\alpha_q$ immunoprecipitation with and appropriate antibody (Fig. 7). $M_3R^{C561/563A}$ mutant showed G protein coupling properties similar to those of $M_3R^{WT}$ (Fig. 7).

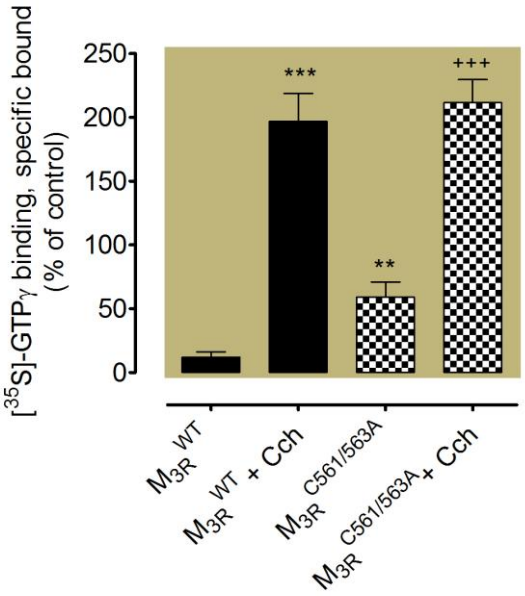


**Figure 7.** Carbachol-induced binding of [$^{35}$S]-GTPγS (0.2 nM) to $G_{\alpha q11}$ proteins onto membrane homogenates expressing $M_3R^{WT}$ or $M_3R^{C561/563A}$ were measured in absence (basal) or presence of 100 µM carbachol for 1 h at 30°C. After reaction stopped, the $G_{\alpha q11}$

proteins were immnunoprecipitated using $G_{\alpha q11}$ protein rabbit antibody at 4°C. Followed incubation with protein-A sepharose the radioactivity of beads was detected by scintillation counting. [$^{35}$S]-GTPγS binding in the presence of 5 µM of unlabeled GTPγS was defined as nonspecific binding. Values are expressed as percentage of specific binding of nontransfected cells in absence of ligand (control). Membranes from COS-7 cells expressing mutated receptor significantly increased [$^{35}$S]-GTPγS binding agonist-independent above control. Data are presented as means ± S.E.M of three independent experiments, each one performed in triplicate. ***, $P$<0.001; ** $P$<0.01: significant difference compared with cell expressing wild-type receptor. ++: is significantly greater ($P$<0.01, by Student´s $t$ test) than cell expressing mutated receptor without treatment.

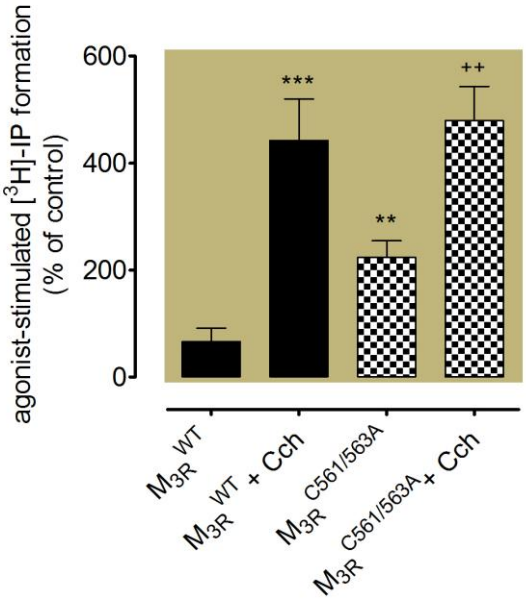


**Figure 8.** Upon carbachol-stimulated COS-7 cells expressing $M_3R^{WT}$ or $M_3R^{C561/563A}$, the [$^3$H]-IP3 production was measured as outlined under *Materials and Methods*. Results are expressed as disintegrations per minute (dpm). Under these experimental conditions, mutated receptor exhibited indistinguishable level of IP3 compared to $M_3R^{WT}$, however, showed significantly IP3 production in agonist-independent manner. Bars represent the mean ± S.E.M of three estimations from three independent experiments. *** and **: Significantly different compared to cell expressing wild-type receptor ($P$<0.001 and $P$<0.01) by One-way analysis of variance (ANOVA), ++: Significantly different compared to cell expressing mutated receptor by Student´s $t$ test, ($P$<0.01).

In addition, $M_3R^{C561/563A}$ did not significantly differ from $M_3R^{WT}$ in its ability to stimulate carbachol-dependent increase in inositol phosphate levels (Fig. 8). In spite of this, we found a significant inositol phosphate level in non-stimulated cells expressing the mutant receptor (Fig. 8). These findings are consistent with the previous observation that changes in the carboxyl tail of $M_3R$ led to constitutive signaling [20,21]. In addition, in experimental demonstrating of GPCR constitutive activity, we found whereas the second messenger production does not increase with expression of the $M_3R^{WT}$, a significant increase was observed for the acylation-deficient receptor, revealing the constitutive activity of the mutant (Fig. 9).

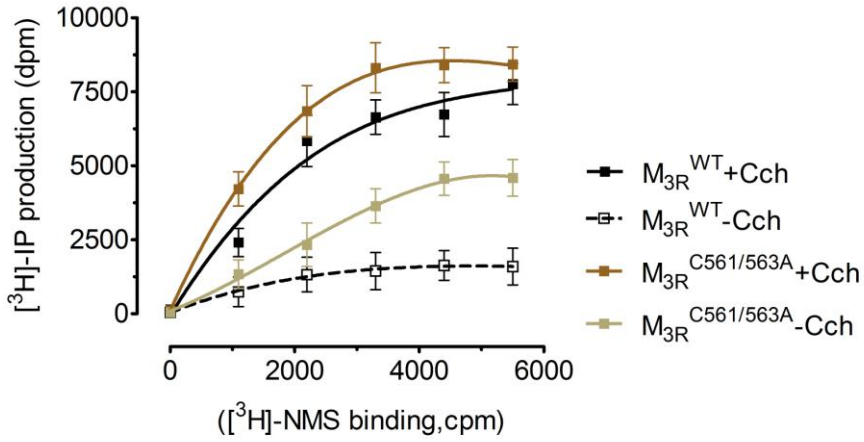


**Figure 9.** COS-7 cells were transfected with increasing concentrations of the wild-type or acylation-deficient mutant receptors indicated. After 24 hours, cells were labelled with *myo*-[$^3$H]-inositol for 24 h. Inositol phosphate formation was determined in non-stimulated cells and cells exposed to 100 µM carbachol for 30 min. Inositol phosphates were separated from inositol by chromatography as described under *Materials and Methods*. Parallel plates were used to determine the receptor density by binding of [$^3$H]-N.metylscopolamine to intact cells and the amount of inositol pohosphate formed was corrected for the different expression levels of the $M_3R$. Unspecific binding was determined in the presence of 5 µM unlabelled NMS. Data, presented as disintegrations per minute (dpm), are mean ± S.E.M values of two independent experiments, each one assayed in triplicate.

## 5.4 Increase constitutive signalling occurred in cell expressing nonpalmitoylated $M_3R$ mutant

Bioluminescent reporter technologies are uniquely suited for high throughput screening due to their inherent high sensitivity, wide dynamic range and low susceptibility to compound interference. Improvement of data quality and reduction of false positives caused by cytotoxic compounds can be achieved by incorporating a control reporter (e.g. a second luciferase) and ratiometric measurement. We probed the effect of acylation in receptor-induced constitutive signaling by determining the ability of the acylation-defective double mutant to increase transcriptional events (NFAT) by means of a luciferase gene reporter activity assay [22,23] (Fig. 10).

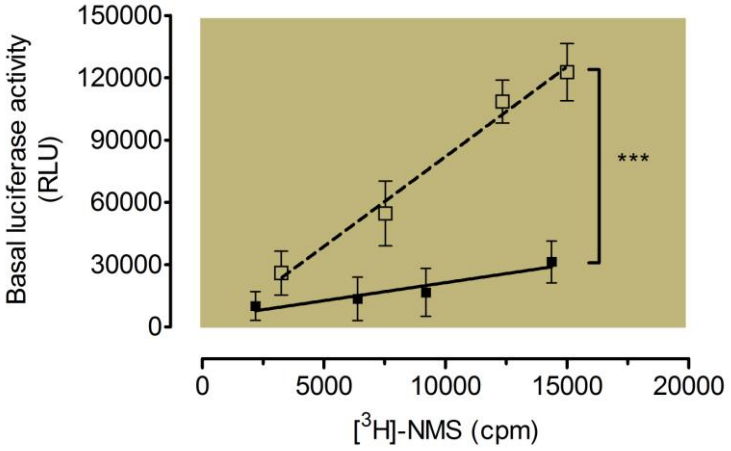


**Figure 10.** Constitutive signalling of the acylation-deficient mutant receptors in COS-7 cells determined by NFAT gene reporter assay. Cells were transiently co-transfected with various amounts of $M_3R^{WT}$ or $M_3R^{C561/563A}$, 1 μg firefly luciferase-encoding experimental plasmid (pGL4-NFAT-luc2p) and 50 ng *Renilla* luciferase-encoding internal control plasmid (phRG-B) followed the signalling in the absence of carbachol was measured using the NFAT luciferase reporter system. The slopes of the lines characterizing the relationship between signalling and receptor expression for mutated receptor was significantly greater that for wild-type receptor. Light emission is expressed as relative light unit (RLU). Data are representative of two independent experiments, each one performed in triplicate.

Different experimental parameters, such as cell number and amount of transfected cDNA were optimized in order to increase the assay sensitivity and reproducibility. We found that the acylation-deficient mutant exhibited marked constitutive signalling in COS-7 cells (Fig. 10). In contrast, non-transfected cells were unable to induce NFAT driven luciferase levels as expected *(data not shown)*.

Carbachol stimulated similar levels of NFAT gene expression for both WT and the mutant receptor, suggesting that the mutations did not significantly affect the receptor/G-protein system (Fig. 10). However, cells expressing the mutant receptor -in a carbachol-independent stimulation assay- showed an increase of at least a 2-fold increase in basal activity according to the NFAT reporter gene assay (Fig. 11). This activity could be completely abolished, by the inverse agonist atropine, suggesting that the mutated receptor constitutively couples to Gq protein (Fig. 11).

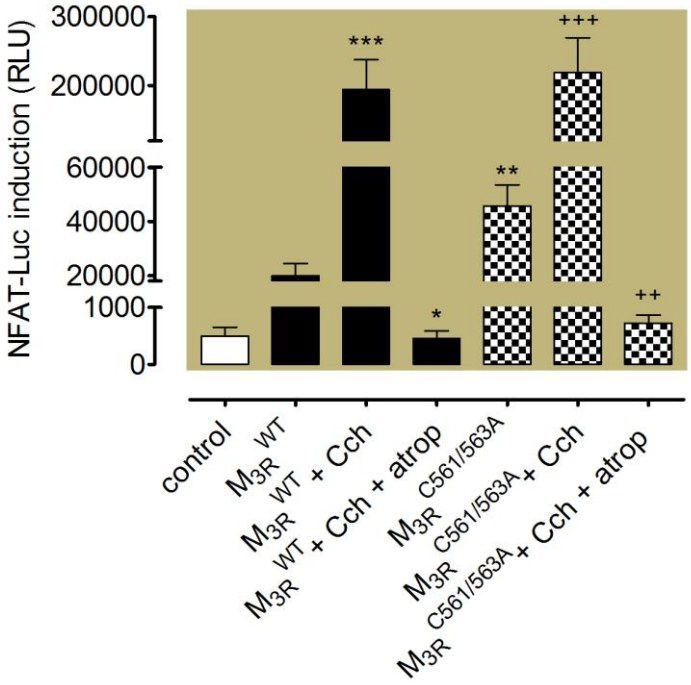

**Figure 11.** Thirty-six hours after transfection, cells were treated 6 h with agonist (carbachol, 100 µM) or antagonist (atropine 10 µM, in presence of agonist) and luciferase activity was measured as described. Bars represent the mean ± S.E.M. of three independent experiments performed in triplicate. ***, ** and *: Significantly different compared to cell expressing wild type ($P < 0.001$, $P < 0.01$ and $P < 0.05$); +++ and ++: Significantly different compared to cell expressing acylation-deficient mutant receptors ($P < 0.001$ and $P < 0.01$).

## 5.5 Inhibition of receptor internalization agonist-dependent and down-regulation by expression of nonpalmitoylated receptor in COS-7 cells

We examined carbachol-induced receptor internalization of both non-palmitoylated mutant and palmitoylated WT receptors in transiently transfected cells using *In-cell Western* assay [24]. COS-7 cells expressing $M_3R^{WT}$ or the mutated receptor were incubated in the presence of carbachol (100 µM) at 37°C -for 5 to 60 min- to monitor receptor internalization (Fig. 12).

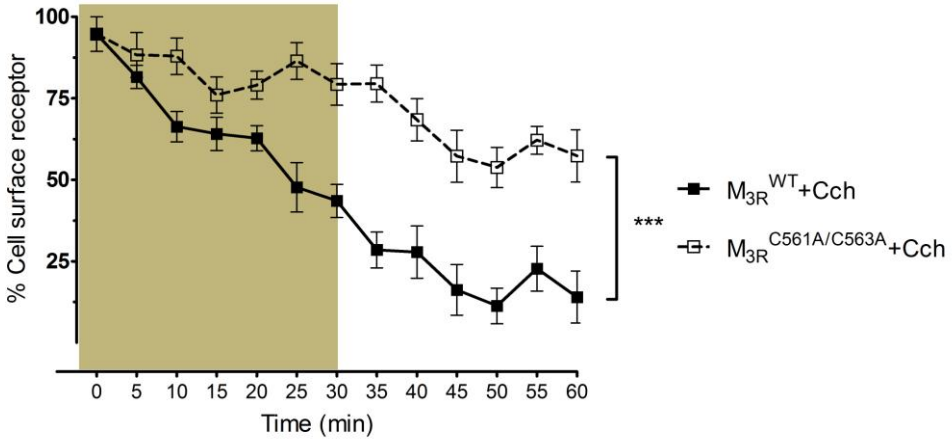


**Figure 12.** Time course agonist-induced receptor internalization was evaluated by an On-cell Western assay in non-permeabilized intact cells, using antibodies against epitope in the N-terminus of the $M_3R$ and the Odyssey IR imaging system. COS-7 cells expressing $M_3R^{WT}$ or $M_3R^{C561/563A}$ were treated with carbachol for 5 min at 37°C and $M_3R$ loss from the cell surface was monitored over time. Points are the means mean ± S.E.M of three independent experiments. *** and *: Significantly different compared to agonist-induce wild-type internalization ($P$<0.001 and $P$<0.05) in the range of 25-60 min by Two-way ANOVA.

Notably, agonist induced rapid internalization of $M_3R^{WT}$ (about 90% reduction of surface-expressed receptor). However, the same treatment reduced surface-expressed non-palmitoylated receptor only about 40% (Fig. 12). Furthermore, cells preincubated with 0.45 M sucrose for 30 min before agonist treatment resulted in a reduction of both $M_3R^{WT}$ and mutated receptor internalization (Fig. 13), suggesting involvement of clathrin-coated pits mediated receptor internalization. Previous studies have shown constitutive internalization of $M_3R$ by clathrin-independent endocytosis [25].

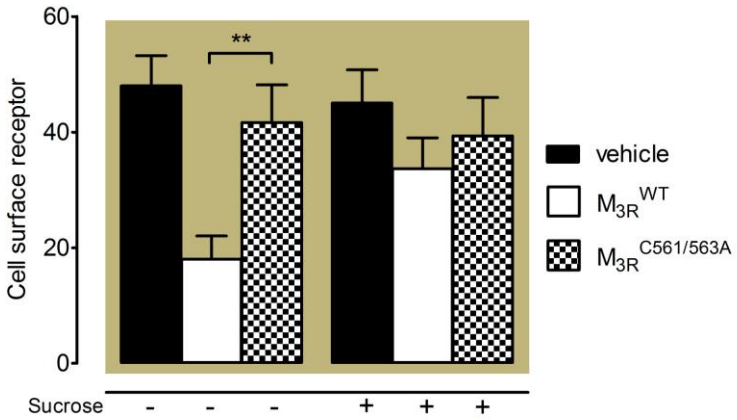


**Figure 13.** $M_3R$ loss from the cell surface after 30 min agonist stimulation was quantified by an On-cell Western assay as described. Cells were preincubated 48 h after transfection in the absence or presence of 0.45 M sucrose for 30 min and then stimulated as indicated. Data represent the mean ± S.E.M of five estimations from three independent experiments. **: Significantly different compared to cell expressing wild-type receptor ($P$<0.01) by One-way analysis of variance (ANOVA).

Hence, due to the reduced ability of the acylation-deficient mutant to undergo agonist-induced internalization, we examined the effect of palmitoylation on constitutive $M_3R$ internalization (Fig. 14). Our results revealed that about 18% of $M_3R^{WT}$ was internalized at 60 min (Fig. 14). In contrast, about 30% of non-palmitoylated mutant receptor, at the cell surface, was internalized (Fig. 14). To check if the constitutive internalization of the mutated receptor was a consequence of basal activity, we blocked this activity with atropine and we found that constitutive endocytosis was not significantly affected *(data not shown)*.

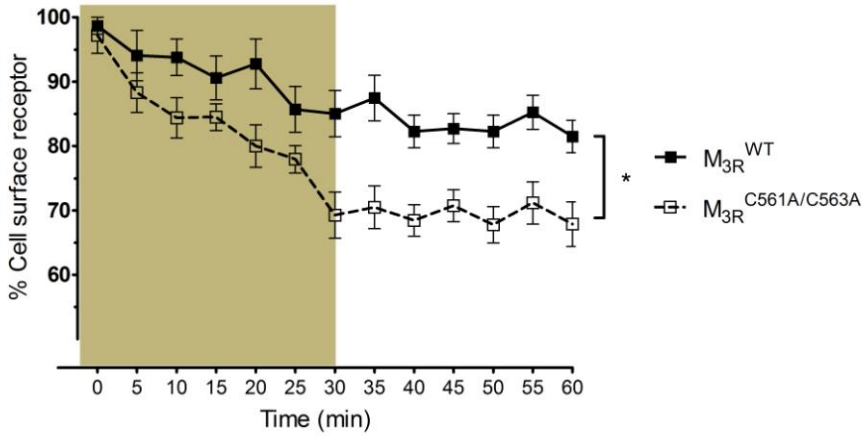


**Figure 14.** Time course constitutive receptor internalization was evaluated by an On-cell Western assay in non-permeabilized intact cells expressing $M_3R^{WT}$ or $M_3R^{C561/563A}$ without agonist treatment, using antibodies against epitope in the N-terminus of the $M_3R$ and the Odyssey IR imaging system as described. Points are the means mean ± S.E.M of three independent experiments. *: Significantly different compared to agonist-induce wild type internalization ($P$<0.05) by Two-way ANOVA.

## Discussion

In the current study we aimed at providing evidence that $M_3R$ is palmitoylated and to investigate the functional consequences of such post-translational modifications. Our experiments, using site-directed mutagenesis and *in vivo* [$^3$H]-palmitate metabolic labeling, revealed that palmitate could be incorporated to $M_3R$ at the conserved Cys-561 and, to a lesser extent at Cys-563. In addition, the sensibility of the receptor-bound fatty acid to hydroxylamine demonstrated that lipid modification occurs via thioester-type linkage [11]. Another important finding of our study is that palmitoylation of $M_3R$ is a dynamic process which can be modified by agonist-stimulation. These results agree with previous studies showing increased palmitoylation or de-palmitoylation in an agonist-dependent manner [11].Many studies have indicated that palmitoylation would be involved in mediating protein-membrane and/or protein-protein interactions in GPCRs [9]. Increasing evidence support the notion that fatty acyl chains can contribute to the efficiency and selectivity of G-protein coupling, receptor phosphorylation and

desensitization, endocytosis and transport to the plasma membrane [3,12]. Our [$^3$H]-NMS binding measurements suggest that impairment of palmitoylation does not affect the overall level of cell-surface expression of $M_3R$. This observation is confirmed by our confocal microscopy analysis. In spite of this, slight changes in the pharmacological properties of the acyl-deficient mutant could be detected. The mutant receptor showed 2-fold enhanced [$^3$H]-NMS affinity. In agreement with this concept, previous studies had shown that mutations within the transmembrane and intracellular domains of $M_3R$, particularly at residues within or adjacent to the NPXXY motif (in tansmembrane helix 7) led to constitutive activity and increased agonist affinity [20,21].

Substitution of either Cys-561 or Cys-563 yielded an acylation-deficient $M_3R$ mutant which exhibited pronounced constitutive signaling in COS-7 cells during agonist-independent activity, but did not affect agonist-mediated receptor coupling with Gq protein and signaling events. However, substitution of either Cys-561 or Cys-563 of the carboxyl tail individually, i.e. the corresponding single mutants, had no significant effect on the receptor binding properties and did not exhibit constitutive signaling *(data not shown)*. Evidence supporting the behavior of the double mutant has been previously reported [4,8,26]. However, mutations of cysteine residues at the carboxyl tail of other GPCRs led to signaling uncoupling [12,27,28], or were found to promote receptor intracellular accumulation [29], suggesting that palmitoylation affected basal and agonist-stimulated G-protein coupling differently in different GPCRs. The physiological role of constitutive signaling for GPCR remains unclear. However, receptor mutations leading to enhanced constitutive activity are associated with certain diseases, *e.g.* retinitis pigmentosa, congenital night blindness, and familial hyperthyroidism [30]. Even less is known about agonist-independent constitutive activity of $M_3R$. There is, however, evidence that increased cholinergic constitutive activity may be an important feature of some diseases, such as chronic obstructive pulmonary disease [31] and sudden infant death syndrome [32].

Rapid internalization of GPCR, after agonist activation, is known to be important for regulation of receptor signalling. In this study, we found that non-palmitoylated

receptor significantly impaired agonist-induced receptor internalization compared to the WT receptor which is in agreement with previous studies [33]. On the other side, internalization of $M_3R$ in the absence of an agonist, occurring via clathrin-independent endocytosis, has been previously reported [25]. The physiologic importance of constitutive internalization is currently unknown. However, constitutive endocytosis of cannabinoid CB1 receptors is responsible for the overall redistribution of receptors from de somatodendritic to the axonal membrane [34], suggesting relocation of the receptor to specific regions of the plasma membrane as one potential role. Our data reveal significant clathrin-independent endocytosis in non-palmitoylated receptors and these results seem to back the proposal that constitutive trafficking of $M_3R$ may occur via clathrin-independent mechanisms, and that these would be switched to clathrin-dependent in the presence of an agonist [25]. On the other hands, it is well documented that GPCR palmitoylation and phosphorylation are closely related in different ways [33]. Many GPCR are not efficiently phosphorylated as a consequence of defects in receptor desensitization and internalization caused by receptor palmitoylation impairment [35]. In this context, recent studies have shown that phosphorylation-deficient $M_3R$ was coupled normally to Gq/11-signaling but was uncoupled from phosphorylation-dependent processes such as receptor internalization and arrestin recruitment [36].

Palmitoylation has been associated with receptor targeting to the membrane lipid microdomains affecting receptor-mediated signaling [10]. We found a high amount of $M_3R$ in the DRM fractions, which was slightly increased in an agonist-stimulation manner. Similarly, $M_2R$ was proposed to migrate (upon agonist-stimulation) into specific lipid microdomains [37], suggesting the existence of a cycle of raft localization where the uncoupled receptor may leave lipid microdomains by lateral diffusion [10]. Our Western blot analysis showed the presence of the palmitoylation-deficient receptor to be reduced in lipid rafts, thus supporting this idea. The possible exclusion from lipid microdomains could affect agonist-induced internalization, or alternatively impairment of palmitoylation may affect internalization events. In this regard, $M_3R$ has been localized to lipid rafts, and disruption of these microdomains promotes loss of receptor localization abolishing $[Ca^{2+}]$ increase [19].

In summary, our combined results confirm that $M_3R$ is palmitoylated ant that this modification is regulated in an agonist-dependent manner. We determined, by using site-directed mutagenesis and *in vivo* metabolic labeling that $M_3R$ is palmitoylated at the conserved Cys-561 and, to a lesser extent at Cys-563. Finally, we demonstrated the functional significance of $M_3R$ palmitoylation for the regulation of receptor constitutive activity and receptor anchorage within lipid rafts, affecting agonist-dependent receptor internalization.

## References


[1] Eglen, R.M. (2006). Muscarinic receptor subtypes in neuronal and non-neuronal cholinergic function. Auton Autacoid Pharmacol 26, 219-33.

[2] Peretto, I., Petrillo, P. and Imbimbo, B.P. (2009). Medicinal chemistry and therapeutic potential of muscarinic M3 antagonists. Med Res Rev 29, 867-902.

[3] Miggin, S.M., Lawler, O.A. and Kinsella, B.T. (2003). Palmitoylation of the human prostacyclin receptor. Functional implications of palmitoylation and isoprenylation. J Biol Chem 278, 6947-58.

[4] Ponimaskin, E., Dumuis, A., Gaven, F., Barthet, G., Heine, M., Glebov, K., Richter, D.W. and Oppermann, M. (2005). Palmitoylation of the 5-hydroxytryptamine4a receptor regulates receptor phosphorylation, desensitization, and beta-arrestin-mediated endocytosis. Mol Pharmacol 67, 1434-43.

[5] Duvernay, M.T., Filipeanu, C.M. and Wu, G. (2005). The regulatory mechanisms of export trafficking of G protein-coupled receptors. Cell Signal 17, 1457-65.

[6] Nathanson, N.M. (2008). Synthesis, trafficking, and localization of muscarinic acetylcholine receptors. Pharmacol Ther 119, 33-43.

[7] Charest, P.G. and Bouvier, M. (2003). Palmitoylation of the V2 vasopressin receptor carboxyl tail enhances beta-arrestin recruitment leading to efficient receptor endocytosis and ERK1/2 activation. J Biol Chem 278, 41541-51.

[8] Du, D., Raaka, B.M., Grimberg, H., Lupu-Meiri, M., Oron, Y. and Gershengorn, M.C. (2005). Carboxyl tail cysteine mutants of the thyrotropin-releasing hormone receptor type 1 exhibit constitutive signaling: role of palmitoylation. Mol Pharmacol 68, 204-9.

[9] Zhong, M., Navratil, A.M., Clay, C. and Sanborn, B.M. (2004). Residues in the hydrophilic face of putative helix 8 of oxytocin receptor are important for receptor function. Biochemistry 43, 3490-8.

[10] Renner, U. et al. (2007). Localization of the mouse 5-hydroxytryptamine(1A) receptor in lipid microdomains depends on its palmitoylation and is involved in receptor-mediated signaling. Mol Pharmacol 72, 502-13.

[11] Kvachnina, E., Dumuis, A., Wlodarczyk, J., Renner, U., Cochet, M., Richter, D.W. and Ponimaskin, E. (2009). Constitutive Gs-mediated, but not G12-mediated, activity of the 5-hydroxytryptamine 5-HT7(a) receptor is modulated by the palmitoylation of its C-terminal domain. Biochim Biophys Acta 1793, 1646-55.

[12] Qanbar, R. and Bouvier, M. (2003). Role of palmitoylation/depalmitoylation reactions in G-protein-coupled receptor function. Pharmacol Ther 97, 1-33.

[13] Borroto-Escuela, D.O., Correia, P.A., Romero-Fernandez, W., Narvaez, M., Fuxe, K., Ciruela, F. and Garriga, P. Muscarinic receptor family interacting proteins: Role in receptor function. J Neurosci Methods

[14] Drisdel, R.C., Alexander, J.K., Sayeed, A. and Green, W.N. (2006). Assays of protein palmitoylation. Methods 40, 127-34.

[15] Borroto-Escuela, D.O., Correia, P.A., Perez Alea, M., Narvaez, M., Garriga, P., Fuxe, K. and Ciruela, F. Impaired M(3) muscarinic acetylcholine receptor signal transduction through blockade of binding of multiple proteins to its third intracellular loop. Cell Physiol Biochem 25, 397-408.

[16] Akam, E.C., Challiss, R.A. and Nahorski, S.R. (2001). G(q/11) and G(i/o) activation profiles in CHO cells expressing human muscarinic acetylcholine receptors: dependence on agonist as well as receptor-subtype. Br J Pharmacol 132, 950-8.

[17] Salah-Uddin, H., Thomas, D.R., Davies, C.H., Hagan, J.J., Wood, M.D., Watson, J.M. and Challiss, R.A. (2008). Pharmacological assessment of m1 muscarinic acetylcholine receptor-gq/11 protein coupling in membranes prepared from postmortem human brain tissue. J Pharmacol Exp Ther 325, 869-74.

[18] Delisle, B.P. et al. (2009). Small GTPase determinants for the Golgi processing and plasmalemmal expression of human ether-a-go-go related (hERG) K+ channels. J Biol Chem 284, 2844-53.

[19] Oldfield, S., Hancock, J., Mason, A., Hobson, S.A., Wynick, D., Kelly, E., Randall, A.D. and Marrion, N.V. (2009). Receptor-mediated suppression of potassium currents requires colocalization within lipid rafts. Mol Pharmacol 76, 1279-89.

[20] Ford, D.J., Essex, A., Spalding, T.A., Burstein, E.S. and Ellis, J. (2002). Homologous mutations near the junction of the sixth transmembrane domain and the third extracellular loop lead to constitutive activity and enhanced agonist affinity at all muscarinic receptor subtypes. J Pharmacol Exp Ther 300, 810-7.

[21] Li, J.H., Hamdan, F.F., Kim, S.K., Jacobson, K.A., Zhang, X., Han, S.J. and Wess, J. (2008). Ligand-specific changes in M3 muscarinic acetylcholine receptor structure detected by a disulfide scanning strategy. Biochemistry 47, 2776-88.

[22] Boss, V., Abbott, K.L., Wang, X.F., Pavlath, G.K. and Murphy, T.J. (1998). The cyclosporin A-sensitive nuclear factor of activated T cells (NFAT) proteins are expressed in vascular smooth muscle cells. Differential localization of NFAT isoforms and induction of NFAT-mediated transcription by phospholipase C-coupled cell surface receptors. J Biol Chem 273, 19664-71.

[23] Borroto-Escuela, D.O., Romero-Fernandez, W., Tarakanov, A.O., Marcellino, D., Ciruela, F., Agnati, L.F. and Fuxe, K. Dopamine D2 and 5-hydroxytryptamine 5-HT(A) receptors assemble into functionally interacting heteromers. Biochem Biophys Res Commun 401, 605-10.

[24] Borroto-Escuela, D.O., Romero-Fernandez, W., Tarakanov, A.O., Ciruela, F., Agnati, L.F. and Fuxe, K. On The Existence of A Possible A2A-D2-b-Arrestin2 Complex: A2A Agonist Modulation of D2 Agonist Induced b-Arrestin2 Recruitment. J Mol Biol

[25] Scarselli, M. and Donaldson, J.G. (2009). Constitutive internalization of G protein-coupled receptors and G proteins via clathrin-independent endocytosis. J Biol Chem 284, 3577-85.

[26] Hauptmann, P., Riel, C., Kunz-Schughart, L.A., Frohlich, K.U., Madeo, F. and Lehle, L. (2006). Defects in N-glycosylation induce apoptosis in yeast. Mol Microbiol 59, 765-78.

[27] Hayashi, M.K. and Haga, T. (1997). Palmitoylation of muscarinic acetylcholine receptor m2 subtypes: reduction in their ability to activate G proteins by mutation of a putative palmitoylation site, cysteine 457, in the carboxyl-terminal tail. Arch Biochem Biophys 340, 376-82.

[28] O'Dowd, B.F., Hnatowich, M., Caron, M.G., Lefkowitz, R.J. and Bouvier, M. (1989). Palmitoylation of the human beta 2-adrenergic receptor. Mutation of Cys341 in the carboxyl tail leads to an uncoupled nonpalmitoylated form of the receptor. J Biol Chem 264, 7564-9.

[29] Percherancier, Y., Planchenault, T., Valenzuela-Fernandez, A., Virelizier, J.L., Arenzana-Seisdedos, F. and Bachelerie, F. (2001). Palmitoylation-dependent control of degradation, life span, and membrane expression of the CCR5 receptor. J Biol Chem 276, 31936-44.

[30] de Ligt, R.A., Kourounakis, A.P. and AP, I.J. (2000). Inverse agonism at G protein-coupled receptors: (patho)physiological relevance and implications for drug discovery. Br J Pharmacol 130, 1-12.

[31] Casarosa, P., Kiechle, T., Sieger, P., Pieper, M. and Gantner, F. The constitutive activity of the human muscarinic M3 receptor unmasks differences in the pharmacology of anticholinergics. J Pharmacol Exp Ther 333, 201-9.

[32] Livolsi, A. et al. Constitutive overexpression of muscarinic receptors leads to vagal hyperreactivity. PLoS One 5, e15618.

[33] Hawtin, S.R., Tobin, A.B., Patel, S. and Wheatley, M. (2001). Palmitoylation of the vasopressin V1a receptor reveals different conformational requirements for signaling, agonist-induced receptor phosphorylation, and sequestration. J Biol Chem 276, 38139-46.

[34] McDonald, N.A., Henstridge, C.M., Connolly, C.N. and Irving, A.J. (2007). An essential role for constitutive endocytosis, but not activity, in the axonal targeting of the CB1 cannabinoid receptor. Mol Pharmacol 71, 976-84.

[35] Kraft, K., Olbrich, H., Majoul, I., Mack, M., Proudfoot, A. and Oppermann, M. (2001). Characterization of sequence determinants within the carboxyl-terminal domain of chemokine receptor CCR5 that regulate signaling and receptor internalization. J Biol Chem 276, 34408-18.

[36] Poulin, B. et al. The M3-muscarinic receptor regulates learning and memory in a receptor phosphorylation/arrestin-dependent manner. Proc Natl Acad Sci U S A 107, 9440-5.

[37] Feron, O., Smith, T.W., Michel, T. and Kelly, R.A. (1997). Dynamic targeting of the agonist-stimulated m2 muscarinic acetylcholine receptor to caveolae in cardiac myocytes. J Biol Chem 272, 17744-8.

# CHAPTER 6

## GENERAL DISCUSSION AND CONCLUSIONS

## General Discussion

G-protein-coupled receptors (GPCRs) represent one of the largest superfamily of proteins in the human body with about 1% of the human genome being encoded by over 1000 genes. Many GPCRs are involved in the pathophysiology of diseases, making them interesting targets for therapeutic intervention. It is estimated that more than half of drugs under current investigation are targets for GPCRs. However, only a small percentage of the drugs under investigation are successfully brought to the market [1]. Part of this growing problem lies in the difficulty to produce an enough quantity of pure receptor for structural analysis. In fact, so far only a few high-resolution GPCR structures are available [2]. Considering that under physiological conditions the expression of GPCRs is relatively low, optimizating receptor overexpression is a pre-requisite for obtaining large amounts of pure receptor. In addition, although is has well established that GPCR undergo post-translational and increase evidences support that it's are tight links to receptor roles, little progress has been made in post-translational modifications field in some GPCR such as the case of $M_3R$.

The human $M_3$ muscarinic acetylcholine receptor ($M_3R$) is a prototypic well-characterized member of the GPCRs and is present in the central and peripheral nervous systems [3]. This receptor mediates important cellular roles, and it has been linked to several neurodegenerative and autoimmune diseases including diabetes type-2, Sjögren's syndrome, chronic obstructive pulmonary disease, overactive bladder, obesity, irritable bowel syndrome, gastrointestinal spasms and cancer [4]. The $M_3R$, as potential therapeutic target, is under intensive investigations. However, the lack of structural information on this receptor subtype hampered the development of new potent drugs with increased selectivity and fewer side effects. Due to low natural abundance of $M_3R$, an early important step in receptor purification is receptor heterologous expression. Heterologous expression of $M_3R$ has been evaluated in several different expression systems including bacterial, yeast, insect and mammalian cells, but with varying degree of success due to differences in host cell metabolism [5].

In the perspective of future biophysical studies, we have overexpressed $M_3R$ using four-engineered tagged receptor genes and codon optimized $M_3R$ gene suitable for high-level expression in mammalian systems, as a first step in the process of large-scale purification. In addition, different heterologous expression systems, including mammalian cells and viral transfection, were employed to overexpress $M_3R$. While codon optimization resulted in an only 2-fold to 3-fold increase of $M_3R$ expression, we found that epitope tagging of the synthetic $M_3R$, especially with haemagglutinin and Flag epitope tags could improve $M_3R$ expression levels. In addition to codon optimization, other techniques have been used to increase the receptor expression with a variable degree of success; for example, incubation agonist/antagonist strategies, amino acid substitution [6], vector optimization [7], and co-expression with chaperones and other GPCRs [8,9]. Our results have shown a slight positive effect on expressing $M_3R$ after 48-hours preincubation with sodium butyrate for both stably and transiently transfected COS-7 cells. In addition, a remarkable boost on the receptor expression level in cells treated with atropine was confirmed by saturation binding assays and Western blot analysis. On the other hand, viral transfection led to a yield of 27 pmol/mg protein, which is the highest level reported so far for this receptor subtype in a mammalian system.

The receptor solubilization is another important early step in receptor purification. Methods for effective solubilization of GPCRs have been previously discussed [10]. The complex relationship between a membrane protein and the lipids in lipid bilayer makes the choice of a proper detergent for a particular receptor solubilization a complicate process, and solubilizing agent selection depends on particular receptor and cell type. A mixture of n-dodecyl-β-D-maltoside/Nonited P40/cholesterol hemisuccinate allowed extraction of a high level of functional receptor from COS-7 cells. MALDI-TOF mass spectrometry analysis confirmed a specific band corresponding to the receptor from different affinity purification systems. Purified receptor yield varied slightly among preparations but was always in the range of 8-14 nmol/l, with the immobilized-nickel affinity chromatography as the best method for purification. Purified $M_3R$ reconstituted into phospholipid vesicles was shown to retain full wild type functionality. However, we did not

produce large amount of $M_3R$ for structural studies, but only $M_3R$ levels to allow functional assays to be performed. It is possible that larger amounts of $M_3R$ could be produced in other expression systems using our purifications strategy.

Our detailed characterization for pos-translational modifications provided clear evidence that, under our experimental conditions, the receptor suffers higher post-translational modifications and suggested a possible map site for N-glycosylation and palmitoylation occurrence at $M_3R$ expressed in COS-7 cells.

N-linked glycosylation is the most common post-translational modification of GPCRs with approximately 70-90% of occurrence in the consensus sequences [11]. The presence of consensus sequences for N-glycosylation in most members of the GPCR family suggests that this post-translational modification may play important roles in receptor expression, structure and/or function. Increasing evidence supports the notion that core N-glycan contributes not only to receptor folding, but also to cell surface transport [11-13]. All muscarinic receptor subtypes contain putative asparagine-linked glycosylation sites but only scarce reports -with differing results- have been previously published for N-glycosylation of muscarinic receptors [14].

In our current study, we analyzed, for the first time, the role of N-glycan chains for human $M_3R$, transiently expressed in COS-7 cells, in both receptor folding and cell-surface traffic. Five potential asparagine-linked glycosylation sites in $M_3R$ were mutated and the mutants subsequently expressed in COS-7 cells. The elimination of N-glycan chains sites did not affect the cellular expression levels of the receptor. However, it did prevent proper receptor localization in the plasma membrane as suggested by reduced [$^3$H]-N-methylscopolamine binding. Confocal microscopy confirmed this observation, and showed that the non-glycosylated receptor was mainly localized in the cytoplasm.

The unexpected activation of ERK1/2 in non agonist-stimulated cells expressing the glycolylation-deficient $M_3R$ mutant, suggested that this pathway may be associated with non-glycosylated-$M_3R$ induced ER-stress elicited by cytoplasmic

mutant accumulation. In order to examine ER-stress induction, we assessed the phosphorylation levels of the α-subunit of eukaryote initiation factor 2, GRP78/Bip, calnexin, calreticulin and CHOP -five well-know ER-stress markers- and our results further support the proposal of the improper intracellular accumulation of the non-glycosylated receptor. Impaired glycosylation in the receptor also rendered the mutant variant more susceptible to apoptosis. Our findings suggest up-regulation of pro-apoptotic Bax protein, down-regulation of anti-apoptotic Bcl-2, and cleavage of caspase-3 effectors. Collectively, our data provide the first evidence of the critical role that N-glycan chains play in determining muscarinic receptor distribution and localization, as well as in cell integrity.

Similarly, the role of acylation of $M_3R$ is another issue which is poorly understood. We undertook the study of this post-translational modification in order to provide evidence about $M_3R$ palmitoylation and to investigate its potential functional consequences. Two cysteines residues located in the C-terminal receptor domain, corresponding to potential fatty acid-linked palmitoylation sites, were mutated and the mutant proteins transiently expressed in COS-7 cells. Our findings, using site-directed mutagenesis and *in vivo* [$^3$H]-palmitate metabolic labeling, revealed that $M_3R$ could be modified by palmitate at the conserved Cys-561 and, to a lower extent, at Cys-563. In addition, the sensibility of fatty acid bound to hydroxylamine demonstrated that lipid modification occurred via thioester-type linkage [15]. Also, our results suggest that palmitoylation of $M_3R$ is a dynamic process occurring in an agonist-dependent manner [15]. The elimination of fatty acid chains sites did not affect significantly the cellular expression levels and cellular localization of the receptor, as suggested by [$^3$H]-N-methylscopolamine binding measurements. This result was confirmed by confocal microscopy analysis which showed that the palmitoylation deficient receptor was mainly localized in the plasma membrane. In addition, although the mutant receptor displayed slight increase in [$^3$H]-N-methylscopolamine binding affinities, it did not differ significantly from the wild-type receptor in its ability to stimulate carbachol-dependent coupled G-protein and to increase inositol phosphate production. However, we found significant inositol

phosphate levels in non-stimulated cells expressing the mutated receptor, suggesting an increase of the constitutive $G_{\alpha q11}$ activity in an agonist-independent fashion. This proposal was confirmed by nuclear transcriptional factor reporter gene assays. Collectively, our data provide evidence for an important role for palmitoylation in determining $M_3R$ residence within lipid rafts, as well as in controlling receptor internalization and down-regulation.

## Conclusions

1. Our findings reveal that the successful strategies used can be helpful tools to increase $M_3R$ expression not only to facilitate purification efforts, but also for subsequent secondary structural trials, functional analyses and three-dimensional structure determination. Furthermore, the results may be useful in future efforts for overproduction of other G protein-coupled receptors.

2. Our results show that a combination of n-dodecyl-β-D-maltoside/Nonited P40 and cholesterol hemisuccinate is able to successfully extract $M_3R$ from cell membranes and to keep $M_3R$ stable in solution. A combination of purification methods, such as nickel affinity chromatography followed by Flag affinity chromatography yielded a receptor purified to near homogeneity in a functional form, as judged by Western blot, radioligand-binding experiments and MALDI-TOF analysis.

3. We demonstrate that $M_3R$ is strongly glycosylated. Using site-directed mutagenesis, we determine $M_3R$ to be glycosylated at four of five of its consensus sequences. Our data provide evidence that impairment in N-glycan chains affects proper receptor localization in the plasma membrane, elicits endoplasmatic reticulum stress and increases susceptibility to cell disruption.

4. We confirmed that $M_3R$ is palmitoylated, and that this post-translational modification responds in an agonist-dependent manner. Using site-directed mutagenesis and *in vivo* metabolic labeling, we have determined that $M_3R$ is palmitoylated at the conserved Cys-561 and, to a lower extent at Cys-563. In addition, we provide evidence for the functional significance of $M_3R$ palmitoylation in the regulation of receptor constitutive activity and receptor anchorage within lipid rafts, affecting agonist-dependent receptor internalization.

## References


[1] Mailman, R.B. (2007). GPCR functional selectivity has therapeutic impact. Trends Pharmacol Sci 28, 390-6.

[2] Kobilka, B. and Schertler, G.F. (2008). New G-protein-coupled receptor crystal structures: insights and limitations. Trends Pharmacol Sci 29, 79-83.

[3] Eglen, R.M. (2006). Muscarinic receptor subtypes in neuronal and non-neuronal cholinergic function. Auton Autacoid Pharmacol 26, 219-33.

[4] Peretto, I., Petrillo, P. and Imbimbo, B.P. (2009). Medicinal chemistry and therapeutic potential of muscarinic M3 antagonists. Med Res Rev 29, 867-902.

[5] Sarramegna, V., Talmont, F., Demange, P. and Milon, A. (2003). Heterologous expression of G-protein-coupled receptors: comparison of expression systems fron the standpoint of large-scale production and purification. Cell Mol Life Sci 60, 1529-46.

[6] Parker, E.M., Kameyama, K., Higashijima, T. and Ross, E.M. (1991). Reconstitutively active G protein-coupled receptors purified from baculovirus-infected insect cells. J Biol Chem 266, 519-27.

[7] Pickering, B.M. and Willis, A.E. (2005). The implications of structured 5' untranslated regions on translation and disease. Semin Cell Dev Biol 16, 39-47.

[8] Huang, D., Gore, P.R. and Shusta, E.V. (2008). Increasing yeast secretion of heterologous proteins by regulating expression rates and post-secretory loss. Biotechnol Bioeng 101, 1264-75.

[9] Leskela, T.T., Markkanen, P.M., Pietila, E.M., Tuusa, J.T. and Petaja-Repo, U.E. (2007). Opioid receptor pharmacological chaperones act by binding and stabilizing newly synthesized receptors in the endoplasmic reticulum. J Biol Chem 282, 23171-83.

[10] Sarramegn, V., Muller, I., Milon, A. and Talmont, F. (2006). Recombinant G protein-coupled receptors from expression to renaturation: a challenge towards structure. Cell Mol Life Sci 63, 1149-64.

[11] Markkanen, P.M. and Petaja-Repo, U.E. (2008). N-glycan-mediated quality control in the endoplasmic reticulum is required for the expression of correctly folded delta-opioid receptors at the cell surface. J Biol Chem 283, 29086-98.

[12] Duvernay, M.T., Filipeanu, C.M. and Wu, G. (2005). The regulatory mechanisms of export trafficking of G protein-coupled receptors. Cell Signal 17, 1457-65.

[13] Roy, S., Perron, B. and Gallo-Payet, N. Role of asparagine-linked glycosylation in cell surface expression and function of the human adrenocorticotropin receptor (melanocortin 2 receptor) in 293/FRT cells. Endocrinology 151, 660-70.

[14] Nathanson, N.M. (2008). Synthesis, trafficking, and localization of muscarinic acetylcholine receptors. Pharmacol Ther 119, 33-43.

[15] Kvachnina, E., Dumuis, A., Wlodarczyk, J., Renner, U., Cochet, M., Richter, D.W. and Ponimaskin, E. (2009). Constitutive Gs-mediated, but not G12-mediated, activity of the 5-hydroxytryptamine 5-HT7(a) receptor is modulated by the palmitoylation of its C-terminal domain. Biochim Biophys Acta 1793, 1646-55.

## List of Publications

1. Enhanced constitutive activity and receptor desensitization changes in non-palmitoylated $M_3$ muscarinic receptor. **Wilber Romero-Fernandez**, Borroto-Escuela, DO and Garriga P. *(Paper submitted for publications in Journal Cell Biology, 2011).*

2. Altered trafficking and unfolded protein response induction as a result of $M_3$ muscarinic receptor impaired N-glycosylation. **Wilber Romero-Fernandez**, Borroto-Escuela, DO, Pérez Alea M and Garriga P. *(Paper submitted for publications in Glycobiology, 2011).*

3. New insights into the intracellular structure and posttranslational modifications of a functional $M_3$ muscarinic receptor. **Wilber Romero-Fernandez**, Borroto-Escuela, DO and Garriga P. *(Paper submitted for publications in Protein Journal, 2011).*

4. Dopamine D4 receptor oligomerization: contribution to receptor biogenesis. Kathleen Van CraenenbroecK, Dasiel O. Borroto-Escuela, **Wilber Romero-Fernandez**, Kamila Skieterska, Pieter Rondou, Béatrice Lintermans, Peter Vanhoenacker, Kjell Fuxe, Francisco Ciruela, Guy Haegeman. *FEBS Letter, 2011.*

5. Dissecting the conserved NPxxY motif of the $M_3$ muscarinic acetylcholine receptor: critical role of Asp-7.49 for receptor signaling and multiprotein complex formation. Borroto-Escuela DO, **Wilber Romero-Fernandez**, Patricia Correia, Pere Garriga, Kjell Fuxe and Francisco Ciruela. *(Paper submitted for publications, 2011).*

6. On the existence of a possible A2A-D2-β-arrestin complex: A2A agonist modulation of D2 agonist induced β-arrestin recruitment. Borroto-Escuela DO, **Wilber Romero-Fernandez**, Tarakanov AO, Ciruela F, Agnati LF and Fuxe K. *Journal of Molecular Biology, 2010.*

7. Dopamine D2 and D4 receptor heteromerization and its allosteric receptor-receptor interactions. Borroto-Escuela DO, Ciruela F, Craenenbroeck KV, **Wilber Romero-Fernandez**, Gómez-Soler M, Guidolin D, Woods AS, Rivera A, Haegeman G, Agnati LF, Tarakanov AO and Fuxe K. *Biochemical and Biophysical Research Communications, 2010.*

8. Overproduction of Human $M_3$ Muscarinic Acetylcholine Receptor: an approach towards structural studies. **Wilber Romero-Fernandez**, Garriga P and Borroto-Escuela DO. *Biotechnology progress (in press 2010).*

9. Muscarinic receptor family interacting proteins: Role in receptor function. Borroto-Escuela DO, Correia PA, **Wilber Romero-Fernandez**, Fuxe K, Ciruela F and Garriga P. *Journal of Neuroscience Methods, 2010.*

10. Characterization of the A2AR-D2R interface: focus on the role the C-terminal tail and the transmembrane helices. Borroto-Escuela DO, **Wilber Romero-Fernandez**, Tarakanov AO, Gómez-Soler M, Corrales F, Marcellino D, Narvaez M, Frankowska M, Flajolet M, Heintz N, Agnati LF, Ciruela F and Fuxe K. *Biochemical and Biophysical Research Communications, 2010.*

11. Dopamine D2 and 5-Hydroxytryptamine 5-HT($_2$A) receptors assemble into functionally interacting heteromers. Borroto-Escuela, DO, **Wilber Romero-Fernandez**, Tarakanov AO, Marcellino D, Ciruela F, Agnati LF and Fuxe. K. *Biochemical and Biophysical Research Communications, 2010.*

12. Vector and P64k gene targeting for tandem affinity purification in *Neisseria meningitides*. Dasiel Oscar Borroto-Escuela, Mileydis Perez Alea, **Wilber Romero-Fernandez** and Daniel Bello Gill. *Journal of Microbiological Methods, 2006.*

**Acknowledgements**

La historia de esta tesis comenzó en San Andrés de Purnio gracias a mi madre, luego Dasiel e Ismel me ayudaron a escapar y el escenario fue otro. Sin ellos estas líneas fueran muy diferentes. No he de olvidar todos los que contribuyeron a la formación recibida en Cuba, con todos aquellos con los que compartí en la Facultad de Biología y en la beca de 12 y Malecón.

Luego Pere Garriga me acepto en su grupo, me ha guiado todo estos años y me permitió compartir con Eva, Laia, Laura, Darwin, Mileidys, Mónica, Marlet y Aram. También cerca estuvieron Margarita Morillo y Margarita Calafell, Tzanko y los chicos del laboratorio de Industrial. Siempre estuvo Irene y Rosa haciendo tan bien su trabajo que todo fue mucho más fácil. Fuera de la UPC, la UAB, la UB, el PCB y el Instituto Karoliska sirvieron de escenario para muchos experimentos.

También encontré apoyo en los viejos y nuevos amigos con los que he compartido de todo.Yoelvis, Francés, Héctor, los pupis, los muñecos, los pirulos, biruta, los lagartijos, Henry y Mary (hay que buscar un nombre para esta pareja) Juan Zapata, Manel, Manuel y familia, Thiago, Felipe, Fifi, Mertxe, Marco Zeta, Martín, Pedrito y a muchos otros que aunque su nombre no este, están.

A mi David y la familia de Canaria y Cuba

**a todos muchas gracias**

**Wilber Romero Fernández**